

POLITECNICO DI MILANO
Facoltà di Ingegneria dei Processi Industriali



Corso di Laurea Specialistica in Ingegneria Nucleare

PRELIMINARY ANALYSIS OF THORIUM FUEL CYCLE
IN A FAST NEUTRON SPECTRUM REACTOR

Relatore: Prof. Marco E. Ricotti

Relatore: Dott. Fausto Franceschini

Relatore: Dott. Mario Carelli

Correlatore: Carlo Fiorina

Tesi di Laurea Specialistica di:

Alberto Sartori

Matr. 736061

Anno Accademico 2010-2011

I wish to thank Prof. Marco Ricotti and Dr. Mario Carelli for the opportunity they have given me to go to Westinghouse Electric Company, where I have done the hereby presented thesis.

I really thank Dr. Fausto Franceschini for he has been an excellent guide throughout the work we performed, from both the technical and the human point of view.

A special acknowledgment is for Dr. Paolo Ferroni, and Micheal Wenner, for their deep suggestions and revisions during the typing of this work.

A particular thank is for Prof. Lelio Luzzi and Prof. Antonio Cammi for their support at the beginning and throught this experience.

I acknowledge Dr. Vincenzo Peluso for the proficuous traning on ERANOS, at ENEA, he offered to us.

I wish to thank also Rahamn Fariz, who gave me a daily lift to the Church, after the work.

A special thank is for Lidia, who is the love of my life.

*The fear of the LORD
is the beginning of knowledge.
Pr 7,1*

Contents

Abstract	ix
Estratto	xi
Introduction	xiii
1 Simulation Tool and Modeling Approach	1
1.1 The ERANOS Code	2
1.1.1 The ECCO Code	3
1.2 Modeling Approach	3
1.2.1 Input Definition	4
1.2.2 Depletion	4
1.2.3 Cooling and Reprocessing	4
1.3 The Multicycle Procedure	5
1.3.1 Materials Definition	6
1.3.2 Calculation of Collapsed Cross Sections	8
1.3.3 Core Building	9
1.3.4 Burnup	13
1.3.5 Cooling	14
1.3.6 Reprocessing	15
2 Thorium Fuel Cycle Performance in the Advanced Recycling Reactor	26
2.1 ARR Core Design and Employed Model	27

2.2	Thorium versus Uranium Fuel Cycles	29
2.2.1	Neutron Spectrum	31
2.2.2	TRU Concentration	36
2.2.3	TRU Transmutation Performance	39
2.3	Metallic, nitride, and Oxide Th-based fuels	41
2.3.1	Neutron Spectrum	45
2.3.2	TRU Transmutation Rate and Breeding Capabilities	48
2.3.3	TRU Concentration	50
2.3.4	Neutron Economy	53
2.4	Summary of Results and Future Works	59
3	Thorium Fuel Cycle Performance in a Heterogeneous Core	
	Design	62
3.1	The THETRU Design	65
3.2	Phase I: THETRU TRU Burning and Breeding Capabilities	67
3.3	Phase II: No TRU External Supply	71
3.3.1	Progressive TRU Content	71
3.3.2	In-bred uranium	76
3.3.3	Th versus U	81
3.4	Summary of Results and Future Works	89
4	Conclusions	92
A	Summary of studies conducted on thorium fuel cycle	95
A.1	Performance in LWRs	95
A.2	Performance in HWRs	101
A.3	Performance in MSR's	105
A.4	Thorium in ADS	109
	Bibliography	112

List of Figures

1	Increase in UNF mass in US and required repositories.	xiv
2	Current versus Westinghouse approach, which is driven by the waste management requirements.	xvi
3	Relative radiotoxicity for major fuel cycle and reprocessing alternatives, versus time after discharge.	xvii
4	Comparison of fission/absorption ratio for thermal spectrum (PWR) and fast spectrum (SFR).	xviii
5	Chain depicting nuclear reactions and decay leading to buildup of higher actinides.	xix
6	The η parameter for ^{233}U (red line) and ^{239}Pu (blue line). Data calculated through JANIS 3.2.	xx
1.1	Procedures developed for the multicycle calculation.	6
1.2	Geometry of real fuel (or blanket) pin, on the left, and the modeled pin, on the right.	7
1.3	The ARR fuel assembly model.	8
1.4	The ARR core radial view with the labels, given by ERANOS, of each assembly position.	11
1.5	Axial representation of the model of the ARR fuel assembly as modeled within the “core building” procedure.	12
1.6	Comparison of calculated k_{eff} values using burnup steps of 1 day and 15 days at BOC for a representative simulation.	14
1.7	Comparison of calculated k_{eff} values using burnup steps of 100, 200, and 500 days.	15

1.8	Trend of k_{eff} for a reactor where TRU enrichment at start-up is too high.	22
1.9	Plutonium content at BOC (a), external feed (b), and the core inventory at BOC (c) for the ARR with a TRU content at start-up too high.	23
1.10	Trend of k_{eff} for a reactor where TRU enrichment at start-up is too low.	24
1.11	Core inventory at BOC (a), and the external feed supply (b), for the ARR with a TRU content at start-up too high.	25
2.1	ARR core cross section.	29
2.2	Axial representation of the model of the ARR fuel assembly.	30
2.3	Neutron flux per unit lethargy versus energy for the three cases analyzed.	33
2.4	One-group macroscopic cross sections of U and Pu at BOC, after 60 EFPYs, for the Th-based fuel containing the recycled in-bred U.	34
2.5	One-group macroscopic cross sections of Pu at BOC, after 60 EFPYs, for the two Th-based fuels.	34
2.6	Percent contribution to total fission (BOC at 60 EFPYs of irradiation).	35
2.7	Plutonium content at EOC for Th-based fuel where in-bred uranium is not recycled (a), Th-based fuel where in-bred uranium is recycled (b), and U-based fuel (c).	38
2.8	Average mass difference (EOC-BOC) for ARR design. Positive values imply accumulation, negative values imply consumption.	40
2.9	α ratio between capture and fission microscopic cross sections, for Am and Cm isotopes.	42
2.10	One-group macroscopic absorption cross sections of the Am and Cm isotopes at BOC, at equilibrium.	43

2.11	Neutron flux per unit lethargy vs energy for metallic, nitride, and oxide fuels.	46
2.12	One-group macroscopic scattering cross sections for the binding elements of the fuels analyzed.	47
2.13	One-group macroscopic absorption cross sections of fuel binding elements.	52
2.14	Percent contribution to total absorption of HM, fuel element binding (Zr, N-14, N-15, O), structure (all but fuel pellet and coolant), and coolant.	53
2.15	The η parameter for the fuels analyzed.	57
2.16	The ε parameter for the fuels analyzed.	58
2.17	The ω parameter for the fuels analyzed.	58
3.1	Visualization of the phases comprising the Th/TRU to Th/U-233 cycle transition, with indication of EOC mass trend for Th, U, and TRU.	64
3.2	THETRU core radial view.	66
3.3	Axial representation of THETRU fuel and radial blanket assemblies.	67
3.4	Uranium generated within each part of the THETRU reactor.	69
3.5	Ratio between uranium generated within a medium and its volume.	70
3.6	Core inventory at discharge for a total of 180 EFPYs of irradiation. For the first 60 EFPYs the external fissile feed consists of legacy TRU. In-bred uranium is the feed thereafter.	72
3.7	Mass vs cycle for Np (a), Pu (b), Am (c), Cm (d), higher isotopes of Cm (e), and Cf (f) throughout the two phases. Note that feed was changed after cycle 20.	74
3.8	Pu content within the core at EOC (a), and the Pu vector (b) throughout the two phases.	76
3.9	Collapsed 1-energy group microscopic fission cross section for the Pu isotopes.	77

3.10	External U to top-up the in-bred U.	77
3.11	U content within the core at EOC (a), and the U vector (b) throughout the two phases.	78
3.12	The concentration, (a), and the mass, (b), of U-232 within the driver, after cooling.	80
3.13	The TRU content within the core at EOC, throughout the two phases for the Th case, (a), and for the U-238 case, (b).	82
3.14	The Pu vector throughout the two phases, for the ARR U fuel design.	83
3.15	On the y axis, the ingested radiotoxicity index <i>at 300 years</i> versus the equivalent U ore, and, on the x axis, the energy produced throughout the two phases for the Th case, (a), and for the U case, (b).	85
3.16	Ingested radiotoxicity isotopic breakdown at 300, 10,000 and 100,000-yr for the Th case, after 60 EFPYS, (a), and after 240 EFPYS, (b).	86
3.17	Ingested radiotoxicity isotopic breakdown at 300, 10,000 and 100,000-yr for the U case, after 60 EFPYS, (a), and after 240 EFPYS, (b).	87
3.18	Radiotoxicity in m^3 of air for the two fuel at the end of each phase.	88
A.1	SBU and WASB fuel assembly design.	97
A.2	LWBR core cross-section.	100
A.3	LWBR fuel module cross-section.	100
A.4	CANFLEX mixed bundle.	103
A.5	Schematic view of a quarter of the MSFR.	108
A.6	Concept of an Accelerator Drive System.	109

List of Tables

1.1	Element masses after 1000 EFPDs, using burnup steps of 100, and 500 days.	16
2.1	Legacy TRU composition assumed for the simulations, in weight % (10-yr cooled, reprocessed LWR, UO ₂ fuel with 4.2 U-235 w/o and 50 GWd/tHM discharge burnup).	28
2.2	Main design parameters of the ARR.	28
2.3	Main parameters of the ARR fuel assembly.	30
2.4	Main design assumptions for the various cases analyzed.	31
2.5	TRU content for the fuels analyzed.	36
2.6	TRU transmutation performance for the fuels analyzed.	39
2.7	Mass difference between EOC and BOC, averaged over 60 EFPYs [kg/GWt-yr]. Positive values imply accumulation, negative values imply consumption.	40
2.8	Main design assumptions for the various fuels analyzed.	44
2.9	TRU transmutation rate and breeding potential for the fuels analyzed.	49
2.10	TRU content for the fuels analyzed.	51
2.11	Classification of isotopes in fissile or fertile, for the fuels analyzed. For this study, a fertile isotope was defined as the isotope which has the one-group microscopic capture cross section higher than the fission cross section.	56
3.1	Main parameters of the THETRU design.	67

3.2	Main parameters of the THETRU driver and radial blanket assemblies.	68
3.3	Comparison of TRU burning and U-233 breeding capabilities between heterogeneous and homogeneous designs, averaged over 60 EFPYs.	69
3.4	Mass of TRU within the core at discharge throughout the three phases [kg/GWt]. Note that 0 EFPYs means at start-up. . . .	73
3.5	Vector of in-bred uranium within each medium, along with the ppm of U-232.	79
3.6	Composition of the external feed for Phase II for the ARR U fuel design.	81

Abstract

In this thesis, the performance of Th-based and U-based fuel cycles has been studied, with particular focus on the destruction of legacy TRU in a fast neutron spectrum environment. The evaluation has been carried out with comprehensive simulations covering all the relevant portions of the fuel cycle, with detailed cycle-by-cycle in-core irradiation performed through an automated procedure developed within the framework of the ERANOS code.

As the first step, a Th-TRU core design for the Advanced Recycling Reactor (ARR), a Toshiba-Westinghouse fast sodium-cooled U-TRU burner reactor, has been developed. This allowed to calibrate the neutronic procedures developed and confirmed the excellent potential of Th for legacy-TRU consumption. In addition, the behavior of different Th fuel forms has been investigated, namely, metallic, nitride (both with natural N and N enriched in N-15), and oxide fuel. The results provided important insights on the TRU transmutation performance and U-233 breeding potential of the various options, and constituted the basis for the selection of an optimum fuel to carry forward into the ensuing design stage.

As the next step, a heterogeneous fast-reactor core design has been developed. The design aimed at improving the U-233 breeding performance of the ARR while maintaining its favorably high TRU transmutation rate. This has been accomplished through the use of radial and axial blankets and N-15 enriched ThN fuel. The results obtained confirm the effectiveness of the design developed in achieving its main objectives: efficient U breeding, nearly doubled from the previous ARR design, maintaining practically intact its high

TRU consumption rate. Additional benefits of the heterogeneous design are the potential for reduced reactivity control requirements and improved safety coefficients.

In the last part of the work, the core design developed has been employed as basis to perform a scenario calculation which encompasses the phases envisaged for thorium implementation, from a Th/TRU fuel cycle to a Th/U-233 fuel cycle. A first phase where legacy-TRU is supplied as an external feed and burned within the fast reactor core is followed by a second phase, where the external TRU stock is assumed to be exhausted, and the in-bred U is used to continue the destruction of the TRU accumulated in the core during the first phase. As the TRUs are being burned also from the fuel core inventory, the cycle transitions to a Th/U-233 fuel, virtually free of TRU. The HWL radiotoxicity from this cycle after 300 years of decay has then been evaluated and showed to be comfortably below that of the natural U ore.

Therefore this work has showed that it is possible, using thorium, to accomplish two main objectives of the Westinghouse backend strategy: deep burn of the legacy TRUs, achievement of a virtually TRU-free fuel with 300-year radiotoxicity comparable to that of the U ore.

Estratto

In questa tesi, le performance del ciclo del combustibile del torio in uno spettro neutronico veloce sono state studiate. Gli studi sono stati condotti simulando il ciclo del combustibile dentro e fuori del nocciolo. L'irraggiamento è stato simulato usando una procedura automatizzata sviluppata nell'ambiente lavoro del codice ERANOS.

Analisi preliminari di combustibili Th-TRU sono state condotte per l'Advanced Recycling Reactor (ARR), un reattore veloce raffreddato a sodio sviluppato per il bruciamento dei TRU, il cui design è Toshiba-Westinghouse. Specificatamente, il ciclo del combustibile del torio è stato prima comparato con quello dell'U-238, al fine di delineare le loro performance relative. Inoltre, sono state comparate anche le performance di quattro diversi tipi di combustibile: combustibile metallico, nitruro (sia con azoto naturale che arricchito in N-15 per evitare la formazione del radiotossico C-14, il quale è generato tramite la reazione (n,p) su N-14) e ossido.

Da questi studi è emerso che, sotto le configurazioni assunte, il combustibile basato sul Th può bruciare fino a tre volte più TRU che il combustibile a uranio: 319 contro 111 kg/GWt-yr. Ciò è dovuto al fatto che il combustibile a U-238 genera direttamente l'isotopo Pu-239, a differenza del Th-232, il quale richiede un maggior numero di catture neutroniche per progredire verso i transuranici.

Tra i combustibili studiati, il tasso di bruciamento di transuranici è simile. Diversamente, la quantità di uranio generata è molto diversa. I nitruri generano il 30% in più di U rispetto ai combustibili metallici e ossidi:

150 kg/GWt-yr contro 114 e 113 kg/GWt-yr rispettivamente. Tra i due nitruri considerati, quello arricchito in N-15 è migliore, in quanto l'isotopo N-14 presenta una sigma di cattura otto volte maggiore di quella di Zr, N-15, e O.

Successivamente, un design di nocciolo eterogeneo è stato sviluppato, chiamato THETRU, al fine di migliorare il breeding del design dell'ARR. Per questo reattore, è stato adottato il combustibile ThN con N arricchito in N-15 al 95% in atomi, poiché presenta la migliore combinazione di tasso di bruciamento di TRU e breeding di U. Di questo design, si è stata studiata la transizione da nocciolo contenente Th/TRU a un puro ciclo del combustibile Th/U-233. Per fare questo, il feed di materiale fissile (TRU) è stato sostituito con l'uranio generato nei blanket. Infine, le prestazioni del reattore THETRU sono state comparate con quelle di una possibile controparte, cioè un reattore veloce basato sul ciclo del combustibile U-238/Pu.

Le conclusioni che si possono trarre dallo studio delle prestazioni del THETRU sono che il combustibile basato sul Th può ridurre del 99% la quantità di TRU presente nel nocciolo, diversamente dal reattore basato su U-238, poiché l'isotopo Pu-239 è continuamente generato. La ridotta quantità di TRU presenti nel reattore a Th, comporta una radiotossicità del combustibile, dopo 300 anni, essere inferiore a quella dell'uranio naturale.

In conclusione, questo lavoro ha dimostrato che, usando il torio, è possibile raggiungere due obiettivi principali per Westinghouse: un consistente bruciamento di TRU, e raggiungimento di un combustibile virtualmente privo di TRU, la cui radiotossicità a 300 anni dopo lo scarico è comparabile con quella del minerale uranio.

Introduction

Historic Perspective

The world electricity demand is projected to grow at an annual rate of about 2.5% through 2030 as a result of increasing population and wealth fare, and industrial development [1]. Finding a large, cheap, clean and secure source of electricity to satisfy the predicted growth of energy consumption is one of the major challenges of the century. Increases in renewable energy installed capacity as well as improvements in energy efficiency are certainly part of the solution. However, to match the energy demand in an environmentally conscientious as well as economically viable way, an increased reliance on a high power density, emission-free energy source, such as nuclear energy, should be pursued.

The nuclear fuel cycle currently pursued in the United States for commercial reactors is the so-called once-through fuel cycle: the fuel, after irradiation within the core is not reprocessed and destined to final disposal as high-level nuclear waste (HLW). On June 3, 2008, after about 30 years of studies on locations and designs of repositories for final storage of HLW, the U.S Department of Energy (DOE) submitted a license application to the U.S Nuclear Regulatory Commission (NRC) for the construction of a geologic repository in Yucca Mountain, in the state of Nevada [2]. However, in 2010 under the Obama administration, funding for the development of the repository was terminated effective with the 2011 fiscal year, and the DOE filed a motion with the NRC to withdraw its license application.

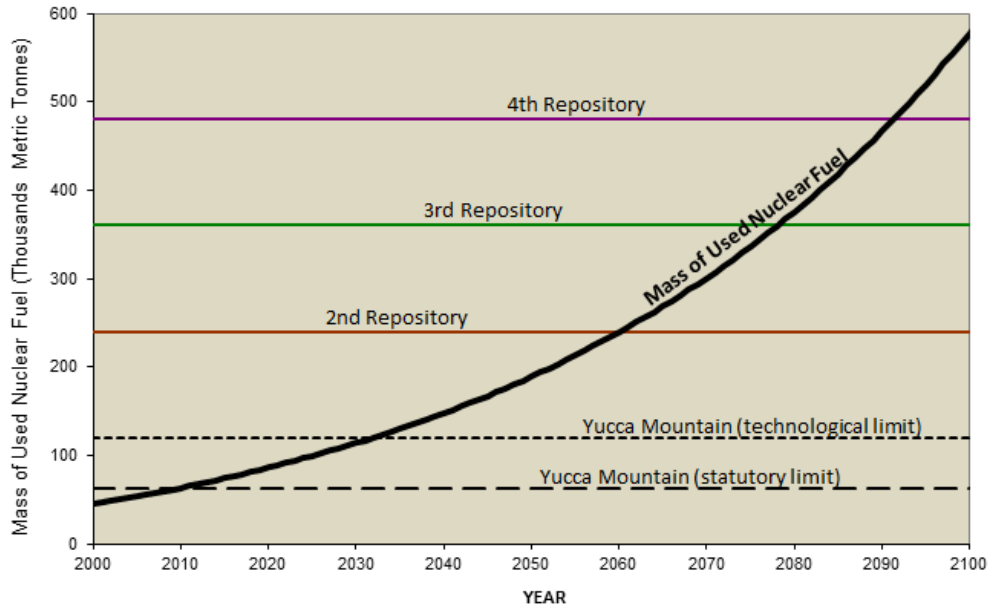


Figure 1: Increase in UNF mass in US and required repositories [3].

Even though the Yucca Mountain repository would have provided storage for all the existing US commercial and defense HLW, the effectiveness of this solution with the continuation of the once-through fuel cycle [3]. Figure 1 shows the increase in used nuclear fuel (UNF) mass in US and the repository capacity needed, assuming an annual growth of 2% in nuclear energy generation. It can be seen that the Yucca Mountain repository would fill up to its statutory limit already around 2014. Although the actual technical limit could be raised to accept waste for about 20 more years, new repositories would still be required every few decades thereafter. A reduction of HLW generation is therefore of paramount importance.

Approach Used and Motivation for Studying Th-based Fuels

To tackle the nuclear waste issue, Westinghouse Electric Company (referred to as “Westinghouse” from now on) has proposed a comprehensive waste-management requirement-driven approach. In this new approach the priority order of the main constituents of the nuclear fuel cycle is reversed from the sequence historically adopted [3]. The top part of Figure 2 shows such historic sequence, i.e. selection of a specific reactor type which best addresses the application requirement, then the fuel form best fitting the chosen reactor, and finally searching for an acceptable waste management solution. The approach presented by Westinghouse, shown at the bottom of the figure, is instead proposing to *start* with the waste management requirement, then select the fuel and/or fuel cycle satisfying the waste objectives, and finally the type of reactors to achieve the objectives.

The requirement chosen is related to the *radiotoxicity* of the nuclear waste. This parameter is a measure of the potential health hazard, for the population, resulting from a postulated release of a radioactive material, the nuclear waste in this context [4]. This hazard is mainly due to some of the elements composing the waste, particularly plutonium, neptunium, americium, curium, and some long-lived fission products such as iodine and technetium. Given a fuel cycle scenario, Westinghouse has set a limit for the waste generated, i.e. not to exceed, after a proper isolation time, the radiotoxicity of the uranium ore needed in a typical PWR once-through cycle to produce the same amount of electricity generated by that waste. Based on the radiotoxicity profiles shown in Figure 3, an isolation period of approximately 300 years was chosen [3]. Figure 3 shows the relative radiotoxicity profiles, with respect to natural uranium ore, for various waste components generated through U-Pu cycles, specifically 1) the transuranic elements (TRUs) generated by a traditional once-through cycle, 2) the TRUs of point 1 excluding plutonium isotopes, 3) the TRUs generated by a mixed-oxide (MOX) fuel cycle with

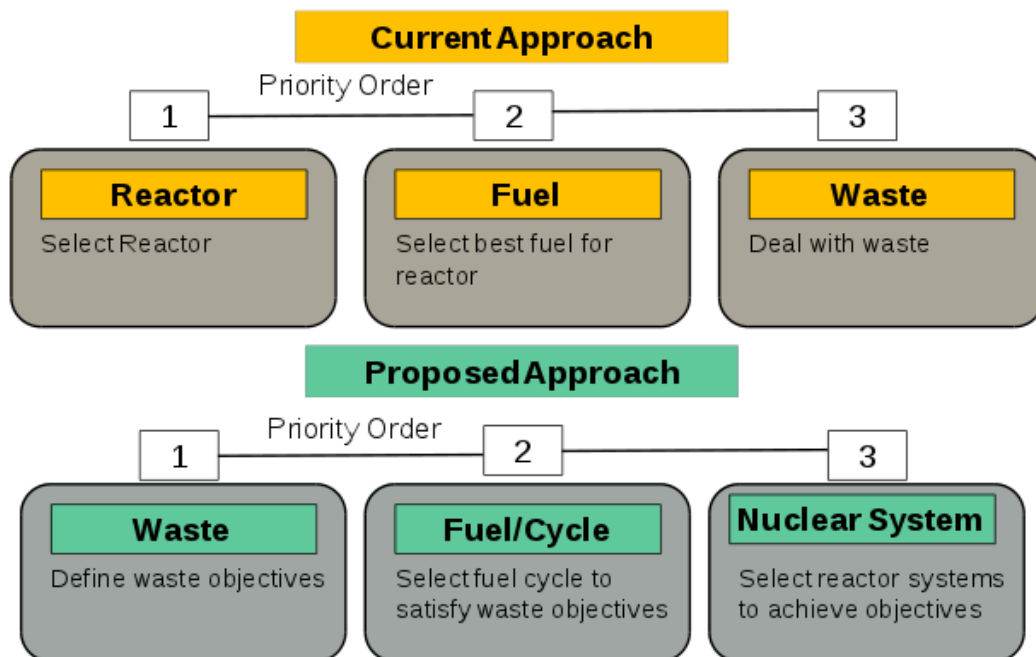


Figure 2: Current versus Westinghouse approach, which is driven by the waste management requirements [3].

single plutonium recycle and 4) the fission products. It can be seen that the traditional once-through cycle takes between one hundred thousand and a million years, significantly longer than a few hundred years, to recede to the uranium ore level. Single plutonium recycle MOX has only a very limited impact on radiotoxicity reduction. Complete recycle of plutonium has a significant effect, reducing the radiotoxicity by about one order of magnitude, but it is still insufficient for reaching the radiotoxicity objective due to the contribution of the remaining transuranics that would be discharged. The fission products decay below the uranium ore radiotoxicity in about 300 years, which makes the objective of the proposed approach practically coincident with being able to fully recycle all the transuranic isotopes.

A comprehensive nuclear waste management strategy should not only cope with the waste accumulated so far (legacy waste) but also with the “future” waste, by steering the cycle towards one with reduced waste generation. One way to achieve this is through a fleet of reactors which are capable

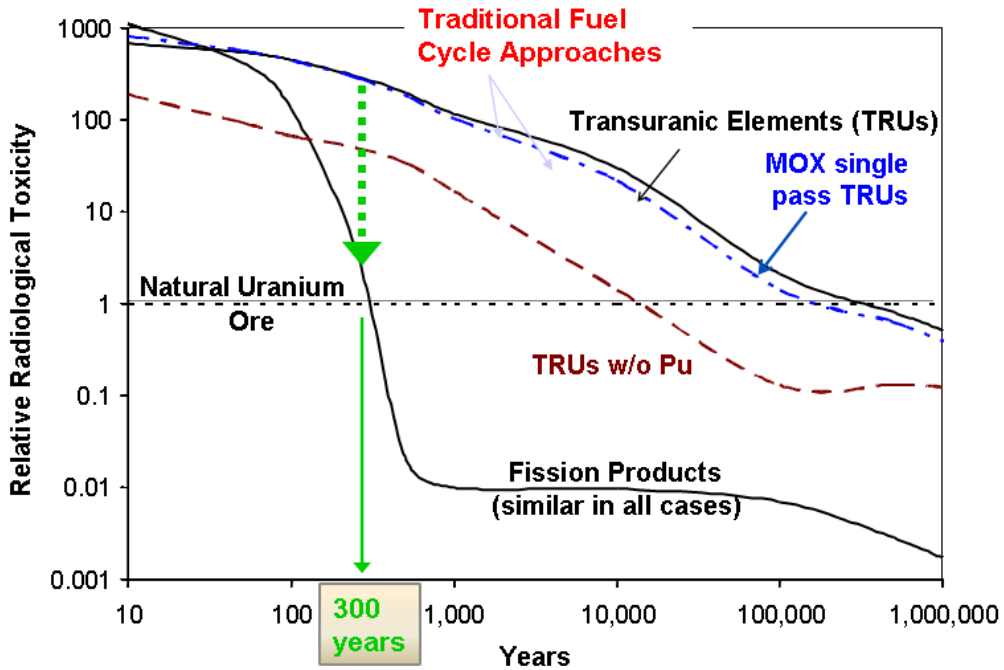


Figure 3: Relative radiotoxicity for major fuel cycle and reprocessing alternatives, versus time after discharge [3].

to burn the current TRUs stock while breeding enough fissile to close and sustain the cycle.

Recycling and transmutation of TRUs can be carried out with homogeneous and heterogeneous configurations [4]. In the homogeneous recycling mode, the TRUs are kept together with the fuel. In the heterogeneous mode, a subset of the actinides (typically Am and Cm) are placed into specific sub-assemblies (*target*) and managed independently from the rest of the fuel. In the present work, the homogeneous recycling mode has been employed for the sake of simplicity.

In general, a fast spectrum is preferred for efficient destruction of TRU because of the larger σ_f/σ_c ratio than in a thermal spectrum, as shown in Figure 4. The larger σ_f/σ_c ratio promotes TRU destruction (by fission) over transmutation (by neutron capture) to higher actinides. The larger fission-to-capture ratio in a fast spectrum is a consequence of the fission cross section

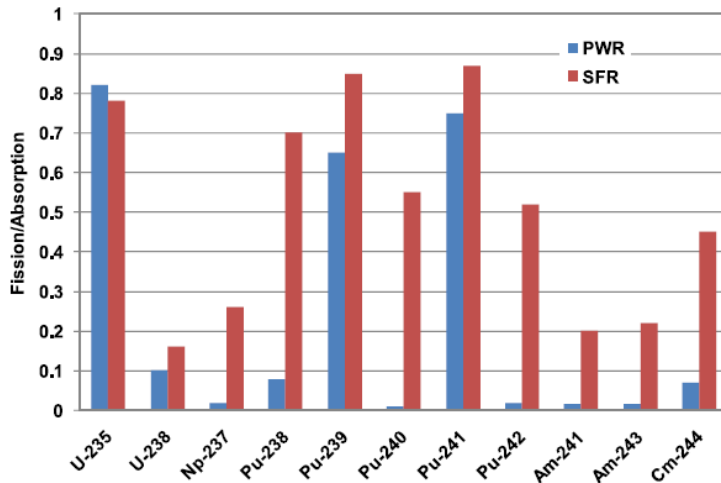


Figure 4: Comparison of fission/absorption ratio for thermal spectrum (PWR) and fast spectrum (SFR) [5].

of the even Pu isotopes and most of the Am and Cm isotopes, which are 1) of the threshold type (i.e. negligible below a certain neutron energy), and 2) approximately constant at high energies, where instead capture cross-section decreases with energy. In addition, the harder spectrum typically yields more fission neutrons available for the TRU destruction [4].

Concerning the fuel cycle, two main options are considered: U-238/Pu, the current standard, and Th/U-233 fuel cycle. From the waste management point of view, thorium-based fuel has the advantage of a lower endogeneous production of TRU. Figure 5 shows the nuclear reactions and decay leading to buildup of the higher actinides mostly responsible for the waste radiotoxicity. Due to its “lower” position, Th-232 requires multiple neutron captures to “advance” to TRU, thereby lowering its generation. A related beneficial consequence is that when Pu or TRU are used as fissile in Th-based fuels, their rate of consumption is much higher than in U-based fuels. In addition, thermal breeding based on the Th/U-233 fuel cycle is possible (see for example the Shippingport Light Water Breeder Reactor [6]), unlike in the U/Pu fuel cycle where breeding is limited to the fast energy range. An indication of the breeding performance is given by the value of the η factor, defined as the

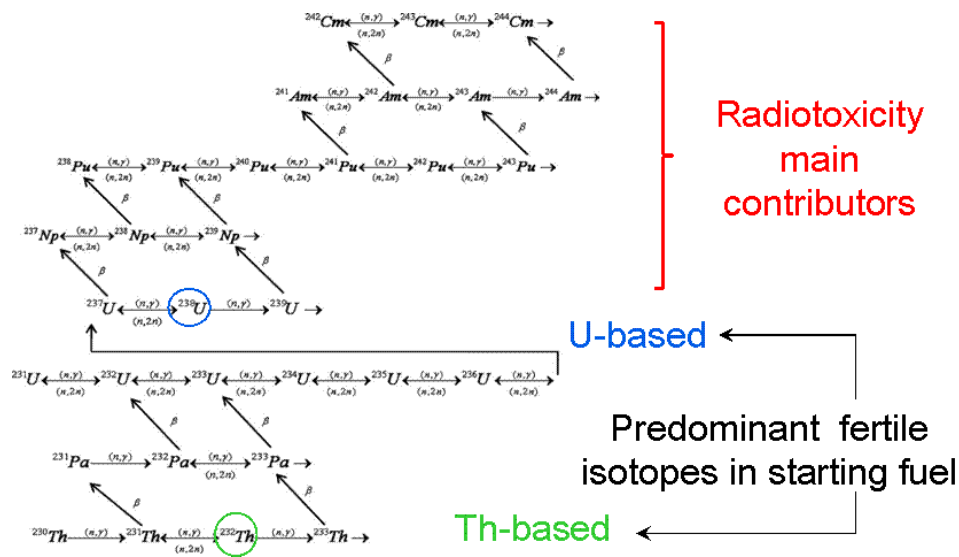


Figure 5: Chain depicting nuclear reactions and decay leading to buildup of higher actinides [3].

average number of neutrons emitted per neutron absorbed, which therefore needs to be higher than 2 to enable breeding. η , as shown in Figure 6, is higher than 2.0 over a wide range of energies for U-233, unlike Pu-239. Note that from a purely breeding standpoint the U-238/Pu fuel cycle outperforms the Th/U-233 fuel cycle, which is why historically a Th fast breeder has never been pursued, but it could be an attractive option now given the shift in emphasis from breeding to waste management.

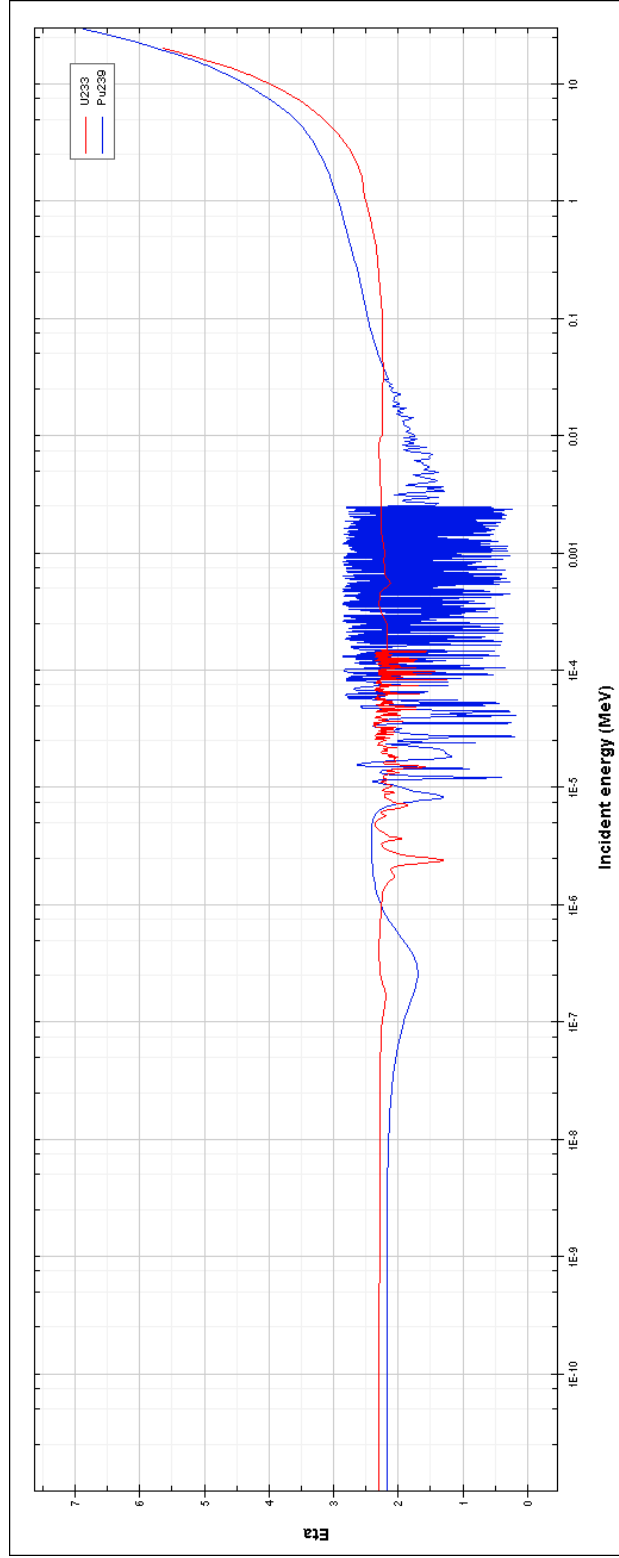


Figure 6: The η parameter for ^{233}U (red line) and ^{239}Pu (blue line). Data calculated through JANIS 3.2 [7].

Organization of the Work

In this thesis, performance of a Th-based fuel cycle in a fast neutron spectrum environment has been studied. The evaluation has been carried out with simulations including the in-core and out-of-core fuel cycle, and cycle-by-cycle irradiation using an automated procedure developed within the framework of the ERANOS code. The ERANOS code and the developed procedure are presented in Chapter 1.

Chapter 2 presents a preliminary performance analysis of Th-TRU fuels. This analysis, which is focused on TRU incineration and breeding capabilities, was carried out for the Advanced Recycling Reactor (ARR) [8], a Toshiba-Westinghouse fast sodium-cooled TRU burner reactor design. Specifically, the Th fuel cycle was first compared to the U-238 fuel cycle to show their relative performance. Additionally, the performance of different types of Th fuels have been compared, namely, metallic, nitride (both with natural nitrogen and nitrogen enriched¹ in N-15), and oxide fuel. The results presented in Chapter 2 provide important insights on the TRU transmutation performance and U-233 breeding potential of the various fuels, which have been used to select the fuel option to carry forward into the ensuing design optimization stage.

Chapter 3 presents results for a heterogeneous core [9, 10] designated as THETRU, with inner and peripheral radial blankets, that was developed to improve the breeding capabilities of the ARR design. ThN, with nitrogen enriched at 95 atom percent in N-15, was chosen since this fuel combines the best performance on TRU incineration and U-233 breeding. For this reactor, the transition phase from a Th/TRU burning phase to a pure Th/U-233 fuel cycle was also explored. Finally, the performance of THETRU has been compared against that of a possible counterpart fast reactor based on the U-238/Pu fuel cycle.

Chapter 4 discusses the conclusions and presents the future work needed.

¹Nitrogen was assumed to be enriched to a 95% atom percent level in N-15, for reducing formation of radiotoxic C-14 via (n,p) reaction from N-14.

Appendix A describes some of the past studies that have been conducted on the Th fuel cycle.

Chapter 1

Simulation Tool and Modeling Approach

To tackle the nuclear waste issue, Westinghouse has proposed a comprehensive waste-management requirement-driven approach. This approach requires that the radiotoxicity of the nuclear waste generated by the reactors employed must not exceed, after 300 years of isolation, the radiotoxicity of the uranium ore needed in a typical PWR open cycle to produce the same amount of electricity. Subsequently, which fuel and/or fuel cycle satisfies the waste objectives is to be investigated, and finally the type of reactors to achieve the objectives.

The objective is practically coincident with being able to *recycle* all TRUs, since the hundreds thousands of years life of the nuclear waste is mainly due to the presence of: Pu, Np, Am, Cm, and some long-lived fission products, such as I and Tc, while the fission products decay below the uranium ore radiotoxicity in about 300 years. Therefore, to assess if a fuel or fuel cycle satisfies the Westinghouse's limit, it is necessary to evaluate the fuel cycle performance, in a closed fuel cycle management, over many cycles.

To this aim, a set of ad hoc procedures for cycle-by-cycle simulation has been developed within the framework of the ERANOS code. Calculations were aimed to address transmutation performance of different fuels (Th-based

and U-based, and metallic, nitride, and oxide) in a fast neutron spectrum environment. The reactors employed were the Advanced Recycling Reactor (ARR), a Toshiba-Westinghouse design, and the THETRU, a heterogeneous core design, which has been developed in this thesis work. This procedure is intended for scoping calculations.

The chapter is organized as follows:

- Section 1.1 gives a general introduction of the ERANOS characteristics and potentials, and, in Section 1.1.1, the cell and lattice code of ERANOS, the ECCO, is briefly introduced.
- Section 1.2 introduces the required objectives to develop a multicycle simulation.
- Section 1.3 describes the multicycle procedure which has been developed within the ERANOS framework.

1.1 The ERANOS Code

The calculation system ERANOS2.2N (European Reactor ANalysis Optimized System) has been used throughout this study. ERANOS (European Reactor ANalysis Optimized System) is a system of neutron and gamma codes developed within a European framework and is particularly suited for fast reactors. ERANOS is a deterministic code system. Neutron physics calculations can be performed at the cell/lattice level, with the ECCO code (see Section 1.1.1), while core level transport calculations, including those in burnup calculations, can be performed with various flux solvers.

ERANOS comes with a huge number of modules (functions) written in ESOPE, an extension of FORTRAN77. A module can generate or modify a SET (Structured ERANOS Tree, or EDL in French). For example, a SET may be the core geometry, or the concentration of isotopes within core, the cross sections, or the flux throughout the core. Calling modules is performed by the interpreter LU (Langage Utilisateur, or User's Language in English).

LU can also manage other variables (integers, reals, string of characters, . . .) or values stored inside SETs. A proper arrangement of such modules and LU instructions is an *ad hoc* procedure.

ERANOS can thus provide a complete simulation of a core, including reactivity, flux, spatial power distributions, feedback coefficients, and control rod worth.

1.1.1 The ECCO Code

Within a ERANOS calculation, the generation of collapsed microscopic, and macroscopic cross sections can be performed. To do so, the ECCO (European Cell COde) is used, which is “included” with ERANOS. ECCO solves the resonant nuclide self-shielding using the sub-group method and computing, with the collision probability method (P_{ij} method), a fine-group solution of the integral transport equation.

ECCO uses different libraries with cross sections stored in several energy meshes: 1968 groups (all-purpose), 175 groups (shielding purposes), 172 XMAS-group structure (refined in the low energy range), and 33 groups (usually used for core calculations). Default libraries that can be used include were derived by: JEF-2.2, ERALIB1, JEFF-3.1, and ENDFB-VI.8.

ECCO can model cells with geometry that is plane, cylindrical, 2D with a rectangular lattice, 2D with a hexagonal lattice or 3D slab geometry. During cross sections calculation, the geometry may be homogenized.

1.2 Modeling Approach

As pointed out in the introduction of this chapter, the simulations must model the fuel cycle performance in a closed fuel cycle, where all the TRUs are recycled. Conceptually, the multicycle simulation can be performed iterating on the following steps:

- Definition of the input for the cycle;

- Perform the depletion;
- Simulate cooling and reprocessing.

1.2.1 Input Definition

The first step is to develop the input for the model geometry. After this, material property definitions are developed and assigned to the appropriate model geometry, e.g. fuel, cladding, coolant, and so forth, at the beginning of each cycle. Note that the composition of the fuel is known at the start-up, but after the depletion it must be recalculated, since a *closed* fuel cycle has to be simulated. This is carried out during the reprocessing and new fuel manufacturing.

1.2.2 Depletion

Once the core geometry and the composition of materials are known, the depletion calculations can begin. In this step the fuel is irradiated simulating the time of residence of the fuel within the core. It is during such step that the TRUs are transmuted.

1.2.3 Cooling and Reprocessing

After the irradiation, the fuel must be cooled before it can be reprocessed. The cooling time depends on the type of fuel and the reprocessing technique employed.

During reprocessing, the elements which are to be recycled, for example Pu, are separated from the rest of the fuel. Subsequently, the new fuel, i.e. the fuel for the following cycle, is made. The new fuel must contain the recycled elements, plus a top-up of fertile and/or fissile material to assure sufficient mass and reactivity. After that, the composition of the fuel is known and can be used for the first step of the next cycle.

1.3 The Multicycle Procedure

As already discussed, a multicycle simulation can be performed iterating a set of steps which simulate a complete fuel cycle, i.e. time step dependent material and cross section development, core transport and burnup calculations, and then reprocessing and fuel manufacturing, which feeds back into the time step and material and cross section development.

A set of ad hoc procedures have been developed, within the ERANOS framework, that permits evaluation of core transmutation performance, cycle by cycle toward equilibrium. Each cycle is composed of the steps shown in Figure 1.1 and for each step a procedure has been developed. The starting point is the definition of materials, i.e. the isotopic composition of each material (fuel, blanket, shield, etc.) at start-up, then the calculation of problem dependent cross sections, followed by the “core building” which creates the 3-D core geometry and associates the proper material to each geometry region. Subsequently, a neutron transport problem is solved, with the output flux utilized for core depletion (BURNUP procedure). Once finished, the fuel has to be cooled and finally reprocessed, which finishes a single cycle and, if desired, gives the input for the following cycle. Note that, even though is not represented in Figure 1.1, the flux calculation is performed several times throughout one cycle, i.e. after the “core building” procedure, after each step of burnup, and before the “cooling” procedure. The flux solver employed is TGV/VARIANT (referred to as “VARIANT” from now on) module of ERANOS, where VARIANT is a flux solver utilizing the variational nodal method developed for the VARIANT code.

The conducted studies were aimed to assess the preliminary transmutation performance of different fuels in two different fast reactors. As a result, significant assumptions were made in developing this process, keeping in mind that it is meant for scoping calculations.

In the following Sections, each procedure will be presented and discussed, giving the philosophy and thoughts that guided their development.

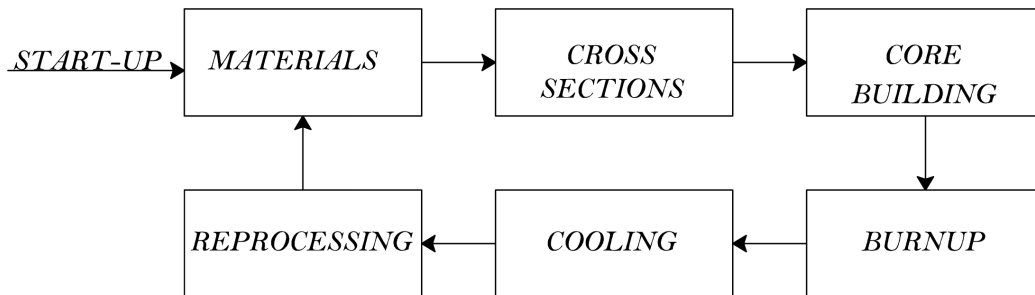


Figure 1.1: Procedures developed for the multicycle calculation.

1.3.1 Materials Definition

The first input required by the ERANOS code is the definition of the materials which compose each part of the core, e.g. fuel, cladding, coolant, and so forth. Along with isotopic composition and temperature, Assembly geometry is defined as well, which is needed for the lattice cell calculations to generate cross sections.

Isotopic compositions are inserted for the first cycle, i.e. at startup. For succeeding cycles, compositions are calculated during reprocessing. In this work, pseudo fission products have been used. A pseudo fission product is not a real, but it is used to represent multiple fission products, by preserving the average properties over the *real* fission products. When a nuclide undergoes fission reaction two pseudo fission products are emitted. Note that every time one isotope undergoes fission reaction, the same two fission products are emitted. The pseudo fission products emitted by, for example, Pu-239 are different from the pseudo fission products emitted by U-235. Simulations using pseudo fission products are faster and still accurate [11]. Simulations are faster because there are less isotopes to be simulated. Pseudo fission products are not tracked. In other words, they do not undergo any nuclear reactions or decay. This is acceptable since the present work is focused on TRU transmutation, and not on the evolution of the fission products, which is similar for all cases.

The geometry model is kept unchanged throughout the analysis. Fuel (or blanket) pins have been modeled already expanded for swelling, i.e. with

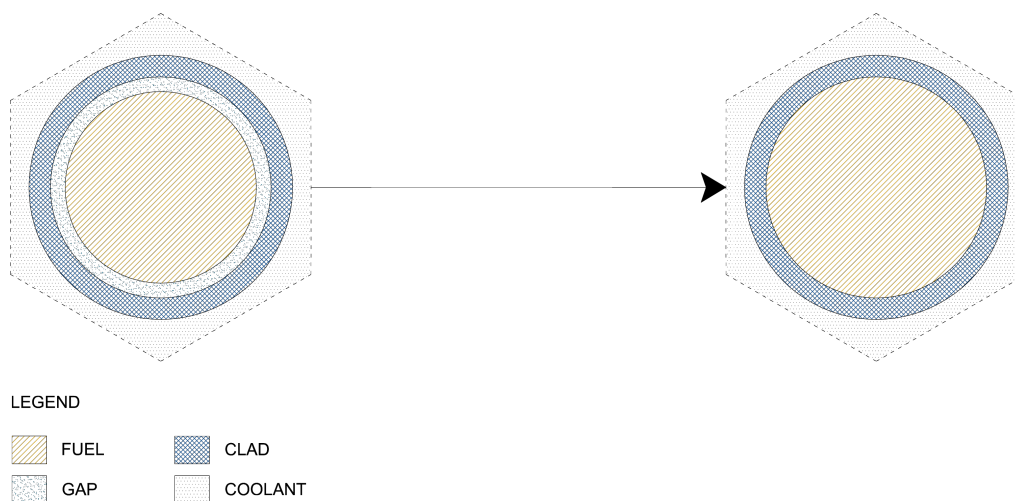


Figure 1.2: Geometry of real fuel (or blanket) pin, on the left, and the modeled pin, on the right.

the fuel pin touching the cladding, as shown in Figure 1.2. The fuel density has been calculated accordingly using the smeared density parameter, which takes into account both the swelling and the porosity of the fuel.

Thermal expansions, both radial and axial, have been avoided by defining a thermal linear expansion coefficient $\alpha = 1$. This choice was made since the expansion coefficients of the fuels that have been studied have not been found in the literature review. So, to compare nuclear properties of such fuels, expansions have been neglected. However, for future and more precise work, in particular for dynamic calculation or for evaluation of feedback coefficients, they should be addressed.

Material temperatures are input corresponding to the reactor operating at the full power. So, as it were, temperatures are hot, while the geometry is cold.

Figure 1.3 shows the modeled ARR fuel assembly, which features 271 pins with a triangular pin lattice. The wire wrapper separating fuel pins has been homogenized within the coolant.

Reflector, shields and control rods has been defined homogeneously at the cell level. Their dimensions are defined through the core building procedure.

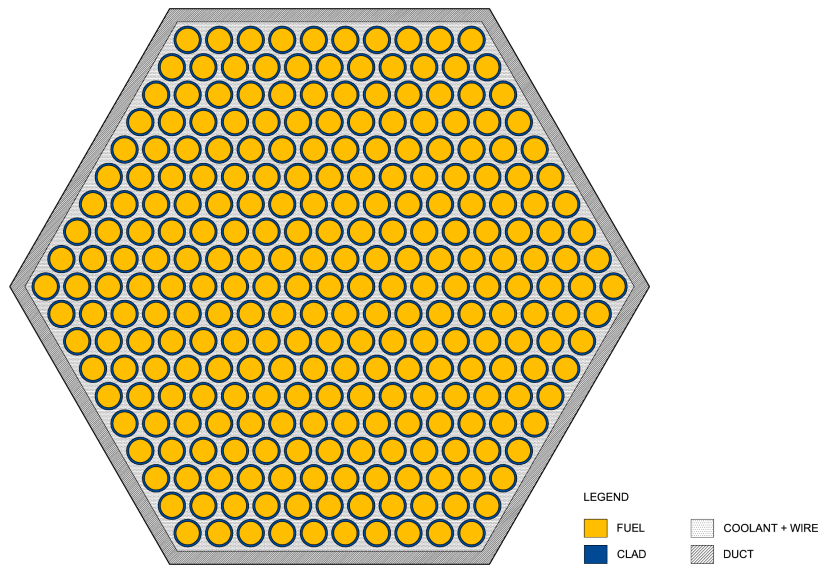


Figure 1.3: The ARR fuel assembly model.

1.3.2 Calculation of Collapsed Cross Sections

After the definition of the materials and the cell geometry, ERANOS requires the generation of the problem dependent cross sections for core calculations. It is mandatory to generate the microscopic cross sections for the first cycle, which are stored in a SET and may be used for many cycles [11]. However, in this multicycle procedure, the cross sections are calculated at each cycle. It is not necessary to regenerate the cross sections often during the irradiation time, unlike for thermal reactors, since there is no significant change in spectrum due to the build-up of fission products, which influence the thermal energy spectrum range.

Cell calculations are performed using ECCO (European Cell COde). ECCO uses the subgroup method to treat resonance self-shielding effects. ECCO prepares self-shielded cross sections and matrices by combining a slowing-down treatment in many groups with the subgroup method within each fine group [12]. The fine group is one energy group. The sub-group method takes into account the resonance structure of heavy nuclides by means of probability tables and by assuming that the neutron source is uni-

form in lethargy within a given fine group. For more information about how ECCO calculates cross sections, see Reference [12].

A library with a 33 energy groups scheme designe for fast reactors, derived from JEFF-3.1, is used.

1.3.3 Core Building

Once materials and cross sections have been calculated, the 3D core model is created. The core is modeled with a hexagonal-3D geometry, where control rods are completely extracted and their in core locations filled with coolant. To develop a 3D model, ERANOS requires two steps.

First, a two coordinate numbering shceme is used to identify each hexagonal element in the radial core dimesion. As an example, the ARR core radial view is shown in Figure 1.4. So, to define the ARR core, input positions must be given for which hexagonal element are occupied by the inner fuel, which by the outer fuel, and so forth.

Second, each assembly type (Inner Fuel, Outer Fuel, etc,) has to be defined axially. Figure 1.5 shows the axial representation of the model of the fuel assembly. From bottom to top, there is the lower plenum, the fuel, and the upper plenum, which is split into two zones. The lower zone, UP1, accommodates sodium bonding relocation due to fuel swelling, while the second zone, UP2, is designed to host fission gases. The composition of the mediums employed is defined in the “materials creation” procedure.

Additionally, an axial mesh is defined as well. The distance between two consecutive points of the mesh must be chosen so that unphysical numerical error is not introduced from the flux solver employed. Throughout this work, the VARIANT module was utilized, which is a nodal diffusion solver. In order to mitigate unnecessary numerical error from VARIANT, the distance between two consecutive points of the axial mesh is set similar to a neutron mean free path within the core [13]. The default distance between two consecutive points of the axial mesh was assumed to be 15 cm.

For the hexagonal 3D geometry, the radial mesh is imposed by ERANOS

and corresponds to the assemblies themselves, so no fine subassembly radial mesh is input.

Within the core building procedure is the definition of a fuel batch, which identifies the fuel assemblies that comprise the first batch, the second batch, and so on.

While a typical fuel management scheme is comprised of three batches, fuel cycle performance for a three batch system can be assessed with a one-batch fuel management scheme [14]. As a result, a one-batch fuel management scheme has been utilized as the default fuel management scheme.

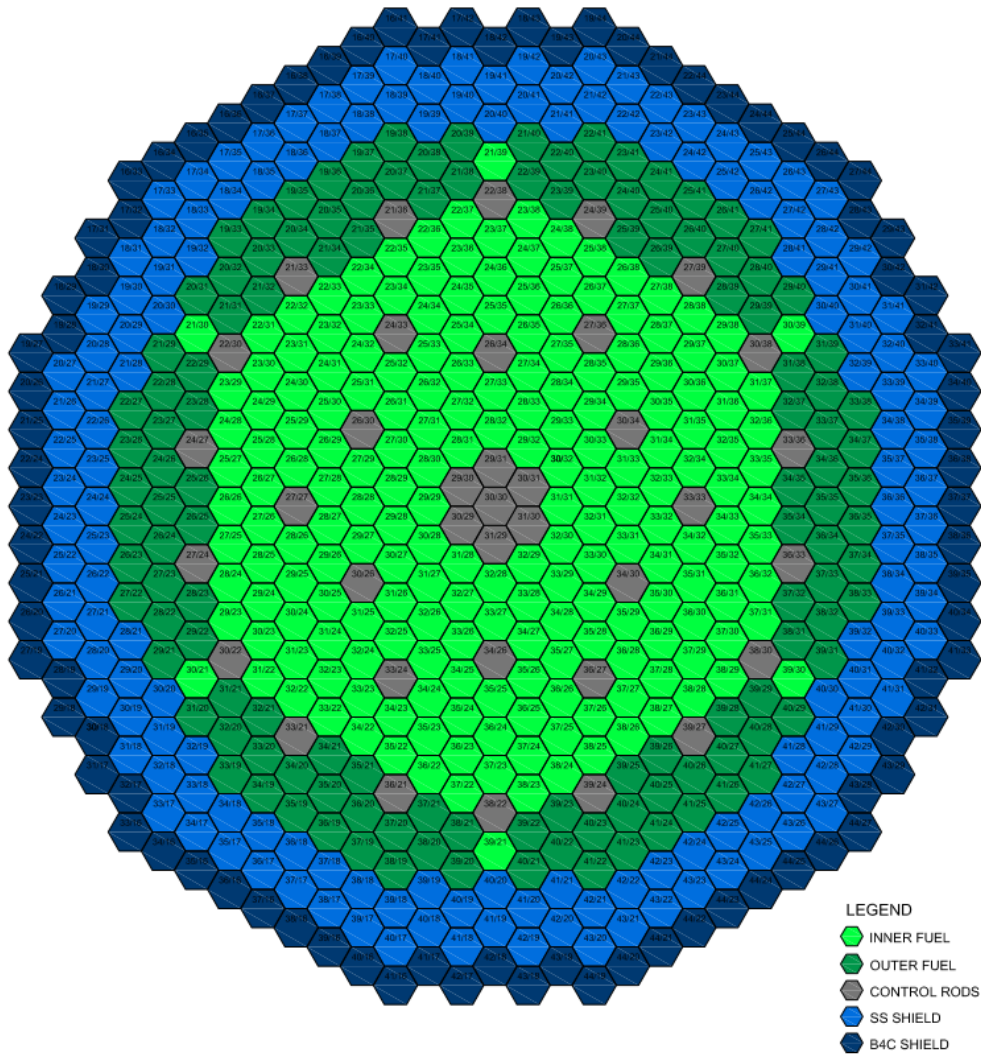


Figure 1.4: The ARR core radial view with the labels, given by ERANOS, of each assembly position.

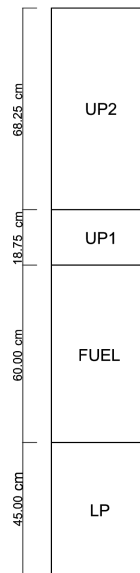


Figure 1.5: Axial representation of the model of the ARR fuel assembly as modeled within the “core building” procedure.

1.3.4 Burnup

ERANOS computes burn-up and decay over a time step t , from a starting nuclide concentration C_0 , using constant flux values within each mesh as determined from the VARIANT solution for the time step, and cross sections as shown in the following equations [13]

$$C(t) = \exp[\mathbf{M}t] C_0 \quad ,$$

where

$$\mathbf{M} = \Phi \mathbf{R} + \mathbf{D}$$

Φ is the scalar flux, \mathbf{R} is the microscopic cross sections matrix, and \mathbf{D} is the decay matrix. As a result, \mathbf{M} is like a flux-dependent decay constant. The evolution of the core material isotopic concentrations depend on the flux, and the flux depends on the isotopic concentrations of the nuclides. Keeping the flux constant for a time step is an approximation. The shorter the time step, the more accurate results, the longer simulation. Therefore, step length optimization is valuable to achieve accurate results in a reasonable time. For a one-batch fuel cycle, three steps of 1 Effective Full Power Year (EFPY) were chosen.

No short steps during beginning of cycle are necessary, contrary to typical LWR burnup calculations, since the build-up of fission products significantly affects the flux in the thermal spectrum energy range only. In the literature review, it was not found where a short step (or more) has been used. To further examine the assumption that no short time steps are required during the beginning of cycle, Figure 1.6 shows a burnup profile for a representative simulation. As can be seen from Figure 1.6, reactivity differences observed are insignificant for scoping calculations throughout the simulation, and a near linear behavior concerning k_{eff} versus Effective Full Power Days (EFPDs) is observed throughout the first 15 EFPDs.

One year time steps were chosen since in a three-batch fuel management scheme, a reactor would be refueled once a year. In addition, to calculate desired reactor performances characteristics, information is needed once a

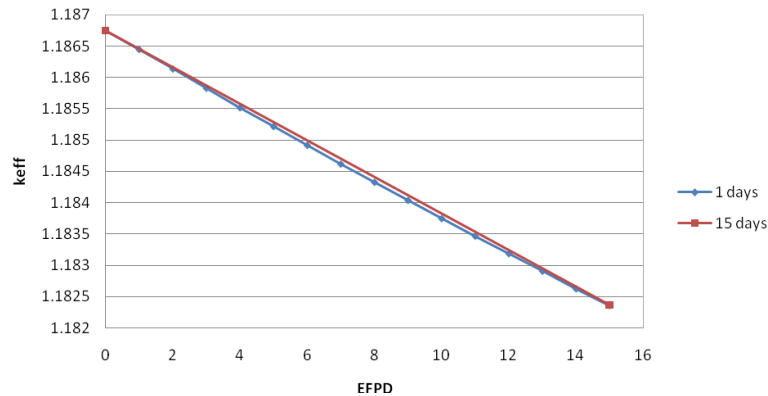


Figure 1.6: Comparison of calculated k_{eff} values using burnup steps of 1 day and 15 days at BOC for a representative simulation.

year to average over each batch. Three representative burnup calculations with different step lengths were performed to assess whether a step of 365 days is too long: one with steps of 100 days, one of 200, and of 500. A total of 1000 EFPDs were simulated.

Figure 1.7 shows k_{eff} for the three cases. As it can be seen, there is no significant difference between the three simulations. At the end of the calculation, the k_{eff} calculated using steps of 500 days, $k_{\text{eff}}|_{500}$, is 361 pcm higher than $k_{\text{eff}}|_{100}$ (0.35%). Recall that this procedure has been developed for *scoping* calculations for which differences of this magnitude are acceptable. Table 1.1 gives the masses of each element at the end of the calculations. The largest mass difference is for Pu, 11.60 kg (0.75%). Therefore, since both the k_{eff} and the composition don't significantly change as the step length is changed, steps of 365 days are acceptable.

1.3.5 Cooling

During cooling, the isotopes undergo decay, which is not driven by the flux. The cooling time depends on the type of reprocessing that must be performed. Throughout this thesis, pyroprocessing was the chosen default reprocessing technique to determine the cooling time, which requires at least

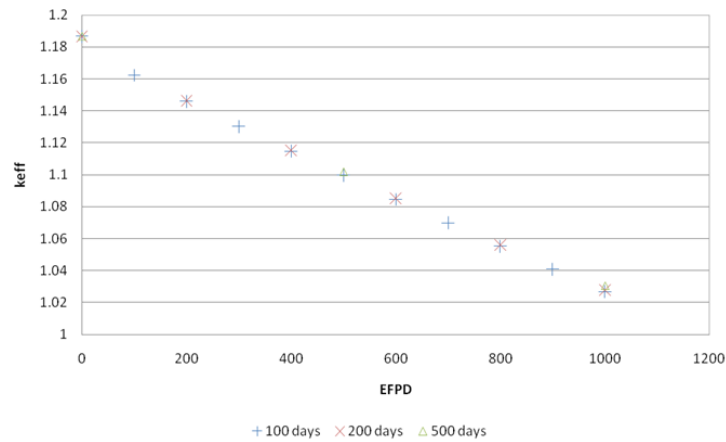


Figure 1.7: Comparison of calculated k_{eff} values using burnup steps of 100, 200, and 500 days.

1 year of cooling. Therefore, the cooling was performed simply as a burnup step of 1 year at a thermal power of 1 mW.

1.3.6 Reprocessing

Reprocessing is the key procedure on which the whole multi-cycle calculation relies. The aim of this procedure is to calculate the composition of the fuel required for the next cycle.

Two constraints are imposed on the fuel composition for the next cycle:

- The mass of heavy metal in the core is kept constant. This is an assumption, which means that fuel density does *not* change throughout the cycles. This should not happen in real fuels. However, from the simulations conducted in this thesis, the density that the fuel should have at BOC after 60 EFPYs, which has been calculated accordingly to the isotopic composition, differs from the fuel density at start-up of less than 2%, which is acceptable for scoping calculations.
- The reactivity of the core at the beginning of each cycle is kept constant.

Table 1.1: Element masses after 1000 EFPDs, using burnup steps of 100, and 500 days.

Element	Mass [kg]	Mass [kg]	Δm
	100 Days Steps	500 Days Steps	[kg]
Th	3.76E+3	3.77E+3	10.75
Pa	1.25E+1	1.17E+1	-0.76
U	1.93E+2	1.88E+2	-5.31
Np	6.36E+1	6.36E+1	0.00
Pu	1.27E+3	1.28E+3	12.51
Am	1.19E+2	1.20E+2	1.35
Cm	2.25E+1	2.19E+1	-0.57
Bk	1.58E-6	1.34E-6	0.00
Cf	7.08E-7	6.09E-7	0.00

Consequently, reactivity at the beginning of cycle is sufficient to yield a k_{eff} equal to 1.0 at the end of cycle.

Mass Constraint

The mass of external feed required can be calculated by a simple mass balance between the beginning of cycle (BOC) and fuel that has been irradiated and cooled. The feed F can be calculated as follows

$$F = \Delta M + M_{\text{fp}} + M_U - M_{\text{blanket}} \quad (1.1)$$

where

- ΔM is the difference between the mass at the beginning of cycle and the mass at the end of cooling. A portion of this ΔM is due to neutron losses and approximation in transmutation chains of heavy nuclides. Such chains are user defined and establish what a heavy nuclide does once a neutron is absorbed. For example, for the Cf-251 nuclide, the

user may want that when Cf-251 absorbs a neutron it becomes Cf-252. However, as an approximation, one may assume that once Cf-252 absorbs a neutron, it remains Cf-252, rather than became Cf-253, so the mass of a neutron disappears. In addition, also the fission reaction itself contributes to the mass “disappearing”, since energy is emitted. Nevertheless, the ΔM is just about several kilos (0.1% of the total feed required).

- M_{fp} is the mass of all fission products. In the present work, when fuel is reprocessed, the mass of all fission products is initialized to 1E-20 kg, since “0” is not recognized by ERANOS. In order to keep fuel mass constant for the next cycle, their mass must be accounted for.
- M_U is the mass of in-bred uranium which may be *extracted* in the Th/U-233 fuel cycle. In the Th fuel cycle, unlike the uranium based fuel cycle, in-bred uranium can be reloaded within the fuel for the next cycle, or sent to another reactor or a repository. If in-bred uranium is *not* reloaded, i.e. is extracted, its mass must be replaced with external feed. Otherwise, $M_U = 0$.
- $M_{blanket}$ is the mass of in-bred fissile material (uranium for Th-based, plutonium for U case) and TRUs from blankets, if any.

The feed F can be divided into two components: fertile and fissile feed

$$F = F_{fertile} + F_{fissile} \quad (1.2)$$

Fertile and fissile feed can be a set of isotopes with a specific isotopic composition. For the U/Pu fuel cycle, fertile feed is depleted uranium, while fissile feed is legacy TRU from spent LWR fuel with a burnup of 50 MWD/ton and cooled for 10 years. For the Th/U fuel cycle, fertile feed is thorium, and fissile is the legacy TRU.

Reactivity Constraint

From the mass constraint, the mass to top-up the fuel is known. However, the split between the mass of fertile and fissile is unknown.

The mass of fissile and fertile feed must assure sufficient reactivity for the irradiation period. An iterative solution to calculate the mass of fissile and fertile needed may be to guess the split between the fertile and fissile mass. Using this feed guess, the next cycle flux calculation can be performed, and if the reactivity is adequate, the result is accepted. If the reactivity is too low or too high, the split between fertile and fissile is adjusted accordingly and another iteration is performed. As an alternative to this iterative procedure, the reactivity can be *estimated* through the concept of *equivalent mass*.

Ideally, if the fuel were made with *only one* isotope, for example Pu-239, the reactivity would be directly proportional to plutonium mass. Thus the mass of Pu-239 can be used as a measure of the reactivity. The more mass, the higher the reactivity. So, if the actual fuel were changed into an *equivalent* fuel formed only by one isotope with an equivalent mass, reactivity could be addressed. Such an approach does not require any iterations.

To determine an equivalent mass, the fuel can be approximated as equivalent fuel formed only by one fissile isotope. Let the total mass of an isotope i be m_i , its equivalent mass m_i^e is then given by

$$m_i^e = c_i m_i \quad (1.3)$$

where c_i is a coefficient. ERANOS calculates these coefficients as

$$c_i = \frac{\sigma_i^+ - \sigma_{\text{fertile}}^+}{\sigma_{\text{fissile}}^+ - \sigma_{\text{fertile}}^+} \quad (1.4)$$

where

$$\sigma^+ = \nu\sigma_f - \sigma_a$$

Subscripts *fertile* and *fissile* stand for a fertile and fissile isotope of reference. For U-based fuel, they are ^{238}U and ^{239}Pu respectively; for Th-based fuel, ^{232}Th and ^{233}U respectively. Equation (1.4) implies that

$$c_{\text{fertile}} = 0 \quad , \quad c_{\text{fissile}} = 1 \quad (1.5)$$

From equation (1.3) and (1.5), the equivalent mass of the fertile feed M_e^{fertile} is

$$M_e^{\text{fertile}} = 0$$

The fact that the equivalent mass of the fertile feed is 0 makes any iterations, to determine the feed split between fertile and fissile, *unnecessary* since the equivalent mass the new fuel should have, which is the goal, can be changed *only* by adding fissile. Note that in reality is not true, however this is an estimation.

The fuel can consist of many isotopes, each one with a mass different from other isotopes. Let $\{C\}$ be the composition of the fuel. The equivalent mass M_e of a fuel with composition $\{C\}$ is given by

$$M_e = \sum_{i \in \{C\}} c_i m_i$$

Let M_e^* be the equivalent mass that the new fuel should have. Defining M_e^{cool} as the equivalent mass of cooled fuel, the feed of equivalent mass, which is given only by the fissile feed, M_e^{fissile} is calculated as

$$M_e^{\text{fissile}} = M_e^* - M_e^{\text{cool}} + M_e^U - M_e^{\text{blanket}} \quad (1.6)$$

where

- M_e^U is the equivalent mass of uranium *extracted* in the Th/U fuel cycle.
- M_e^{blanket} is the equivalent mass coming from blankets (if any).

In the equation (1.6), there are two unknowns: M_e^* and M_e^{fissile} . As already pointed out, M_e^* is the equivalent mass which the fuel for the next cycle should have. M_e^{fissile} is the equivalent mass of fissile feed which has to be added to make the new fuel have the desired M_e^* . The equivalent mass M_e^* is not known *a priori* so it must be guessed. A first guess might be the equivalent mass at start-up. The value of M_e^* is input by the user, which is then unchanged throughout all cycles. The reactivity swing does not change significantly throughout the cycles, so a unique value for the M_e^* is acceptable.

Let M_e^{fissile} be measured in “equivalent kilograms” $[\text{kg}|_e]$, which must be converted into real kilograms. Thus, the next step is calculating the equivalent mass of a unit of mass, 1 kg, of the fissile feed.

$$W_{\text{fissile}} = \sum_{i \in \text{fissile}} c_i w_i \quad , \quad [W_{\text{fissile}}] = \frac{\text{kg}|_e}{\text{kg}}$$

where w_i is the weight percent of isotope i in the fissile feed composition.

Finally, fissile and fertile feed can be calculated as follows

$$F_{\text{fissile}} = \frac{M_e^{\text{fissile}}}{W_{\text{fissile}}} \quad , \quad F_{\text{fertile}} = F - F_{\text{fissile}} \quad (1.7)$$

F_{fissile} can be positive, null or negative, based on the kind of reactor, as follows:

$F_{\text{fissile}} > 0$: Burners – external fissile feed is needed to continue the cycle.

$F_{\text{fissile}} = 0$: Isobreeders – only fertile feed is needed since in-bred fissile is just sufficient.

$F_{\text{fissile}} < 0$: Breeders – in-bred fissile is in excess.

Before the simulation reaches equilibrium, all of the three cases may occur despite the final result. For example, if the initial fissile material content is very high, during the reprocessing procedure, there is too much fissile material in the cooled fuel, so the third case will occur even if the reactor is a burner. Conversely, if the initial fissile material content is low, F_{fissile} might be higher than F . In that case the procedure implemented imposes $F_{\text{fissile}} = F$. These behaviors take place when poor initial guesses are made in estimation of the initial fissile content. Note that, the F_{fissile} is calculated from the input M_e^* , which is a user defined input. If the M_e^* is too small, for the procedure is as it there were too much fissile in the fuel. On the other hand, if the input M_e^* is too large, for the procedure is as it there were a low concentration of fissile.

For a better understanding, two examples are given. One which the TRU enrichment at start-up is higher than required, i.e. k_{eff} at EOC will be much greater than 1, and one with the TRU enrichment at start-up lower than needed. The reactor simulated was the ARR fueled with Th-TRU-Zr metallic fuel, and in-bred uranium was not reloaded.

First, the trend of k_{eff} vs EFPDs is shown in Figure 1.8. At the beginning of reactor life $k_{\text{eff}} = 1.184$, and at the end of the first cycle $k_{\text{eff}} = 1.043$. Additionally, Figure 1.9 shows the composition change throughout cycles: (a) shows the plutonium content vs cycles, (a) the external feed supply, and (c) the core inventory at BOC – uranium is not present since it is not reloaded. As can be seen in Figure (a), at the first cycle there is a large content of Pu-239, and the plutonium vector is not degraded yet. During reprocessing, since TRU content is high, the equivalent mass is high as well. Therefore, as shown in Figure (b), the TRU feed is low, which has a positive equivalent mass. A significant amount of thorium is added, in order to keep the mass constant (mass constraint), which counterbalances the mass of all fission products, see Figure (b) cycle 1. Thus, the second cycle starts with a lower plutonium content (Figure (a) cycle 2), and with a higher content of Th, as shown in Figure (c) cycle 2. As a result, at EOC $k_{\text{eff}} = 0.958$. Reactivity at BOC, then needs to be increased, since it was not sufficient to lead the k_{eff} to be 1 at EOC. However, the feed mass that can be added for each cycle is limited, due to the mass constraint, so, for several cycles feed will be only TRU and no more fertile feed is added during that time, as shown in Figure (b). A better reloading scheme might extract some Th and replace it with TRU.

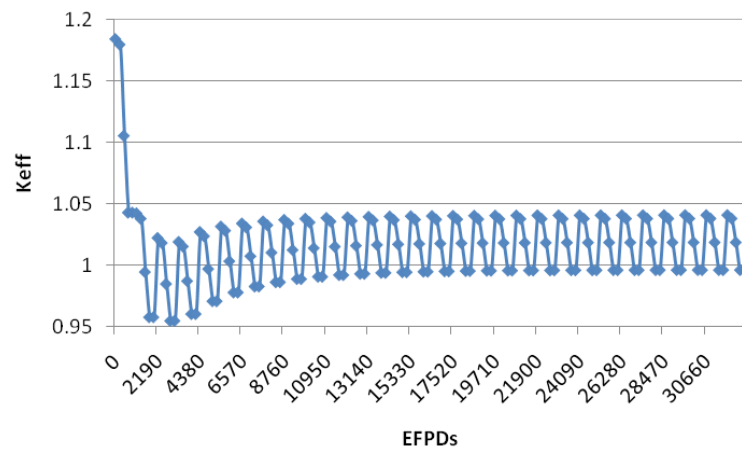
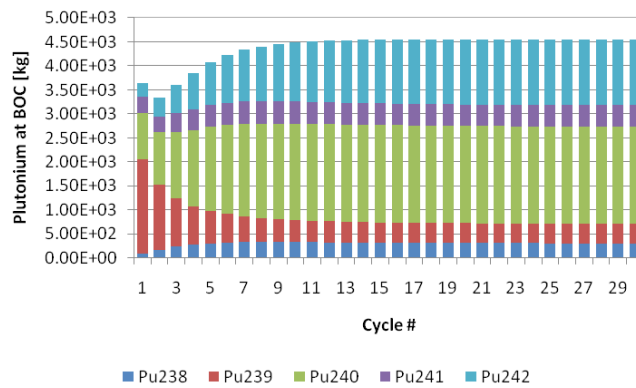
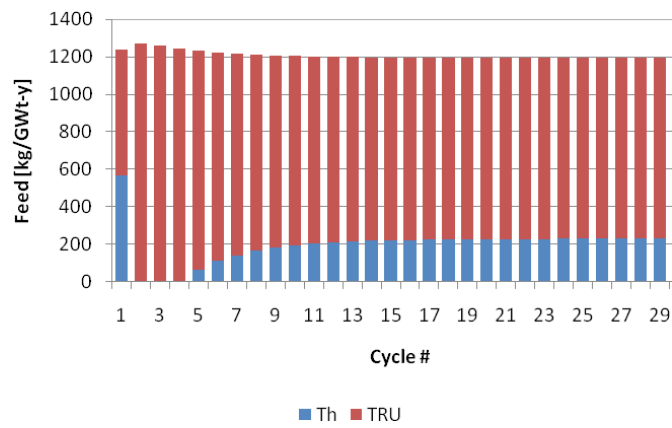


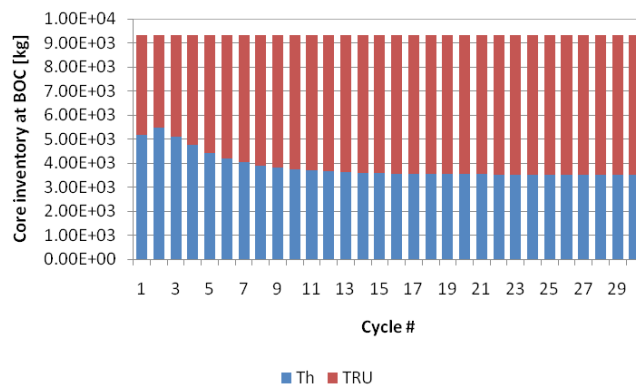
Figure 1.8: Trend of k_{eff} for a reactor where TRU enrichment at start-up is too high.



(a) Plutonium content at BOC.



(b) External feed.



(c) Core inventory at BOC.

Figure 1.9: Plutonium content at BOC (a), external feed (b), and the core inventory at BOC (c) for the ARR with a TRU content at stat-up too high.

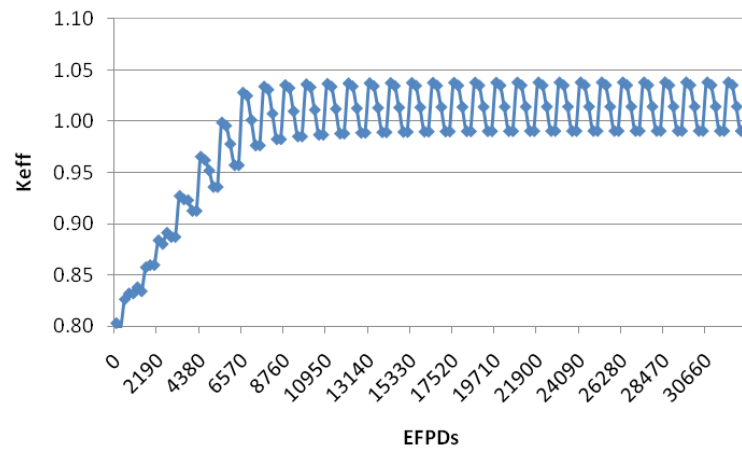
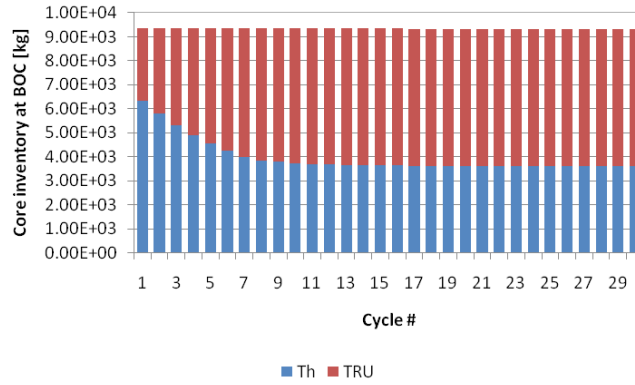
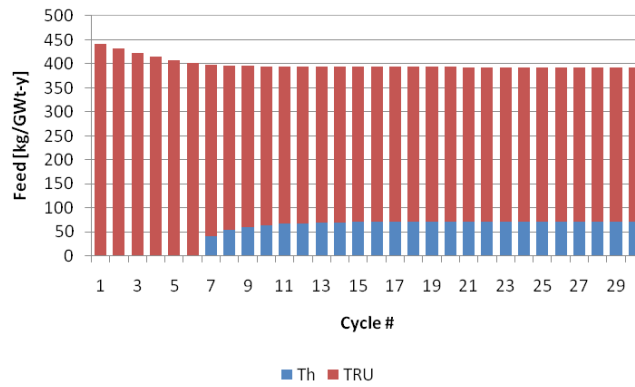


Figure 1.10: Trend of k_{eff} for a reactor where TRU enrichment at start-up is too low.

Next, Figure 1.10 shows the k_{eff} when the initial TRU content is too low. At start-up, $k_{\text{eff}} = 0.803$. The increasing trend of k_{eff} during first cycles is due to the large breeding of ^{233}U fostered by the high content of Th, as shown in Figure 1.11 (a) cycle 1. Then, once there is a lower amount of Th there is no more breeding. As can be seen in Figure 1.11 (b), from the first cycle feed is made up only by fissile because of mass constraint. The trend of TRU inventory is similar to the above case from the second cycle.



(a) Core inventory at BOC.



(b) External feed.

Figure 1.11: Core inventory at BOC (a), and the external feed supply (b), for the ARR with a TRU content at start-up too high.

Chapter 2

Thorium Fuel Cycle Performance in the Advanced Recycling Reactor

The goal of this chapter is to assess the performance of thorium fuel cycle in a fast neutron flux environment. In particular, the focus is on the analysis of the legacy TRU burning potential of thorium. The Advanced Recycling Reactor (ARR) [8], a Toshiba-Westinghouse design sodium cooled fast reactor, has been employed for the purpose. The chapter is organized as follows:

- Section 2.1 describes core design and model employed;
- Sections 2.2 and 2.3 present the results. Specifically:
 - Section 2.2 compares the result of Th-based versus U-based fuel, to show the main differences in the TRU burning potential of the two cycles. Metallic fuel has been assumed as the fuel form for this comparison. In the Th case, two management techniques are compared for the in-bred uranium, which is either recycled back into the core, or it is sent (or stored) to another reactor (or

repository) . Simulations cover the period from start-up core to 60 Effective Full Power Years (EFPYs) of irradiation.

- Section 2.3 is focused on Th-based fuel cycles only, and compares results referred to metallic, nitride (both with natural nitrogen and nitrogen enriched with 95 atom percent of N-15, to reduce formation of C-14), and oxide fuels. In all cases, in-bred uranium is not recycled. Metallic fuel has been studied because it yields the fastest spectrum, which enhances actinide transmutation, and because it is the reference fuel for the ARR core. Nitride fuel fosters an increased HM inventory due to the higher density, improving breeding capabilities and helping to overcome the smaller density of Th compared to U; in addition, nitrides have been recognized as advanced fast reactor fuels also for their high thermal conductivity and excellent compatibility with sodium coolant [15]. Finally, oxide fuels have been studied based on the vast knowledge available from their extensive usage throughout the history of nuclear power.
- Section 2.4 presents a summary of the results and some recommendation for future works.

The results obtained will be the basis for the development of an improved fast reactor design, optimized for TRU burning as well as U-233 generation, presented in Chapter3.

The TRU external feed assumed for all the simulations is 10-yr cooled, reprocessed LWR UO₂ , discharged at 50 GWd/tHM burnup and with initial U-235 enrichment of 4.2% in weight. Its composition is given in Table 2.1.

2.1 ARR Core Design and Employed Model

The core design chosen for this set of studies is based on the Toshiba-Westinghouse Advanced Recycling Reactor (ARR), which is a sodium-cooled

Table 2.1: Legacy TRU composition assumed for the simulations, in weight % (10-yr cooled, reprocessed LWR, UO₂ fuel with 4.2 U-235 w/o and 50 GWd/tHM discharge burnup).

Np-237	4.72	Am-241	5.61
Pu-238	2.17	Am-242m	0.01
Pu-239	47.38	Am-243	1.55
Pu-240	22.80	Cm-243	0.00
Pu-241	8.41	Cm-244	0.45
Pu-242	6.83	Cm-245	0.04
Pu-244	0.00	Cm-246	0.00

Table 2.2: Main design parameters of the ARR.

Core thermal power	1000 MWth
Coolant	Na
Number of inner/outer assemblies	198/126
Number of stainless steel shield assemblies	150
Number of B ₄ C shield assemblies	84
Number of primary control assemblies	24
number of secondary shutdown assemblies	6
number of assembly locations for tertiary shutdown system	7
number of batches	3
Refueling interval	1 year
Coolant inlet/outlet T	395/550 °C

fast reactor.

A summary of the main design parameters is given in Table 2.2.

Figure 2.1 shows the core cross section. As it can be seen, the core is composed of an inner and an outer region, surrounded by two rings of stainless steel (SS) shield assemblies and an outer ring of B₄C shield assemblies. While the SS assemblies act both as reflector and shield, the B₄C assemblies

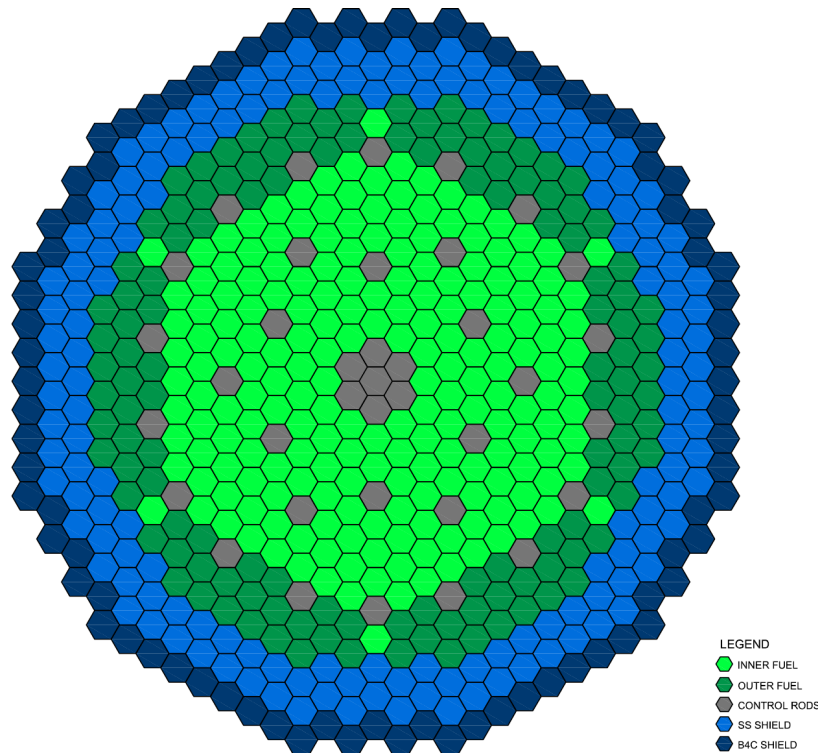


Figure 2.1: ARR core cross section.

are used to reduce the fast fluence on the vessel wall. Control rods are divided into three sets, each independent and different from the other sets in order to ensure reliability of the shutdown system.

Table 2.3 gives the main parameters of the fuel assembly, while Figure 2.2 shows the axial representation of the model of the fuel assembly. From bottom to top, there is the lower plenum, the fuel, and the upper plenum, which is split into two zones. The lower zone, UP1, accommodates sodium bonding relocation due to fuel swelling, while the second zone, UP2, is designed to host fission gases.

2.2 Thorium versus Uranium Fuel Cycles

The performance of the Th versus U fuel cycles have been investigated with core physics simulations of the ARR using either Th or U metallic fuel

Table 2.3: Main parameters of the ARR fuel assembly.

Assembly type	Hexagonal with duct
Clad/Duct material	HT-9
Pin Lattice	Triangular
Pin pitch	7.41 mm
Pins per assembly	271
Pellet diameter	4.71 mm
Clad inner diameter	5.44 mm
Clad outer diameter	6.50 mm
Fuel/Coolant/Structure vol %	41.1/32.7/26.2

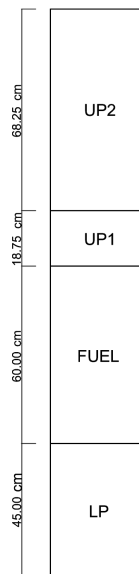


Figure 2.2: Axial representation of the model of the ARR fuel assembly.

containing TRUs. For Th, the in-bred uranium is managed in two alternative ways: it is either recycled, together with the other actinides, into the next batch of fuel or it is separated out and sent to storage.

The main design assumptions for the various cases analyzed are provided in Table 2.4. The differences between fuels reflect the difference of density

Table 2.4: Main design assumptions for the various cases analyzed.

Fuel Constituents	Th-TRU-Zr	Th-U-TRU-Zr	U-TRU-Zr
Fuel Form	Metal	Metal	Metal
Smear density, %	75	75	75
Fuel density [g/cm ³]	12.01	12.01	15.85
Zr content in fuel (w/o)	10	10	10
Actinide Recycle	All but U	All	All
Make-Up Fertile/Fissile	Th/TRU	Th/TRU	U/TRU
Composition of external TRU feed	Table 2.1	Table 2.1	Table 2.1
HM loading [kg/GWt]	10,000	10,000	13,100

of Th versus U metal, i.e. 11.5 versus 19.07 g/cm³, whereas smear density and Zr content are the same in all the cases analyzed. As a consequence, the heavy metal (HM) content is $\sim 30\%$ lower in the Th case, i.e. 10 versus 13.1 MT/GWt. The two Th-based fuels have the same density since at start-up there is no U-233, so the composition is the same. Throughout the cycles, due to the “mass constraint” imposed by the developed procedure (see Section 1.3 for details), the fuel density is kept constant. Such approximation was found acceptable for scoping calculations.

The main characteristics of the three fuels are further discussed in the following Sections. Specifically, the flux spectral behavior, TRU content, TRU and transmutation performance are analyzed.

2.2.1 Neutron Spectrum

Fine energy group neutron spectra have been calculated using the ECCO cell code with the 1968 energy-group library. A 2D heterogeneous fuel assembly model with fuel compositions at BOC representative of the respective cores at 60 EFPYs of depletion has been employed.

Different fuel compositions lead to different flux spectra, as shown in Figure 2.3. Thorium fuels yield a harder spectrum than U fuel due to

their higher relative TRU content which, as shown later in Section 2.2.2, is 28.90% (41.50%) for the case of recycled (not-recycled) in-bred uranium, versus 24.10% for the U fuel.

Among Th fuels, that containing the in-bred recycled U yields the hardest spectrum. A possible explanation for that, may be found in the lower scattering cross section featured by the U element versus Pu. Figure 2.4 compares the one-group macroscopic cross sections of U and Pu, for the case where in-bred U is reinserted in the fuel. As it can be seen, in-bred U has a lower scattering cross section than Pu. Figure 2.5 shows the one-group macroscopic cross section for Pu, at BOC after 60 EFPYs, for the two Th-based fuels. As it can be seen, the one-group macroscopic scattering cross section of Pu in the fuel without the recycled in-bred uranium, is almost two times the scattering cross section of Pu in the fuel with the recycled U. Notably, the sum of the one-group macroscopic scattering cross section of U and Pu is lower than the one-group macroscopic scattering cross section of Pu for the case without the in-bred U. In addition, U-233 features a harder fission spectrum than Pu-239. Figure 2.6 shows the percent contribution of the main nuclides to total fission for the Th and U fuels. For the U reinserted case, the contribution by U-233, which has a harder fission spectrum emission, is ~ 1.5 higher than that of Pu-239.

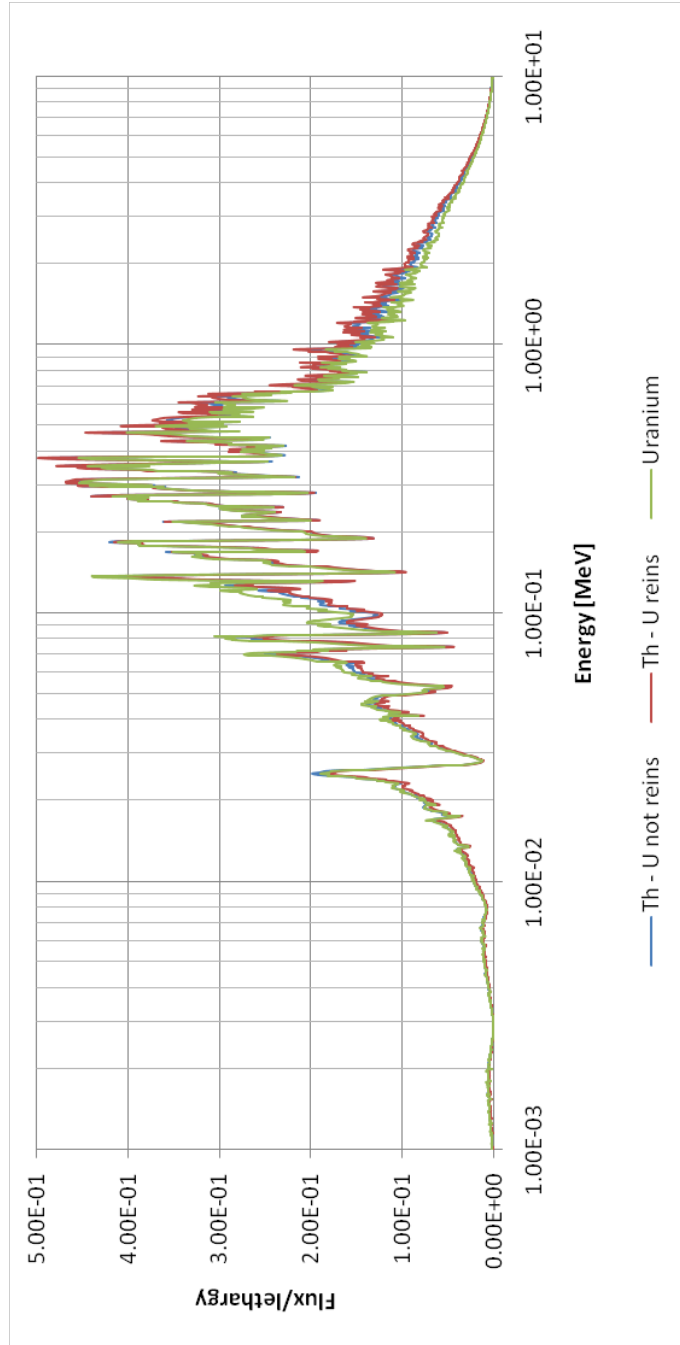


Figure 2.3: Neutron flux per unit lethargy versus energy for the three cases analyzed.

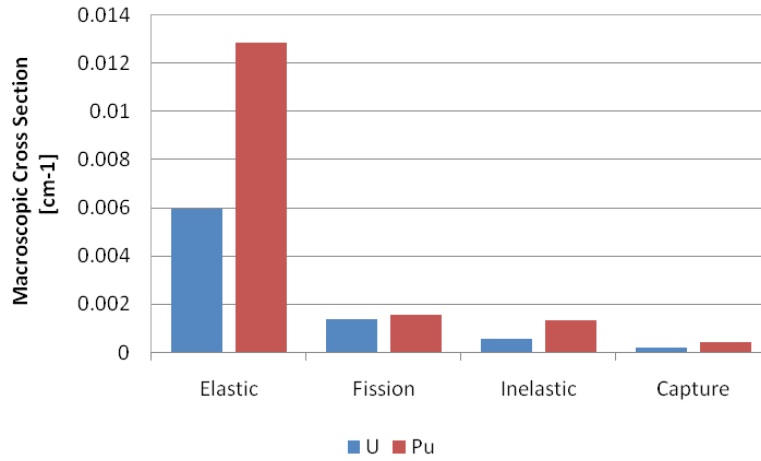


Figure 2.4: One-group macroscopic cross sections of U and Pu at BOC, after 60 EFYs, for the Th-based fuel containing the recycled in-bred U.

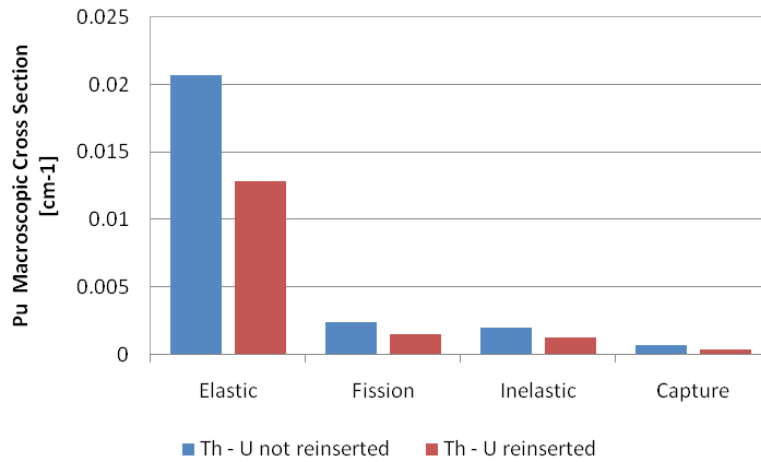


Figure 2.5: One-group macroscopic cross sections of Pu at BOC, after 60 EFYs, for the two Th-based fuels.

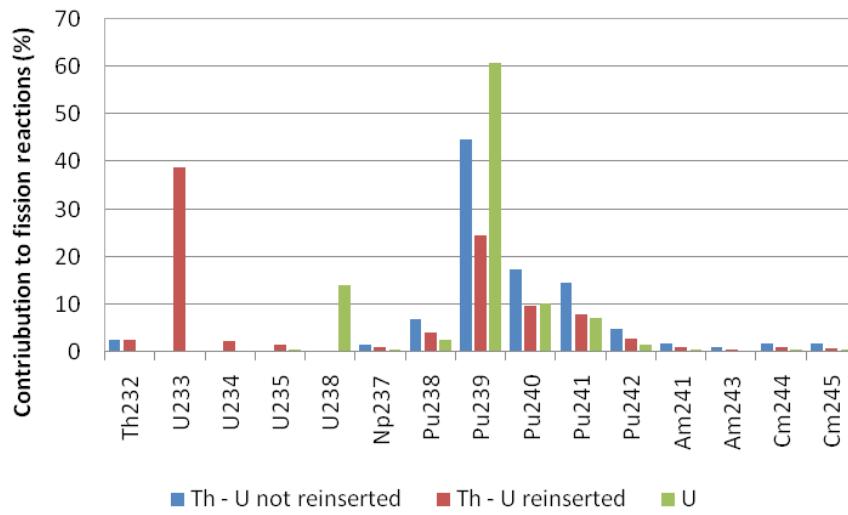


Figure 2.6: Percent contribution to total fission (BOC at 60 EFPYs of irradiation).

Table 2.5: TRU content for the fuels analyzed.

Fuel Constituents	Th-TRU-Zr	Th-U-TRU-Zr	U-TRU-Zr
BOC TRU start-up [kg/GWt]	3,580	3,580	3,161
(% of HM)	35.8	35.8	24.1
BOC TRU 60 EFPY [kg/GWt]	4,147	2,895	3,155
(% of HM)	41.5	28.9	24.1

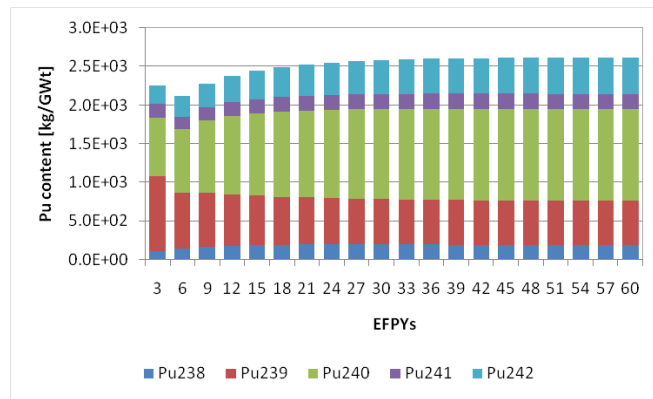
2.2.2 TRU Concentration

As shown in Table 2.5, U-based design requires a lower TRU concentration due to the better neutron economy of U-based versus Th-based fuel. The main reasons for this are:

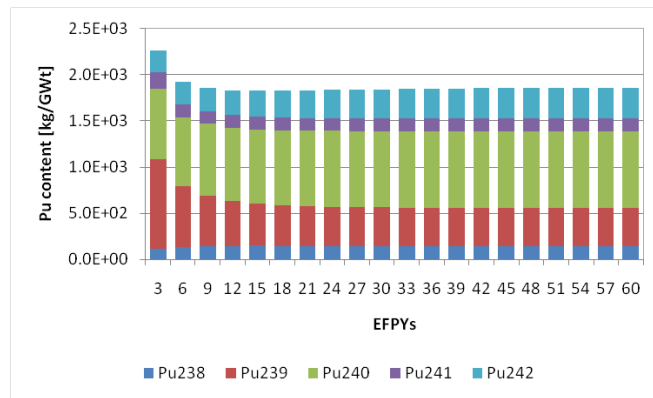
- Larger contribution to fission of U-238 versus Th-232. Uranium has a microscopic fission cross section that is 3.4 times that of thorium; in addition, U-based fuel is more dense. Thus, as can be seen from Figure 2.6, U-238 contributes for about 15% of the total fissions versus 2% for Th.
- Higher number of fission neutrons per absorption in the respective main fissile isotopes, i.e. 2.44 for Pu-239 vs 2.23 of U-233.
- More efficient breeding mechanism in U versus Th because of fewer parasitic absorption in Np-239 versus Pa-233. This is because, in spite of the lower microscopic capture cross section of the protoactinium isotope, 0.52 barn, than the neptunium isotope, 1.07 barn, Np-239 has a shorter half-life than Pa-233, i.e. 2.36 versus 27 days.
- Reduced leakage in U due to larger HM content and neutron scattering compared to Th.

Figure 2.7 shows the plutonium content at EOC throughout the cycles for the three cases studied. For Th-based fuels the Pu-239 content is typically

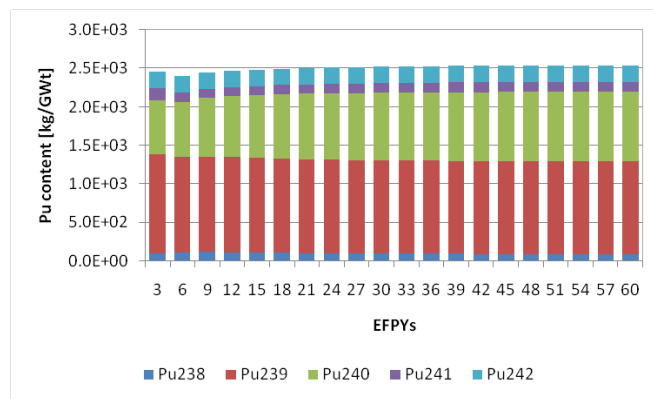
smaller than for U-based fuel, since for the latter its consumption is counterbalanced by the Pu-239 breeding. This is reflected in the small change in TRU concentration from start up to 60 EFPYs of depletion for the U case. On the other hand, Th-based fuel where the in-bred uranium is not recycled requires the highest TRU enrichment and shows the largest variation in TRU content from start-up to 60 EFPYs. When the in-bred uranium is recycled, its contribution lowers the TRU requirement and leads to its decreasing concentration from start-up to equilibrium.



(a) Th-based, uranium not recycled.



(b) Th-based, uranium recycled.



(c) U-based.

Figure 2.7: Plutonium content at EOC for Th-based fuel where in-bred uranium is not recycled (a), Th-based fuel where in-bred uranium is recycled (b), and U-based fuel (c).

Table 2.6: TRU transmutation performance for the fuels analyzed.

Fuel Constituents	Th-TRU-Zr	Th-U-TRU-Zr	U-TRU-Zr
TRU [kg/GWt-yr]	318.9	214.5	110.9
U bred [kg/GWt-yr]	114.2	-	-
% TRU burned	23.1	22.2	10.6
% Pu-239 burned	44.5	42.0	11.8

2.2.3 TRU Transmutation Performance

As shown in Table 2.6, Th-based fuels can burn up to three times more TRU legacy than U-based fuel, under the configuration analyzed here. This stems from the much lower generation of TRU in Th versus U, due to the “lower” position of Th-232, which requires multiple neutron captures to “progress” to TRUs. In terms of relative TRU consumption, the Th case with in-bred uranium not recycled within the fuel yields the highest relative TRU consumption rate, i.e. 23.1%. Then the Th fuel with the in-bred uranium recycled follows, 22.2%. U fuel comes last, featuring a relative TRU consumption of 10.6%.

The mass difference between EOC and BOC for each element, averaged over 60 EFPYs, is presented in Table 2.7 and graphically shown in Figure 2.8. In all cases, plutonium incineration drives the TRU consumption rates, with a mass of about 88% of the total legacy TRU.

As shown in Table 2.7, Cm is the first transuranic element which actually builds-up during the irradiation, instead of being destroyed. This is because the transmutation of one isotope may occur either via fission reaction, leading to destruction, or via neutron capture, leading to accumulation. Figure 2.9 shows the ratio α between the one-group capture and fission microscopic cross sections of the Am and Cm isotopes. If α is higher than 1 the neutron capture reaction is more likely to occur than the fission reaction. The different spectrum hardness characterizing the three fuels yields different α values. The harder the spectrum, the lower the α is. As shown in

Table 2.7: Mass difference between EOC and BOC, averaged over 60 EFYs [kg/GWt-yr]. Positive values imply accumulation, negative values imply consumption.

Fuel Constituents	Th-TRU-Zr	Th-U-TRU-Zr	U-TRU-Zr
Th	-1.71E+02	-1.70E+02	-
Pa	6.16E+00	6.29E+00	-
U	1.14E+02	1.40E+01	-2.70E+02
Np	-1.73E+01	-1.21E+01	-6.90E+00
Pu	-2.98E+02	-2.09E+02	-1.02E+02
Am	-2.49E+01	-1.73E+01	-1.13E+01
Cm	5.24E+00	3.87E+00	2.97E+00
Bk	1.91E-03	1.20E-03	1.24E-03
Cf	1.62E-04	9.04E-05	3.47E-05

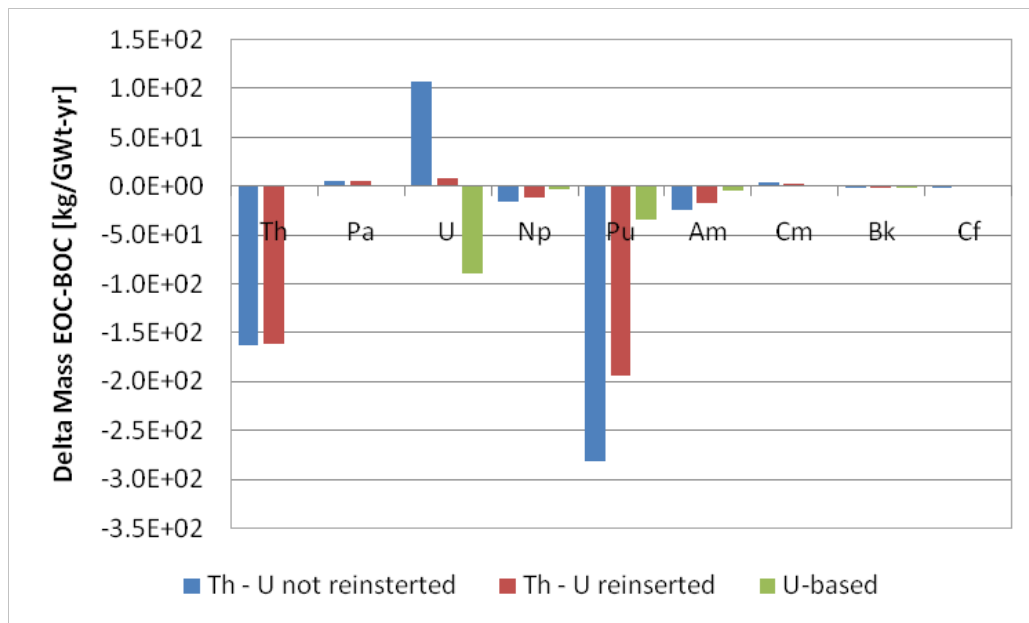


Figure 2.8: Average mass difference (EOC-BOC) for ARR design. Positive values imply accumulation, negative values imply consumption.

Figure 2.9, for Am-241 and Am-243 α is greater than 1, i.e., 3.31 and 3.78 respectively. When the Am-241 isotope captures a neutron either the Am-242 or the metastable Am-242m isotope is formed, which decay to Cm-242 with half-lives of ~ 16 hours and ~ 26 min respectively. Similarly, when the Am-243 isotope captures a neutron either the Am-244 or the metastable Am-244m isotope is formed, which decay to Cm-244 with half-lives of ~ 10 hours and ~ 26 min respectively.

In addition, Figure 2.10 shows the one-group macroscopic absorption cross sections of the Am and Cm isotopes. It can be seen that macroscopic absorption cross sections of Am isotopes is higher than that of Cm isotopes. This means that more neutrons are absorbed by Am than by Cm. As a result, Cm builds-up via neutron capture reactions, and following decays, of Am isotopes. The values of the absorption cross sections of Am for the three different fuels, i.e., the highest for Th-based fuel without the in-bred U recycled, then Th-based fuel with the in-bred U, and last the U-based fuel, explain the different transmutation rate of Am by the three fuels, as shown in Table 2.7.

Higher actinides such as Bk and Cf are generated via neutron capture by Cm-248 and following decay. However, as shown in Figure 2.10, the macroscopic cross section of Cm-248 is very low, yielding a slow build-up of these actinides.

2.3 Metallic, nitride, and Oxide Th-based fuels

From the previous Section, it was concluded that Th fuels can burn up to 3 times more TRU legacy than U fuel. If the aim is to burn this legacy, as it is in the Westinghouse's approach, Th-based fuels are preferable over U-based fuels.

To explore the effect of the Th-based fuel form on the TRU destruction performance, as well as the breeding potential, four types of Th-based fuels

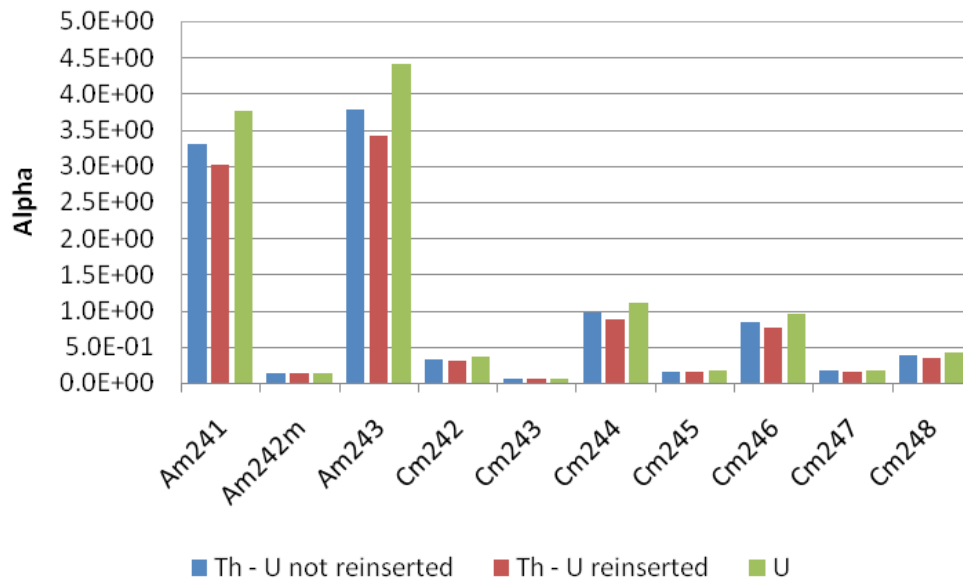


Figure 2.9: α ratio between capture and fission microscopic cross sections, for Am and Cm isotopes.

are analyzed: metallic, nitride (with natural nitrogen as well as 95 atom percent enriched in N-15), and oxide. For this study, the default actinide recycle scheme assumed is to recycle all actinides except in-bred U, since if in-bred uranium is not reinserted within the fuel after the separation, the TRU destruction rate is the highest.

The main design assumptions for the various fuels analyzed are provided in Table 2.8. A smeared density of 85% has been employed for the oxide and nitride fuels, higher than for the metallic fuel, crediting their reduced swelling rate. The higher smeared density and fuel density of nitride fuels yield the largest HM inventory among the options analyzed.

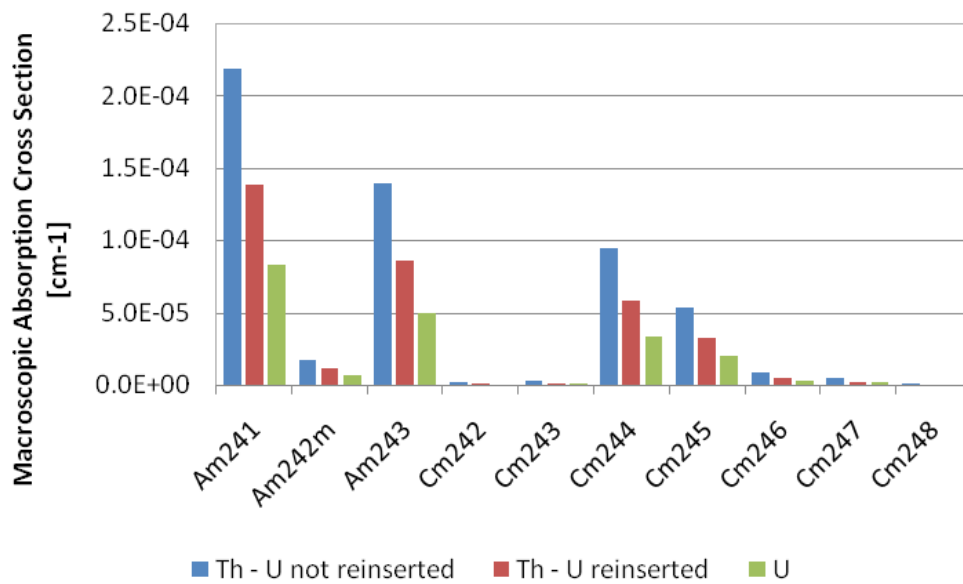


Figure 2.10: One-group macroscopic absorption cross sections of the Am and Cm isotopes at BOC, at equilibrium.

Table 2.8: Main design assumptions for the various fuels analyzed.

Fuel Constituents	Th-TRU-Zr	Th-TRU-14N	Th-TRU-15N	Th-TRU-O2
Fuel Form	Metal	Nitride	Nitride	Oxide
Smear density, %	75	85	85	85
Fuel density [g/cm ³]	12.01	12.53	12.62	10.42
Actinide Recycle	All but U	All but U	All but U	All but U
Make-Up Fertile/Fissile	Th/TRU	Th/TRU	Th/TRU	Th/TRU
Composition of external TRU feed	Table 2.1	Table 2.1	Table 2.1	Table 2.1
HM loading [kg/GWt]	10,000	12,360	12,380	9,490

The four fuel types have been compared on the basis of their neutron spectrum (Section 2.3.1), TRU concentration (Section 2.3.3), TRU transmutation and breeding capabilities (Section 2.3.2), and neutron economy (Section 2.3.4)

2.3.1 Neutron Spectrum

Fine energy group neutron spectra have been calculated using the ECCO cell code with the 1968 energy-group library. A 2D heterogeneous fuel assembly model with fuel compositions at BOC representative of the respective cores at 60 EFPYs of depletion has been employed.

As shown in Figure 2.11, the hardest spectrum pertains to the metallic fuel, due to the reduced neutron moderation of Zr with respect to N (intermediate spectrum) and O (softest spectrum). Figure 2.12, showing the one-group macroscopic scattering cross section for the four fuels binding elements (Zr, N-14, N-15, and O), supports the above consideration.

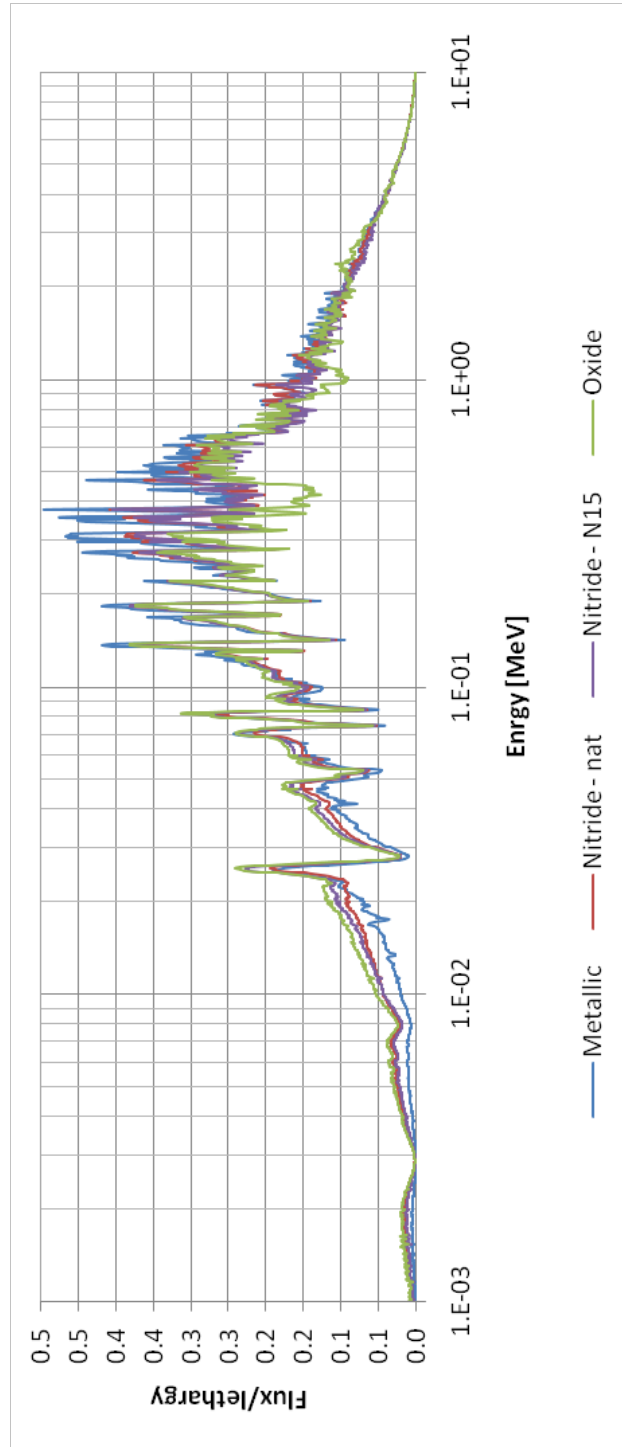


Figure 2.11: Neutron flux per unit lethargy vs energy for metallic, nitride, and oxide fuels.

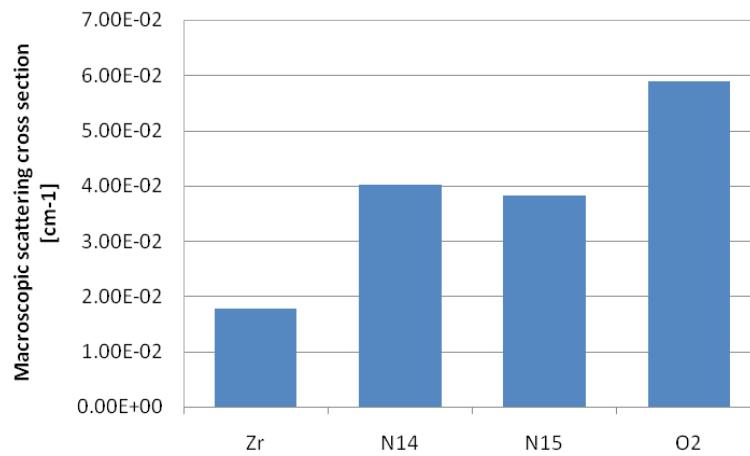


Figure 2.12: One-group macroscopic scattering cross sections for the binding elements of the fuels analyzed.

2.3.2 TRU Transmutation Rate and Breeding Capabilities

Table 2.9 shows TRU transmutation rate and breeding potential for the fuel analyzed. It can be seen that:

- The TRU transmutation performance is similar among the fuels analyzed and proportional to the TRU concentration.
- Breeding potential of nitride fuels is much larger than for metallic and oxide fuels, which are similar to each other. This is related to the Th content in the core, which is responsible for the generation of in-bred uranium. The larger the Th content, the larger the mass of in-bred U. Therefore, nitride fuels yield the highest amount of in-bred uranium. As a result of the large mass of in-bred U, the reactivity swing for the ThN fuels is the lowest.

Table 2.9: TRU transmutation rate and breeding potential for the fuels analyzed.

Fuel Constituents	Th-TRU-Zr	Th-TRU-14N	Th-TRU-15N	Th-TRU-O2
TRU consumption rate [kg/GWt-yr]	-318.9	-317.1	-313.6	-321.8
% TRU burned	23.1	20.3	20.8	21.9
% Pu239 burned	44.5	40.4	41.6	43.7
U bred [kg/GWt-yr]	114.2	142.0	149.7	112.9
BOC Th averaged [kg/GWt]	6020	7800	7950	5190
Burnup reactivity loss, %delta k	3.44	1.93	1.62	3.14

2.3.3 TRU Concentration

Table 2.10 shows composition-related results for the Th-based fuels considered, at BOC of both start-up and 60 EFPYs. The following considerations can be made:

- Even though metallic and oxide fuels have similar HM inventories, metallic fuel has a lower TRU concentration, both at start-up and at 60 EFPYs. This results from the better neutron economy of metal fuel versus oxide fuel, which makes criticality achievable with less fissile material. In addition, the slightly higher Th content in metal yields to a bit more in-bred uranium.
- Nitride fuels have the highest Th content, as shown in Table 2.9, and therefore the largest content of in-bred U. As a result of the enhanced U in-bred during the cycle, ThN features the lowest TRU concentration among the fuels analyzed.
- The TRU concentration in “natural” nitride is larger than in “enriched” nitride. This is because, as shown in Figure 2.13, the absorption cross section of N-14 is significantly higher than that of N-15, resulting in more fissile needed.

Table 2.10: TRU content for the fuels analyzed.

Fuel Constituents	Th-TRU-Zr	Th-TRU-14N	Th-TRU-15N	Th-TRU-O2
HM loading [kg/GWt]	10,000	12,360	12,380	9,490
BOC TRU start-up [kg/GWt]	3,580	4,099	3,835	3,973
(% of HM)	35.8	33.3	31.2	41.8
BOC TRU 60 EFPY [kg/GWt]	4,147	4,695	4,521	4,416
(% of HM)	41.5	38.2	36.7	46.5
Average Discharge burnup, MWd/kg	75	61	61	80

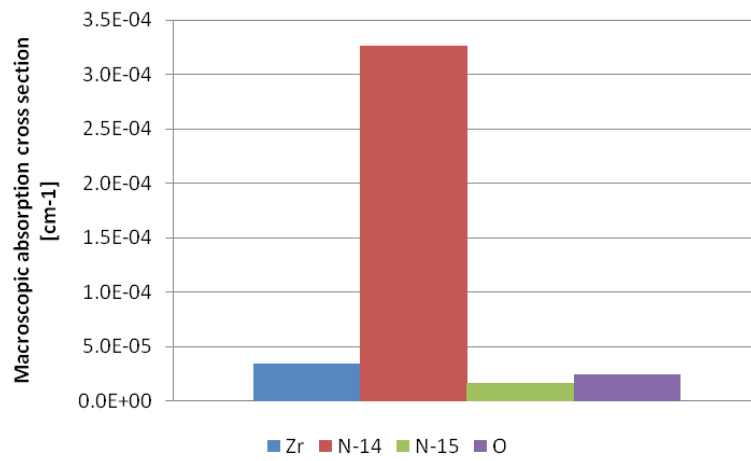


Figure 2.13: One-group macroscopic absorption cross sections of fuel binding elements.

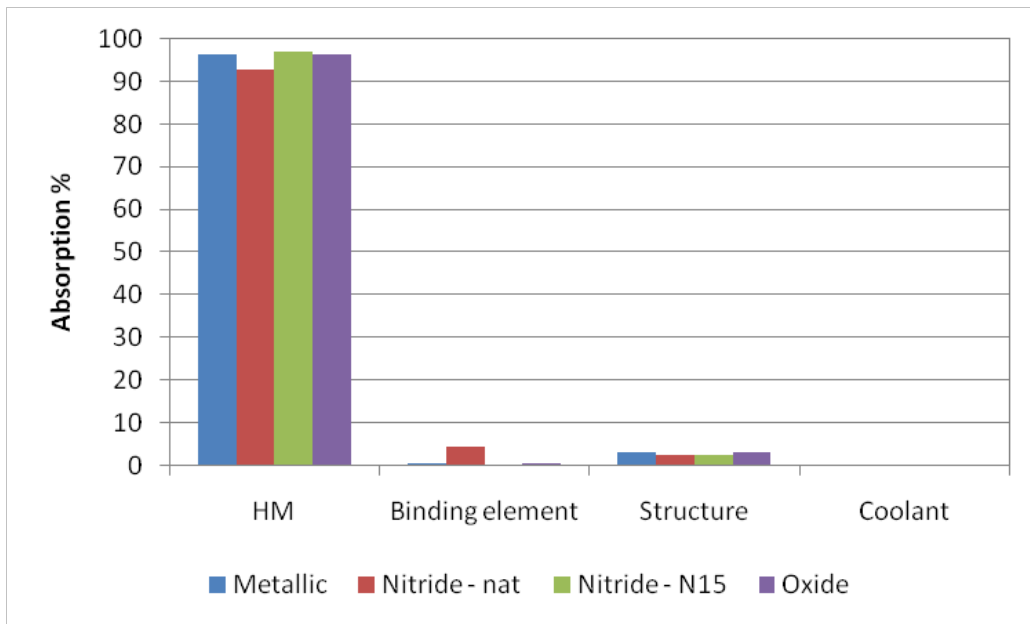


Figure 2.14: Percent contribution to total absorption of HM, fuel element binding (Zr, N-14, N-15, O), structure (all but fuel pellet and coolant), and coolant.

2.3.4 Neutron Economy

Figure 2.14 shows the contribution percentages, to total absorptions, corresponding to HM, fuel binding elements (Zr, N-14, N-15, O), structure (all but fuel and coolant), and coolant. It can be seen that:

- For all fuels, HM is responsible for more than 90% of the absorptions;
- unlike Zr, N-15, and O, whose absorption contributions are negligible (0.68%, 0.24%, and 0.39%, respectively), the binding element N-14 is responsible for 4.53% of all the absorptions;
- for all fuels, absorptions in the structure materials count for about 3-4%;
- for all fuels, absorptions in the coolant is practically zero.

To sustain the breeding, more than two neutrons per neutron absorbed must be emitted: one neutron to sustain the fission reaction chain, one for the breeding and a fraction to account for the leakages, since the reactor has a finite volume. Two parameters describing the neutrons available for the breeding are η and ε [16]. The η parameter is defined as follows

$$\eta = \frac{\sum_{\text{fissile}} \nu_i \Sigma_f^i}{\sum_{\text{fissile}} \Sigma_{\text{abs}}^i} \quad (2.1)$$

where ν_i is the average number of emitted neutron per fission reaction by isotope i , while Σ_f^i and Σ_{abs}^i are the macroscopic fission and absorption cross section for the same isotope. As it is defined, η accounts the neutrons emitted by the fissile isotopes per neutron absorbed by fissile isotopes. If $\eta = 1$, the neutrons emitted by the fissile isotopes are just enough to sustain the fission reaction, without counting for the leakages nor the absorption by fertile isotopes to breed new fissile.

The ε parameter is a measure of the extra neutrons emitted by fertile isotopes, with respect to those absorbed by fissile isotopes, and it is calculated as:

$$\varepsilon = \frac{\sum_{\text{fertile}} (\nu_j - 1) \Sigma_f^j}{\sum_{\text{fissile}} \Sigma_{\text{abs}}^i} \quad (2.2)$$

A high value of ε means that many neutrons are emitted by fertile isotopes with respect to neutrons absorbed by fissile isotopes. Or, in other words, few neutrons are absorbed by fissile isotopes among the neutrons emitted by fertile isotopes. So such neutrons are valuable for breeding. They are *extra* neutrons because the absorption by the fertile isotopes is already counted with the “-1” in the equation.

The distinction between fertile and fissile isotope is not well defined in a fast neutron spectrum environment. For this study, the fertile was defined as the isotope which has the one-group microscopic capture cross section higher than the fission cross section. Such definition is flux-dependent. For a

given fuel composition, the harder the spectrum, the higher number isotopes classified as “fissile”. Table 2.11 shows which isotope is fissile and which is fertile, according to the above definition, for the fuels analyzed. As it can be seen, some isotopes (e.g. U-234, Pu-242, Cm-244, and Cm-246) are classified as “fissile” for the metallic fuel, which features the hardest spectrum (see Section 2.3.1), while they are “fertile” for the oxide fuel, which features the softest spectrum (see Section 2.3.1).

Table 2.11: Classification of isotopes in fissile or fertile, for the fuels analyzed. For this study, a fertile isotope was defined as the isotope which has the one-group microscopic capture cross section higher than the fission cross section.

	Th232	Pa231	Pa233	U232	U233	U234	U235	U236	U237	U238	Np237
Metallc	fertile	fertile	fertile	fissile	fissile	fissile	fissile	fertile	fissile	fertile	fertile
N-14	fertile	fertile	fertile	fissile	fissile	fissile	fissile	fertile	fissile	fertile	fertile
N-15	fertile	fertile	fertile	fissile	fissile	fissile	fissile	fertile	fissile	fertile	fertile
Oxide	fertile	fertile	fertile	fissile	fissile	fertile	fissile	fertile	fissile	fertile	fertile
	Np238	Np239	Pu238	Pu239	Pu240	Pu241	Pu242	Am241	Am242m	Am243	Cm242
Metallc	fissile	fertile	fissile	fissile	fissile	fissile	fissile	fertile	fissile	fertile	fissile
N-14	fissile	fertile	fissile	fissile	fissile	fissile	fissile	fertile	fissile	fertile	fissile
N-15	fissile	fertile	fissile	fissile	fissile	fissile	fissile	fertile	fissile	fertile	fissile
Oxide	fissile	fertile	fissile	fissile	fissile	fissile	fertile	fertile	fissile	fertile	fissile
	Cm243	Cm244	Cm245	Cm246	Cm247	Cm248	Bk249	Cf249	Cf250	Cf251	Cf252
Metallc	fissile	fissile	fissile	fissile	fissile	fissile	fertile	fissile	fissile	fissile	fissile
N-14	fissile	fertile	fissile	fertile	fissile	fissile	fertile	fissile	fissile	fissile	fissile
N-15	fissile	fertile	fissile	fertile	fissile	fissile	fertile	fissile	fissile	fissile	fissile
Oxide	fissile	fertile	fissile	fertile	fissile	fissile	fertile	fissile	fissile	fissile	fissile

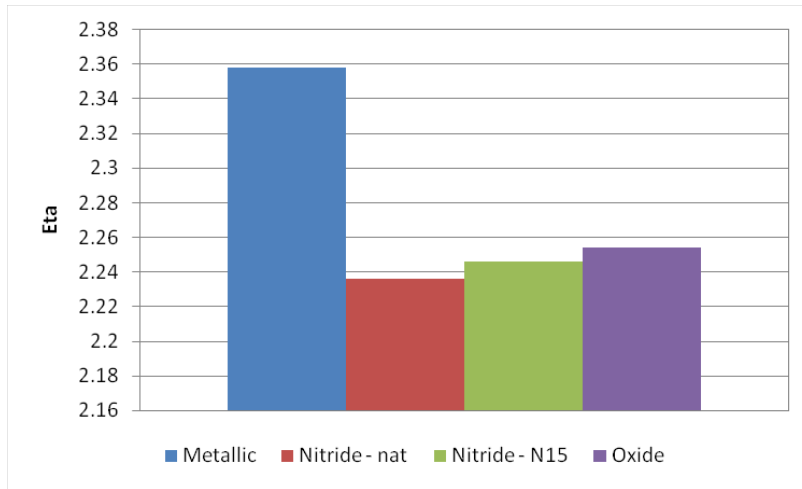


Figure 2.15: The η parameter for the fuels analyzed.

Figure 2.15 shows the η parameter for the fuels analyzed. As it can be seen, the metallic fuel features the highest η . This is due to the hardest spectrum characterizing this fuel: the harder the spectrum, the higher the number of neutrons emitted per fission [4]. In addition, there are more isotopes which are classified as “fissile” and the concentration of TRU is high (41.5% of HM, per Table 2.10), if compared to nitride fuels (38.2 and 36.7% of total HM for natural and enriched N, respectively), which have, on the other hand, the lowest η .

Figure 2.16 shows the ε parameter for the four fuels studied. Oxide fuel features the highest ε , nitride fuels have intermediate values, and metallic has the lowest ε .

The total excess of neutrons available for breeding, ω , can be calculated as follows

$$\omega = \eta - 1 + \varepsilon. \quad (2.3)$$

Figure 2.17 shows the ω parameter for the fuels analyzed. The oxide has the highest number of neutrons available for breeding, metallic is second, and nitrides, despite their large amount of in-bred U, come last.

Hence, oxide fuel has the best neutron economy characteristics for breeding; however, its low Th content, resulting from the low fuel density, yields a

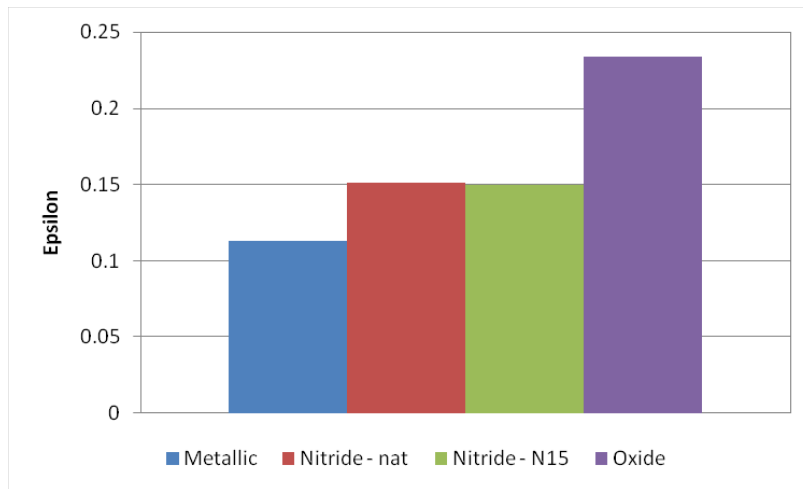


Figure 2.16: The ε parameter for the fuels analyzed.

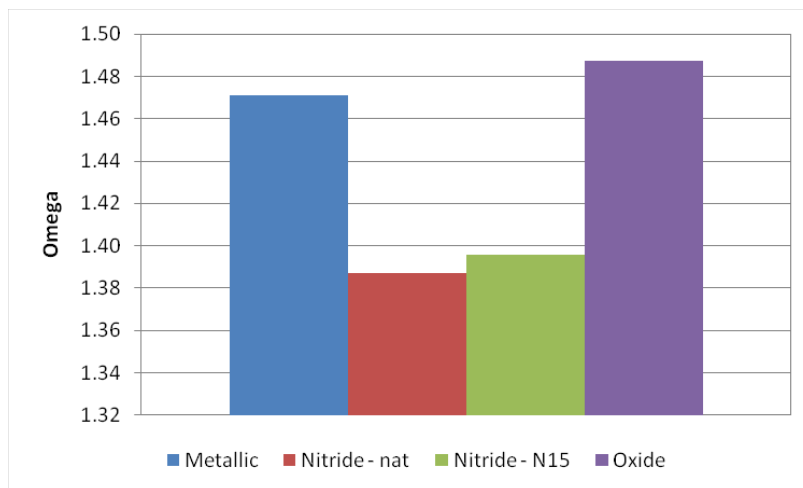


Figure 2.17: The ω parameter for the fuels analyzed.

smaller amount of U bred when compared to nitride fuels. Notwithstanding, in order to start other reactors based on the pure Th/U-233 fuel cycle, it is important to breed as much U as possible. From this point of view, nitride fuels are therefore preferable. Of the two nitrides, that enriched in N-15 is the best option.

2.4 Summary of Results and Future Works

Preliminary performance analysis of Th-TRU metallic fuels were carried out for the Advanced Recycling Reactor (ARR), a Toshiba-Westinghouse fast sodium-cooled reactor design, focusing on the TRU incineration and breeding capabilities. First, the Th fuel cycle was compared to the U-238 fuel cycle. For the Th case, the in-bred uranium can either be recycled along with the other actinides, or not recycled (it may be used to start a different reactor based on the pure Th/U-233 fuel cycle). Both options were studied. The main conclusions that can be drawn, from this study, are as follows:

- Th fuels feature a harder spectrum versus U fuel, due to the higher relative TRU content versus U fuel. Among Th fuels, the fuel containing the in-bred recycled U yields the hardest spectrum. This is due mainly to the higher absorption cross sections of Pu-240 and Pu-239 in the fast spectrum energy range, versus U-233.
- U-based design requires a lower TRU concentration (24.10% of HM) due to the better neutron economy yielded by U versus Th. The principal reasons are: 1) larger contribution to fission of U-238 versus Th-232; 2) higher number of fission neutrons per absorption in the respective main fissile isotope; 3) more efficient breeding mechanism in U versus Th because of fewer parasitic absorption in Np-239 versus Pa-233; 3) reduced leakage in U due to larger HM content and neutron scattering compared to Th.
- U fuel presents a small change in TRU content from start-up to 60 EFPYs, from 3.16 to 3.15 MT. This small change is fostered by the Pu-239 breeding, which counterbalances its consumption. On the other hand, Th fuel where the in-bred U is not recycled requires the highest TRU concentration (41.50% of HM after 60 EFPYs) and shows the largest variation in TRU content from start-up to 60 EFPYs of depletion, from 3.5 to 4.1 MT. When the in-bred uranium is recycled, its contribution

lowers the TRU requirement and leads to its decreasing concentration from start-up to equilibrium, from 3.5 to 2.9 MT.

- Th fuels can burn up to 3 times TRU legacy than U fuel, under the configuration analyzed here. This stems from the much lower generation of TRU in Th versus U already discussed.

Then, the ARR core design is used to assess four types of Th-based fuels: metallic, nitride (natural nitrogen and 95 N-15 a/o, for reducing formation of radiotoxic C-14 via (n,p) reaction from N-14), and oxide. For this study, the default actinides recycle scheme assumed is to recycle all actinides but in-bred U, since if in-bred uranium is not reinserted within the fuel after the separation, the TRU consumption rate is the highest. The main conclusions, drawn from this study, are summarized as follows:

- The hardest spectrum pertains to the metallic fuel, due to the reduced neutron moderation of Zr with respect to N (intermediate spectrum) and O (softest spectrum).
- Nitride fuels lead to up to 30% more in-bred U than the other fuels analyzed, 150 kg/GWt-yr for nitride enriched versus 114 and 113 kg/GWt-yr by metallic and oxide fuel respectively. This is due to the largest content of Th within ThN, fostered by their high density and assumed slow swelling rate. Mass of in-bred U within metallic and oxide fuel is similar.

Oxide fuel features the highest number of neutrons available for breeding per neutron absorbed, 1.49, then metallic fuel follows, 1.47. Nitride fuels show the smallest number of neutrons available, 1.40 and 1.39 for nitride enriched and natural respectively. Notwithstanding, the dominant factor which leads to the highest generation of in-bred uranium is the Th content, as already pointed out.

- ThN features the lowest TRU concentration, among the fuels analyzed, 33.30% and 31.20% of HM, at start-up for natural and enriched respectively. This stems from the largest in-bred U generation. Metallic fuel

requires a lower TRU concentration versus oxide fuel, 35.80% of HM versus 41.80% at start-up, because of the harder spectrum featured by metallic. Among nitride fuels, ThN with natural nitrogen needs a higher TRU content due to the large absorption cross section of N-14 versus N-15.

- The TRU transmutation rate is similar for each fuel analyzed and proportional to the TRU concentration: oxide, 321.8 kg/GWt-yr, metallic, 318.9 kg/GWt-yr, nitride natural, 317.1 kg/GWt-yr, and nitride enriched, 313.6 kg/GWt-yr.

Several aspects remain to be explored before claiming the viability, or superiority, of the options proposed. This includes not only design aspects but also experimental work, such as Th-TRU fuel manufacturing, irradiation and separation. The potential proliferation concerns represented by fuel with high content of TRU as well as U in-bred from Th should also be examined. Dynamics simulations should be carried out in order to address the controllability of reactors with proposed fuels studying the feedback coefficients.

Chapter 3

Thorium Fuel Cycle Performance in a Heterogeneous Core Design

In the previous chapter, the legacy TRU burning capabilities of U-based and Th-based fuels were compared. It was shown that Th fuels outperform U fuels, both because their TRU content needs to be higher than in U fuel and because with thorium there is no breeding of Pu-239.

Also, for the Th-based fuel it was shown that, among the two options of recycling U-233 back in the same reactor, or send it as fissile feed to other reactor types, the latter yields a higher TRU consumption, since more TRU feed is needed to achieve criticality. To pursue this venue, reactors based on the pure Th/U-233 fuel cycle must be started. Thus, along with the TRU consumption, the mass of in-bred U is an important parameter. These two parameters have been studied for metallic, nitride, and oxide fuel. While the TRU consumption is almost constant for the fuels studied, the mass of in-bred uranium is significantly different. Specifically, it was shown that Th-based nitride fuel, with nitrogen enriched in N-15 to 95% in atom, features the best combination of TRU consumption and breeding of U-233. Since this large breeding fostered from the high density and smeared density of

nitride fuel, it can be inferred that to increase the generation of in-bred U-233 further, the Th content must be increased. A possible solution may be to make the core bigger. However, size increase for sodium-cooled fast reactors is constrained by the need of limiting void reactivity coefficient, and the ARR features a small core just to make this coefficient negative [8]. Instead, a heterogeneous core design, i.e. with radial blankets, could increase the generation of U-233 still guaranteeing the safety of the reactor. This is because heterogeneity enhances breeding and improves void feedback when compared to its homogeneous counterpart [17].

A new design of a heterogeneous core, named THETRU, has been proposed and it is presented in Section 3.1. The THETRU has been developed for devising the transition from a TRU burning phase to a self-sufficient Th fuel cycle. One of the key elements of the transition is the generation of a sufficient amount of U-233 to offset the decreasing TRU external supply, which could not be achieved with an homogeneous ARR.

Because of the reasons mentioned above, the fuel of choice for THETRU is nitride fuel enriched in N-15.

The transition from a TRU burning phase to a self-sufficient Th fuel cycle can be divided into three Phases. In Phase I, the external fissile feed employed is legacy TRU and in-bred U is assumed to be partitioned out of the recycled fuel. Subsequently, once the TRU external supply is exhausted, Phase II begins. During Phase II, the feed is changed from TRU to in-bred uranium, which is now recycled into the reactor together with the rest of the actinides. Phase II is characterized by a decreasing trend in the amount of TRUs contained in the recycled fuel. Eventually, TRUs will decrease to negligible amount and the cycle becomes effectively a pure Th-U fuel cycle (Phase III). Figure 3.1 anticipates the results, which are discussed in the following sections, showing the mass of Th, U, and TRU in the core at EOC throughout the three phases. The end of the Phase I was arbitrarily chosen to correspond at the end of the reactor life, i.e. 60 EFPYs. Conceptually, the distinction between Phase II and Phase III is clear, but it is difficult to

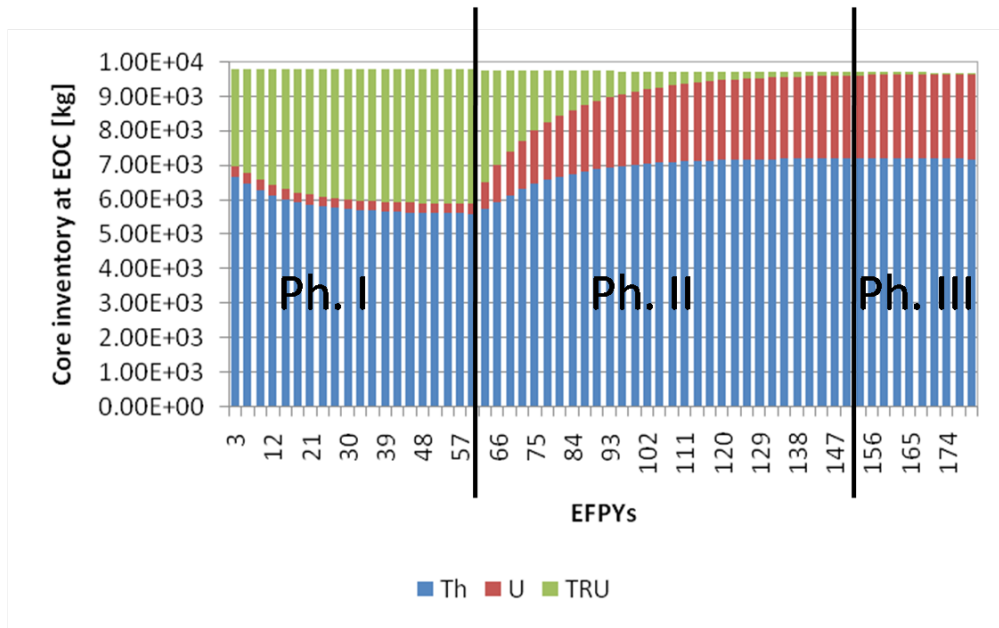


Figure 3.1: Visualization of the phases comprising the Th/TRU to Th/U-233 cycle transition, with indication of EOC mass trend for Th, U, and TRU.

quantitatively define when one ends and the following begins, since the TRU content does not suddenly decrease to negligible values. In Figure 3.1 an indicative border between the two phases was drawn after 150 EFPYs, i.e. 90 EFPYs after the external TRU supply is interrupted.

Notably, to sustain the transition to the pure Th/U-233 fuel cycle, a sufficient amount of U needs to be available during Phase II. This requires that either the reactor breeds enough uranium, i.e. a breeding gain¹ BR of 1 or higher, or that a sufficient amount of U stock has been accumulated during Phase I. However, during Phase II and III, a $BR \sim 0.95$ was achieved, which is insufficient for self-sustainability. Instead of changing the reactor design, to achieve the target BR, it was preferred for simplicity to keep the current configuration and assume that a U stock would be available to top-up the in-bred U. The U composition for this feed is that characterizing

¹Th breeding gain BR has been calculated as the ratio between the integral amount of uranium burned and produced at EOC [18].

in-bred U during Phase I. The design of a Th-U breeder is a complex task which is left for future studies. The TRU consumption in the breeder design could decrease, since the in-bred uranium would increase, but the trends and general conclusions presented herein would still be valid.

Section 3.2 analyzes Phase I and compares the THETRU design to its homogeneous, i.e. the ARR featuring the same fuel.

Section 3.3 analyzes Phase II, and shows the difference between the THETRU design and a self-sufficient fast reactor based on the U-238/Pu fuel cycle.

3.1 The THETRU Design

The THETRU core, shown in Figure 3.2, contains 294 fuel assemblies and 139 radial blanket assemblies. The 139 radial blanket assemblies are divided into four rings, which we refer to as RAB1 to RAB4, moving from the center to the periphery. The innermost radial blanket, RAB1, occupies the central location. The reflector thickness has been reduced crediting the reduction in neutron leakages resulting from the addition of the peripheral blanket. A single enrichment has been used for the driver fuel throughout the core. In addition of being the practice for the Clinch River breeder reactor [9], having one type of driver fuel simplifies the calculation of the BOC TRU content, thanks to the elimination of the driver fuel enrichment ratio (inner/outer), which was an unknown in the ARR analysis.

Figure 3.3 shows an axial view of driver fuel and radial blanket assemblies. With respect to the ARR, an upper and a lower axial blankets have also been added in the driver fuel assemblies, increasing the core active fuel height by 30 cm. The driver fuel height remains unchanged, and equal to 60 cm.

Table 3.1 and Table 3.2 present key characteristics of the core and geometry of the assemblies, respectively. The geometry of the driver assemblies is the same as in the ARR. The blanket assembly design has been obtained from the S-PRISM core design [10] by preserving the same ratio between the

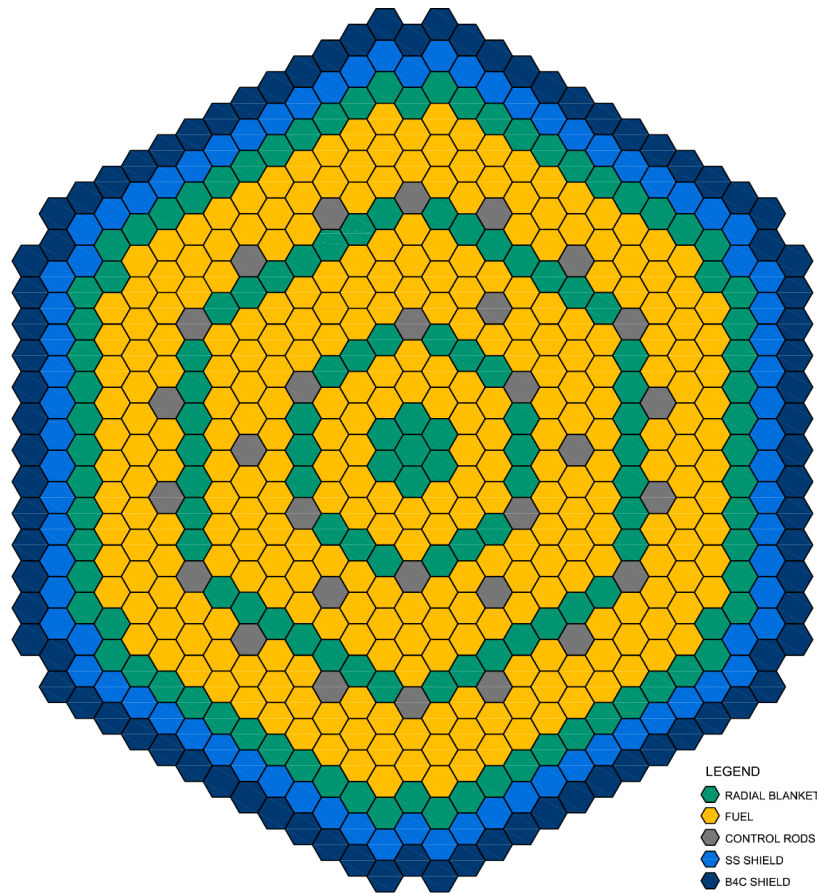


Figure 3.2: THETRU core radial view.

driver and blanket pin dimensions as in the S-PRISM core. The pin diameter, both for driver and blanket assembly, has not been optimized, leaving such studies for future improvements.

The fuel type is ThN, with nitrogen enriched to 95% in atom in the N-15 isotope. This is because, as showed in the previous chapter, this type of fuel yields the highest breeding capabilities when compared to the other type of fuels studied.

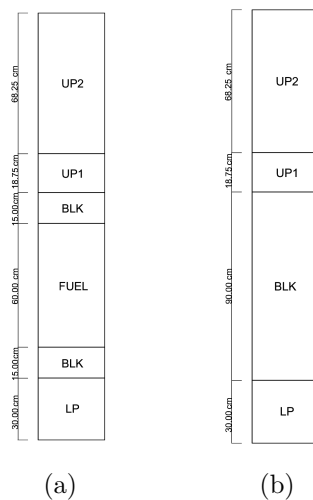


Figure 3.3: Axial representation of THETRU fuel and radial blanket assemblies.

Table 3.1: Main parameters of the THETRU design.

Core thermal power	1,000 MWth
Coolant	Na
Number of fuel assemblies	294
Number of radial blankets assemblies	139
Number of batches	3
Refueling interval	1 year

3.2 Phase I: THETRU TRU Burning and Breeding Capabilities

During Phase I, the external feed consists of TRUs from LWR UNF with composition already reported in Table 2.1. The in-bred U is assumed to be partitioned out of the recycled fuel and set aside for later use.

Table 3.3 compares the results obtained for the THETRU design with those of the ARR counterpart (ThN-TRU with enriched N, taken from Section 2.3). It can be seen that:

Table 3.2: Main parameters of the THETRU driver and radial blanket assemblies.

	Driver	Blanket
Assembly type	Hexagonal with duct	Hexagonal with duct
Clad/Duct material	HT-9	HT-9
Pin Lattice	Triangular	Triangular
Pin pitch	7.41 mm	10.91 mm
Pins per assembly	271	127
Pellet diameter	4.71 mm	8.50 mm
Smear density, %	82	85
Clad inner diameter	5.44 mm	9.00 mm
Clad outer diameter	6.50 mm	10.00 mm
Fuel/Coolant/Structure vol %	41.1/32.7/26.2	52.7/26.3/21.3

- the TRU burning rate for the THETRU design is only slightly lower than for the homogeneous design, i.e. 296 vs 315 kg/GWt-yr, due to the higher content of in-bred U-233 (which undergoes fission reactions as well), but it is still significant, especially if compared to that characterizing the ARR fueled with U-TRU-Zr, i.e. 110 kg/GWt-yr (see Section 2.2);
- the U-233 breeding rate for the THETRU design is much higher than for the homogeneous counterpart, i.e. 272 vs 146 kg/GWt-yr, due to the higher Th content in the core, which is in turn motivated by the addition of the blankets.

Figure 3.4 shows the amount of uranium produced by the various reactor zones. It can be noticed that the majority of the in-bred uranium is produced in the driver fuel, which however also occupies the largest volume. The breeding efficiency, shown in Figure 3.5, and defined as the ratio between in-bred uranium and medium volume, reveals that the higher efficiency is reached in the radial blankets. In particular, the inner blankets RAB1 to

3.2. PHASE I: THETRU TRU BURNING AND BREEDING CAPABILITIES

Table 3.3: Comparison of TRU burning and U-233 breeding capabilities between heterogeneous and homogeneous designs, averaged over 60 EFPYs.

	Heterogeneous	Homogeneous
TRU burned [kg/GWt y]	2.96E+02	3.15E+02
TRU inventory per batch [kg]	1.60E+03	1.50E+03
U extracted [kg/GWt y]	2.72E+02	1.46E+02
TRU % burned	18.55	20.93
Pu239 % burned	36.13	41.64

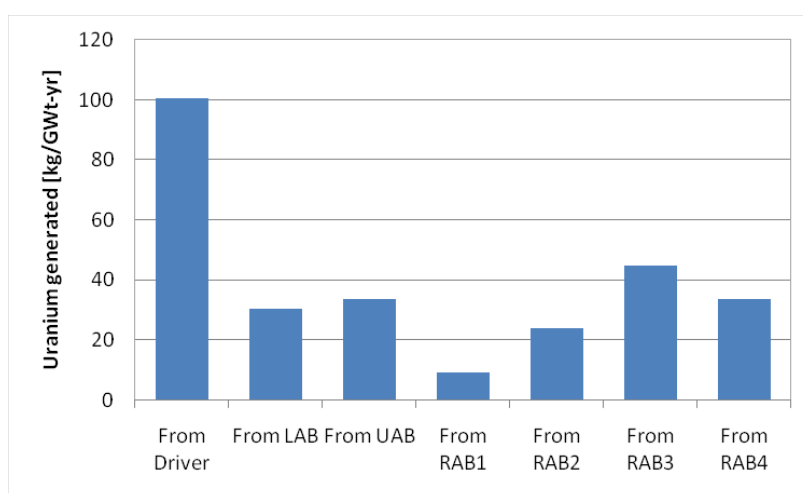


Figure 3.4: Uranium generated within each part of the THETRU reactor.

RAB3 have higher breeding efficiencies than the outermost blanket RAB4. This is due to the more intense flux in the inner zones compared to the periphery. A higher TRU content in the outer zones, or a thicker reflector, or both, may improve the efficiency in RAB4.

From Figure 3.4 it can also be seen that the upper axial blanket has a higher efficiency compared to the lower one. This is because it benefits from the presence of a large amount of sodium in the upper plenum, due to the assumed fuel swelling-induced sodium bonding relocation, which reflects neutrons back into the upper blanket.

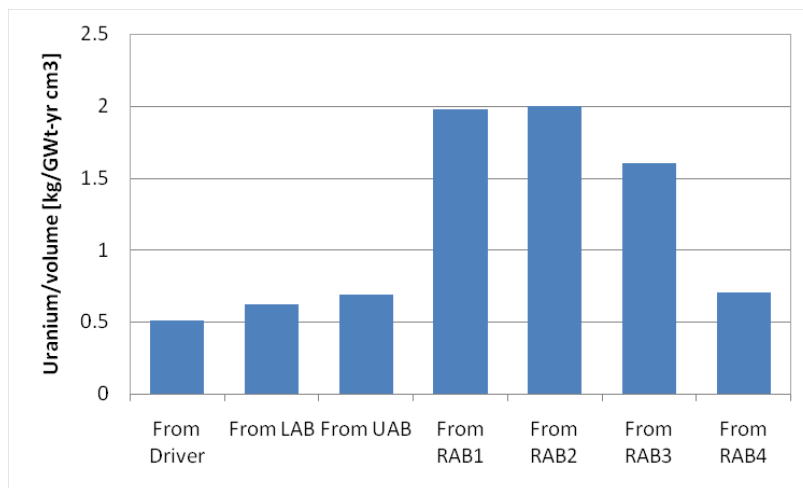


Figure 3.5: Ratio between uranium generated within a medium and its volume.

3.3 Phase II: No TRU External Supply

The end of Phase I, which simulates the exhaustion of the TRU external supply, was arbitrarily chosen to correspond to the end of the reactor life, i.e. 60 EFPYs. As anticipated in Figure 3.1, at this point in time there are still ~ 4 MT of TRUs within the core. The challenge is how to burn this residual legacy. While in Phase I the in-bred uranium was not recycled back with TRUs, the lack of external TRU feed assumed for Phase II requires uranium to be now recycled. In this way, the reactor can move toward a pure Th/U-233 fuel cycle since plutonium, whose mass is almost the $\sim 82\%$ of the TRU, is not directly bred, unlike for the U/Pu fuel cycle.

To achieve the transition to a pure Th/U-233 fuel cycle, the reactor should breed enough uranium to sustain the cycle. As already discussed at the beginning of this chapter, this is not the case for the current configuration, so it was decided to rely on an assumed external U feed to top-up the recycled U and therefore maintain the reference 3-year cycle length.

3.3.1 Progressive TRU Content

Figure 3.6 shows the core inventory at discharge throughout the three phases. As it can be seen, the TRU content of the core is greatly reduced once the external TRU supply is extinguished, i.e. after 60 EFPYs. From Table 3.4, which shows the inventories at five discrete time steps, it can be seen that, with respect to the total TRU content at the time of TRU external feed interruption, the TRU content is reduced by $\sim 93\%$ at 120 EFPYs, i.e. from 3.90 to 0.25 MT/GWt, while at 180 EFPYs is reduced by $\sim 99\%$.

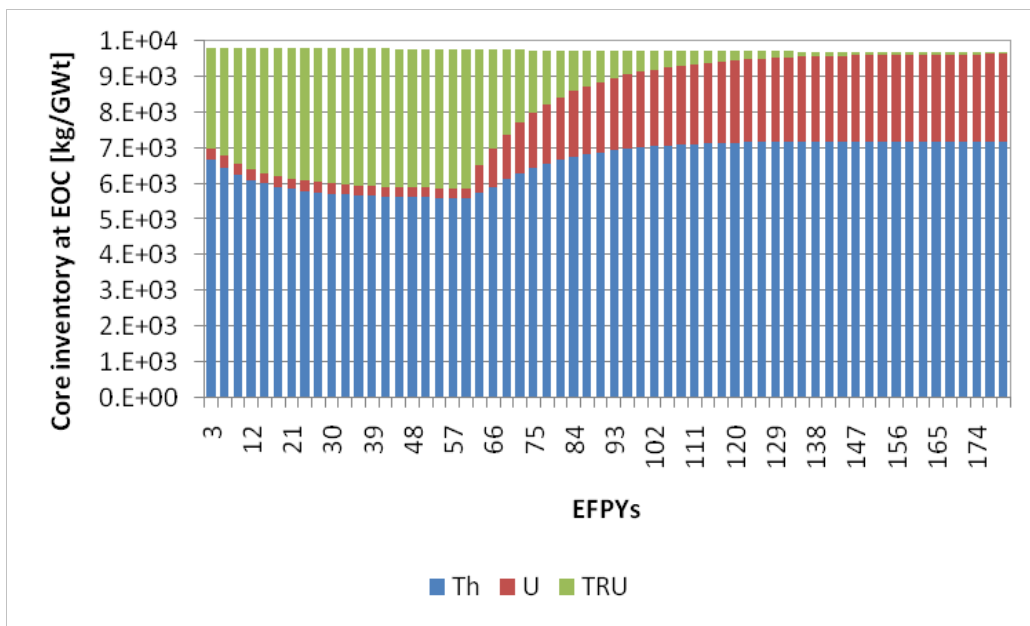


Figure 3.6: Core inventory at discharge for a total of 180 EFPYs of irradiation. For the first 60 EFPYs the external fissile feed consists of legacy TRU. In-bred uranium is the feed thereafter.

Table 3.4: Mass of TRU within the core at discharge throughout the three phases [kg/GWt]. Note that 0 EFPYs means at start-up.

Feed	TRU		TRU		In-bred U		In-bred U	
	Actinide	Recycle	All but U	All but U	All	All	All	All
EFPYs			0	60	120	180	240	
Np	1.74E+02		1.02E+02	1.03E+01	1.92E+01	2.18E+01	2.18E+01	
Pu	3.23E+03		3.22E+03	1.75E+02	2.77E+01	1.88E+01	1.88E+01	
Am	2.64E+02		3.92E+02	3.26E+01	2.80E+00	3.12E-01	3.12E-01	
Cm	1.85E+01		1.87E+02	3.56E+01	4.15E+00	4.51E-01	4.51E-01	
Bk	0		1.50E-02	1.66E-02	5.55E-03	1.10E-03	1.10E-03	
Cf	0		7.07E-02	1.04E-01	3.86E-02	8.08E-03	8.08E-03	
Tot	3.68E+03		3.90E+03	2.54E+02	5.39E+01	4.14E+01	4.14E+01	

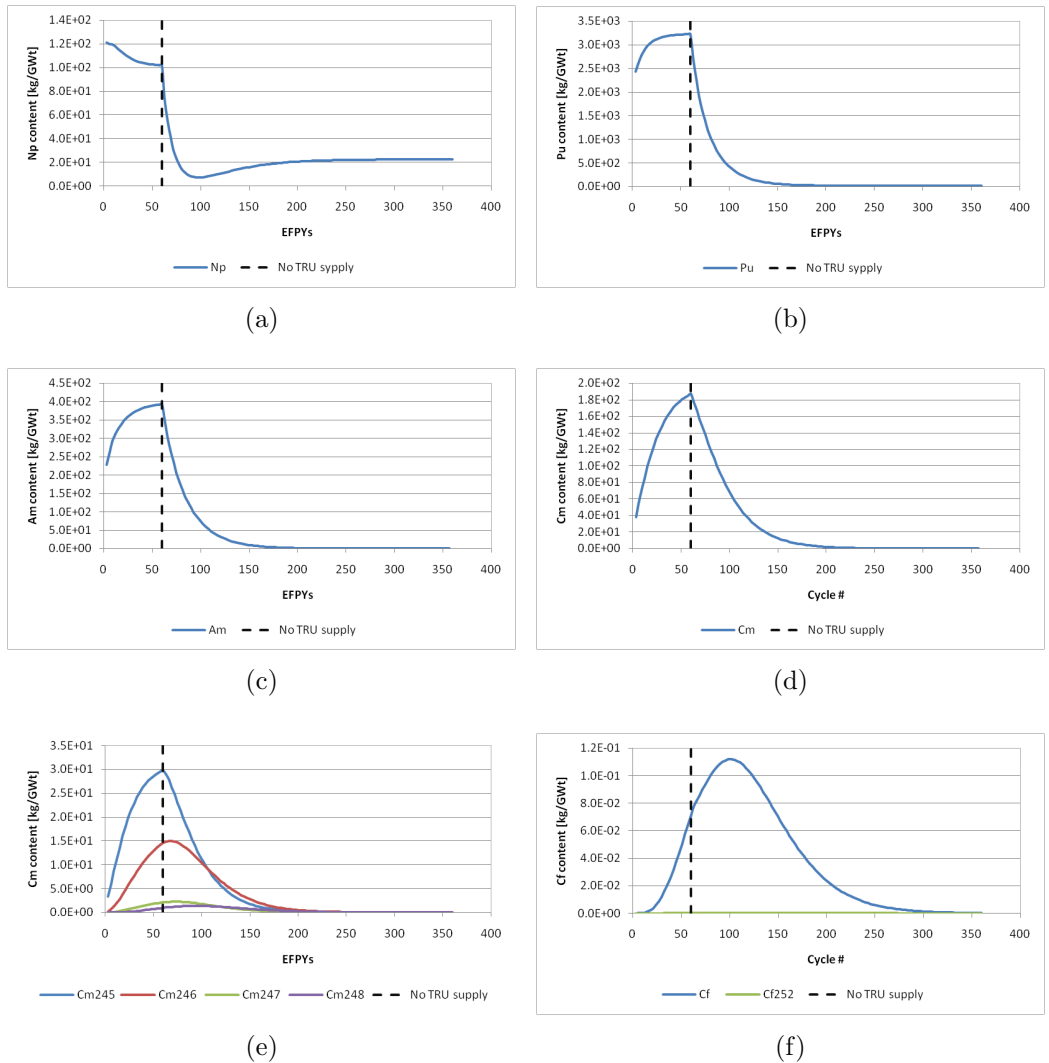


Figure 3.7: Mass vs cycle for Np (a), Pu (b), Am (c), Cm (d), higher isotopes of Cm (e), and Cf (f) throughout the two phases. Note that feed was changed after cycle 20.

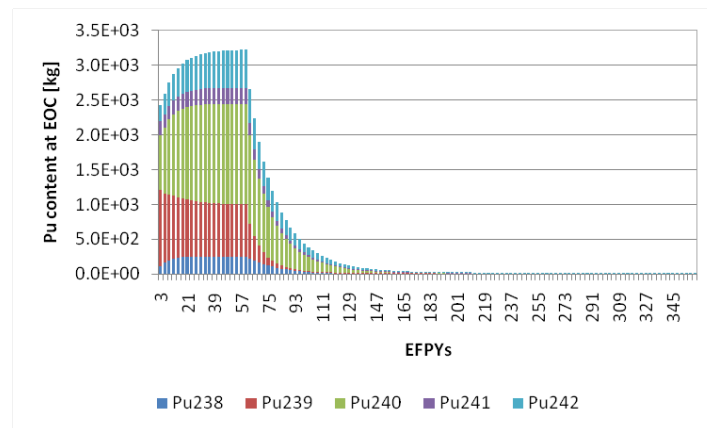
From Figure 3.7, which the trends of the inventories of the elements reported in Table 3.4, it can be seen that:

- after the TRU supply stops, masses of Pu, Am, and Cm decrease rapidly. Plutonium mass is greatly reduced but not completely burned since it is still bred from neptunium. At the end of Phase I, the mass of

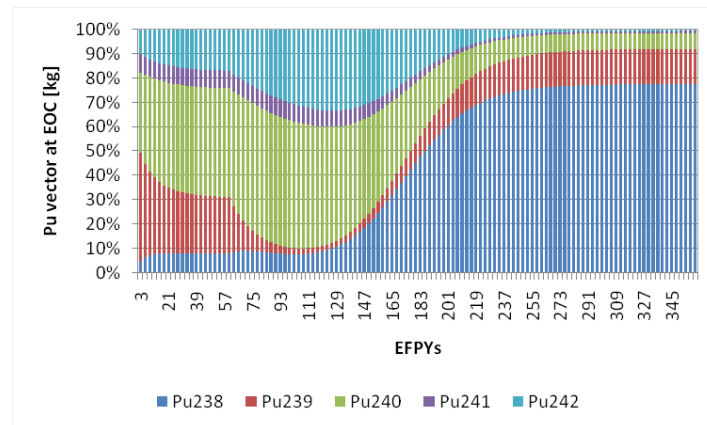
Pu is ~ 3 MT/GWt, while at the end of Phase II it is about 18 kg/GWt. Americium and curium are also significantly reduced. The mass of Am falls from ~ 392 kg/GWt at the end of Phase I, to ~ 98 g/GWt at the end of Phase II. The mass of Cm is ~ 187 kg/GWt at the end of Phase I, and decreases to ~ 30 g/GWt at the end of Phase II.

- after the TRU supply stops, the Np mass, which is practically only Np-237, first decreases rapidly but then, at about 90 EFPYs, begins to increase due to the build-up of U-236, which prevails over its consumption until a new equilibrium value is established. Notably, this equilibrium value is still 4 times lower than during Phase I, i.e. from ~ 100 kg/GWt, at the end of Phase I, to ~ 22 kg/GWt at the end of Phase II.
- unlike Pu, which builds up before TRU supply interruption but is progressively destroyed thereafter, the higher actinides Bk and Cf continue to build up even after the interruption of TRU feed. Then, with a delay compared to the other elements, they also start to be consumed.

Figure 3.8 shows the Pu content, (a), and the Pu vector, (b), at EOC throughout the two phases. As already discussed, the total mass of Pu, as soon as the TRU external supply is interrupted, decreases. However, Np-237 build-up leads to increasing content of Pu-238 in Pu, as shown in Figure (b). The percent of Pu-239 decreases first and then raises due to generation via neutron capture in Pu-238. The percent of Pu-240 and Pu-242 isotopes, once the TRU supply is interrupted, increases at first and then decreases. The initial increase in the relative content of the even Pu isotopes in Pu is the result of the more rapid fissioning of the odd isotopes, which have higher σ_f , as shown in Figure 3.9. Note that the masses of Pu-240 and Pu-242 are also on a decreasing trend.



(a)



(b)

Figure 3.8: Pu content within the core at EOC (a), and the Pu vector (b) throughout the two phases.

3.3.2 In-bred uranium

As the core configuration features a $BR=0.95$, external uranium has to be added to maintain the 3-year cycle length. Such external U, which tops-up the in-bred U, has the composition that characterizes in-bred U during Phase I. Figure 3.10 shows the mass of external U needed. During the first EFPYs, such external feed is not required, since the reactivity granted by the TRU and the in-bred U is sufficient. After 15 EFPYs, when the TRU are diminished by $\sim 55\%$, the external U is needed. The amount of such feed

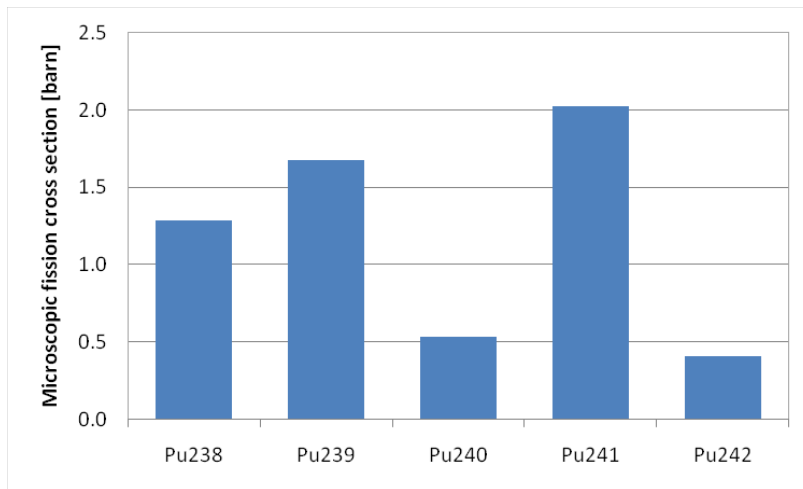


Figure 3.9: Collapsed 1-energy group microscopic fission cross section for the Pu isotopes.

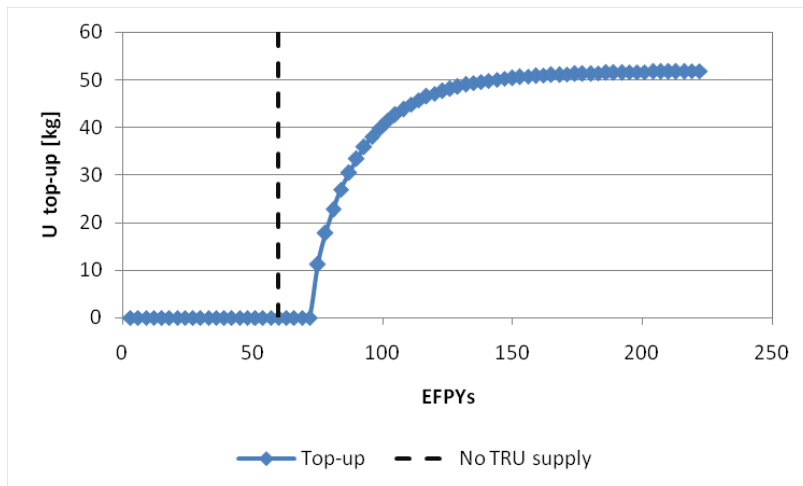
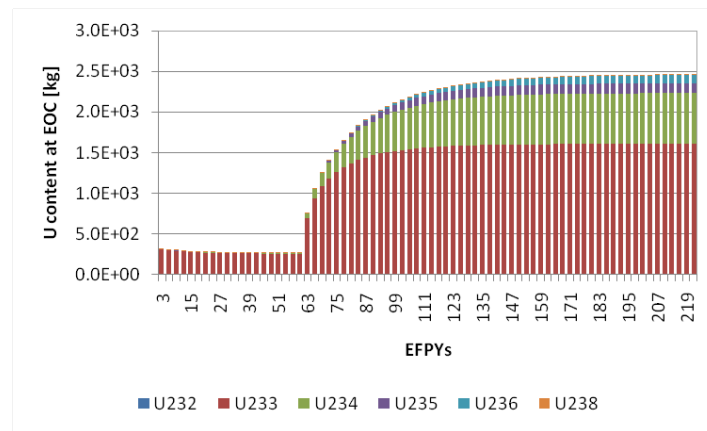


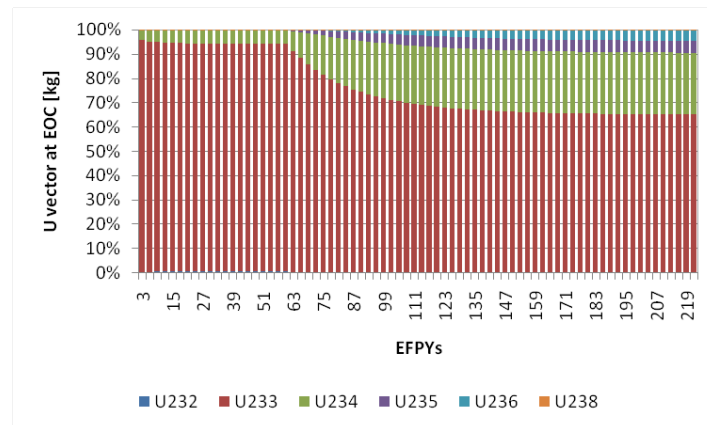
Figure 3.10: External U to top-up the in-bred U.

increases as the TRU are decreasing, then it stabilizes. At equilibrium, the U to top-up is ~ 52 kg/GWt-y. Note that the U content within the driver at BOC, at equilibrium, is ~ 3 MT. Therefore the expedient devised of topping-up the in-bred U with external U feed is not certainly acceptable for scoping calculations.

Figure 3.11 shows the U content, (a), and the U vector, (b), within the



(a)



(b)

Figure 3.11: U content within the core at EOC (a), and the U vector (b) throughout the two phases.

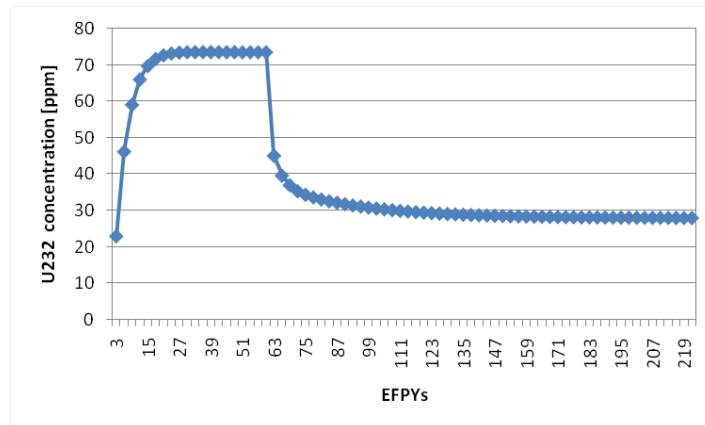
driver at EOC throughout the two phases. During the Phase I, the U vector does not change since it is not recycled. During the Phase II, the in-bred uranium is recycled, and, at equilibrium, the mass of uranium is 5 times that during Phase I, as shown in Figure (a). As can be seen in Figure (a) and (b), when in-bred uranium is recycled, the higher isotopes of U build up, such as U-236, from which the Np-237 isotope is bred.

In Th-based fuel, the U-232 isotope builds-up, whose decay chain produces penetrating gamma ray. The most important gamma emitter, ac-

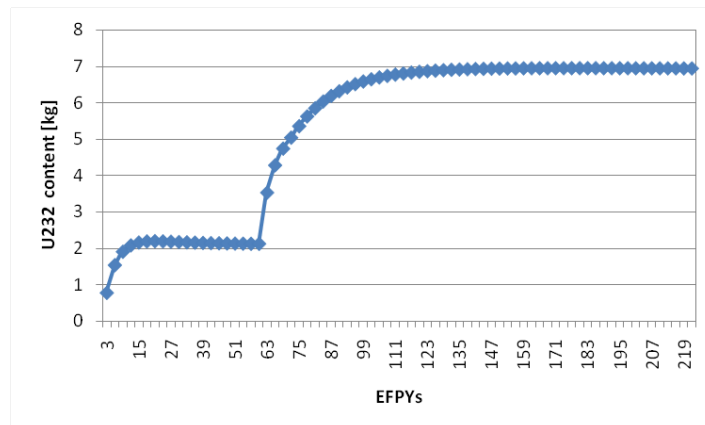
Table 3.5: Vector of in-bred uranium within each medium, along with the ppm of U-232.

	Driver	UAB	LAB	RAB1	RAB2	RAB3	RAB4
U-232	0.78%	0.07%	0.06%	0.14%	0.18%	0.13%	0.04%
U-233	93.42%	96.61%	97.23%	95.01%	94.82%	96.30%	98.60%
U-234	5.39%	3.18%	2.61%	4.62%	4.76%	3.44%	1.33%
U-235	0.23%	0.14%	0.09%	0.22%	0.23%	0.13%	0.02%
U-236	0.18%	0.00%	0.00%	0.01%	0.01%	0.00%	0.00%
U-238	0.00%	0.00%	0.00%	0.00%	0.00%	0.00%	0.00%
ppm U-232	78	7	6	14	18	13	4

counting for about 85 percent of the total dose from U-232 after 2 years, is Tl-208, which emits a 2.6-MeV gamma ray when it decays [19]. As a result, handling fuel with even few parts per millions (ppm) of U-232 requires shields. Figure 3.12 shows the concentration, (a), and the mass, (b), of U-232 within the driver, after the cooling. It is interesting to note that, once the in-bred uranium is recycled, the concentration of U-232 decreases, as shown in Figure (a), even though the mass of U-232 increases, as can be seen in Figure (b). The fall of U-232 concentration is due to the adding of “cleaner” uranium, i.e. with lower concentration of U-232, from the blankets, as given in Table 3.5.



(a)



(b)

Figure 3.12: The concentration, (a), and the mass, (b), of U-232 within the driver, after cooling.

Table 3.6: Composition of the external feed for Phase II for the ARR U fuel design.

Np237	0.28
Pu238	0.04
Pu239	94.79
Pu240	4.74
Pu241	0.14
Pu242	0.00
Am241	0.01

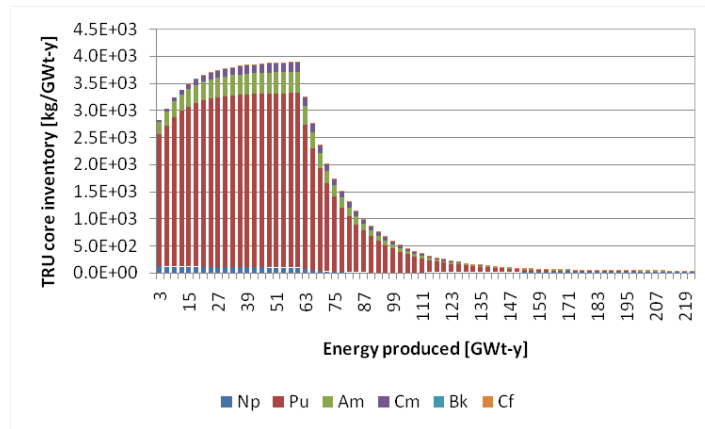
3.3.3 Th versus U

In U based fuel cycles, the capability to burn TRU is intrinsically limited by the conversion of U-238 into Pu-239. TRU burner designs based on U fuel are certainly possible, and a wide range of conversion ratios has been claimed by varying the amount of U admixed with the TRU, for example [20]. These U-based TRU-burner designs could be employed during Phase I of the scenario described above, as counterpart of the Th-TRU transmuters. An example will be provided using the ARR U fuel design described in Chapter 2.

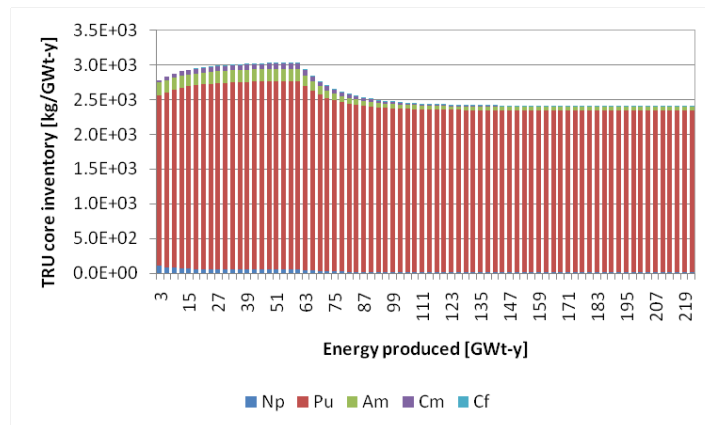
However, a self-sufficient U design will eventually be needed once the TRU external supply is exhausted. This is achieved providing that a sufficient amount of fissile (Pu-239 from U-238 primarily) is generated during the cycle. Therefore the long-term reduction of TRU achievable by this class of reactors is limited, with an example shown in the following.

Since the ARR U fuel design does not breed enough fissile, similarly to the expedient adopted to overcome the breeding shortfall in THETRU Th design, an external feed of Pu is added, with the composition of characterizing in-bred Pu within U-238 blankets after 3 EFPYs of irradiation. The composition is given in Table 3.6.

Figure 3.13 shows the TRU content within the core at EOC, throughout the two phases, for the Th case, (a), and for the U-238 case, (b). As can be



(a)



(b)

Figure 3.13: The TRU content within the core at EOC, throughout the two phases for the Th case, (a), and for the U-238 case, (b).

seen, in the U case, the TRU cannot be deeply burned, unlike the Th case, since new Pu is directly bred from the U-238 isotope. The little decrease of the higher actinides, (Am, Cm, and so forth), is due to the stop of the external supply of Am and Cm. While the decrease of Pu content is due to the better Pu vector composition, i.e. with higher percent of Pu-239, as shown in Figure 3.14.

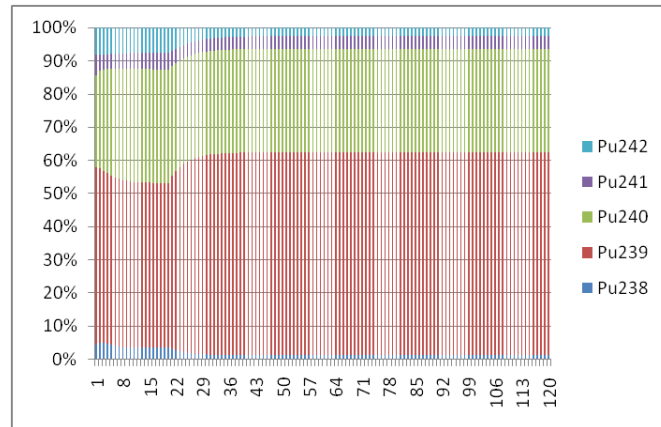


Figure 3.14: The Pu vector throughout the two phases, for the ARR U fuel design.

Radiotoxicity

Most of the hazards in dealing with spent fuel stem from some of the following chemical elements: plutonium, neptunium, americium, curium, and some long-lived fission products such as iodine and technetium. A measure of their health potential hazard is conveyed by *radiotoxicity*, which accounts for the radiological impact due to the exposure of the population following a postulated release of these elements [4].

The objective in the Westinghouse backend approach is for the HLW generated to have a radiotoxicity not to exceed, after 300 years of decay, the radiotoxicity of the uranium ore needed in a typical PWR open cycle to produce the same amount of electricity [3].

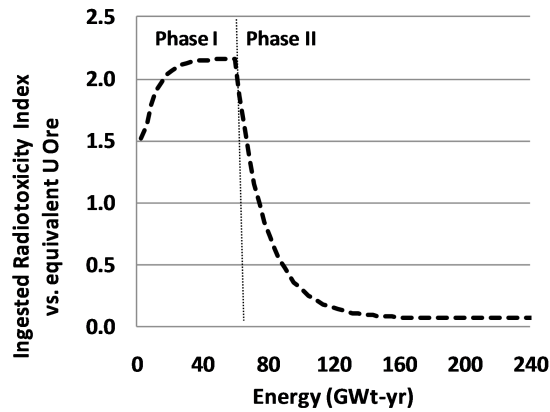
Figure 3.15 shows on the y axis the ingested radiotoxicity index *at 300 years* versus the equivalent U ore, and on the x axis the energy produced throughout the two phases for the Th case, (a), and for the U case, (b). The plots were generated assuming the same heavy metal process losses, 0.1% of total HM. As can be seen, the smaller TRU core inventory of the Th design fosters a much lower long-term radiotoxicity, $\sim 1/10$, when compared to the U design.

Figure 3.16 shows the ingested radiotoxicity isotopic breakdown at 300,

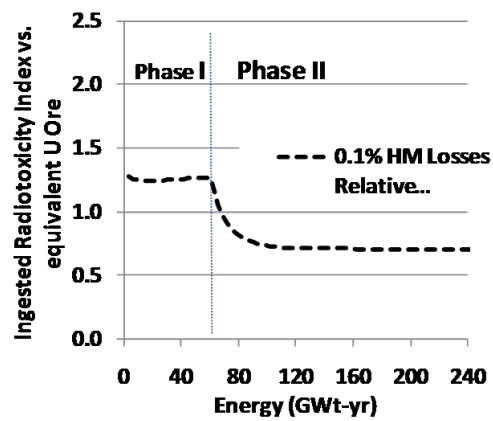
10,000 and 100,000-yr for the Th case, after 60 EFPYS, (a), and after 240 EFPYS, (b). As can be seen, with the Th-based reactor is capable to complete the TRU transmutation once the TRU external stream is exhausted. The ingested radiotoxicity evolves toward the typical one for the Th/U-233 fuel cycle, which is dominated by the U isotopes.

Figure 3.17 shows the ingested radiotoxicity isotopic breakdown at 300, 10,000 and 100,000-yr for the U case, after 60 EFPYS, (a), and after 240 EFPYS, (b). As can be seen, the U-based reactor can just reduce the content, and so the radiotoxicity, of the higher actinides, such as Am and Cm. After the change of the feed, from the TRU supply to the in-bred Pu, the ingested radiotoxicity is dominated by the Pu isotopes.

Figure 3.18 shows the trend, throughout the years, of the radiotoxicity index for inhalation of the discharged fuel (Th case and the U case, at the end of Phase I and Phase II). The radiotoxicity of the U ore needed in a typical PWR open cycle to produce the same amount of electricity is also plotted. As can be seen in the Figure 3.18 only the “Th-phase 2” radiotoxicity curve satisfies the “300-year” HLW objective. At the end of Phase II the fuel inventory is, as shown above, typical of a pure Th/U-233 fuel cycle. Therefore, to satisfy the Westinghouse’s objective, the TRU must to be completely burned.

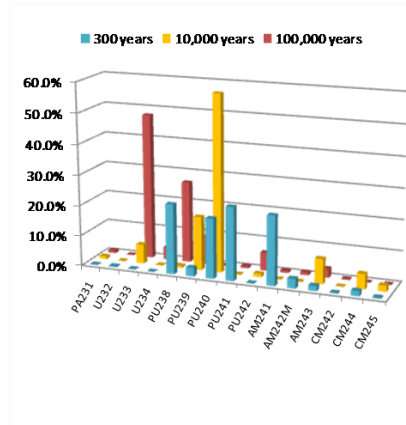


(a)

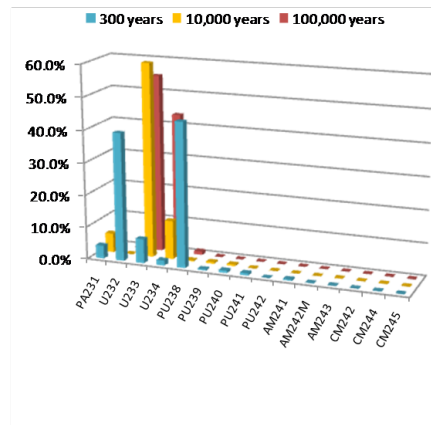


(b)

Figure 3.15: On the y axis, the ingested radiotoxicity index *at 300 years* versus the equivalent U ore, and, on the x axis, the energy produced throughout the two phases for the Th case, (a), and for the U case, (b).

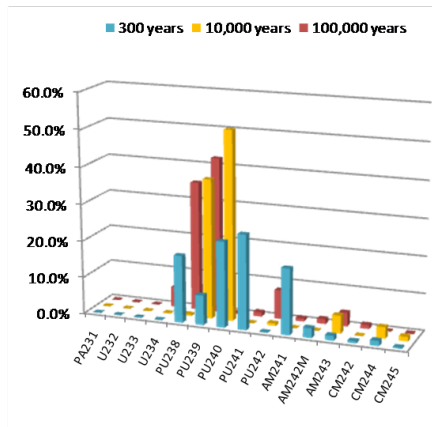


(a)

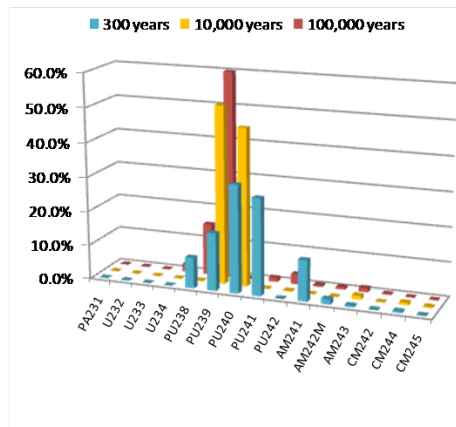


(b)

Figure 3.16: Ingested radiotoxicity isotopic breakdown at 300, 10,000 and 100,000-yr for the Th case, after 60 EFPYs, (a), and after 240 EFPYs, (b).



(a)



(b)

Figure 3.17: Ingested radiotoxicity isotopic breakdown at 300, 10,000 and 100,000-yr for the U case, after 60 EFPYS, (a), and after 240 EFPYS, (b).

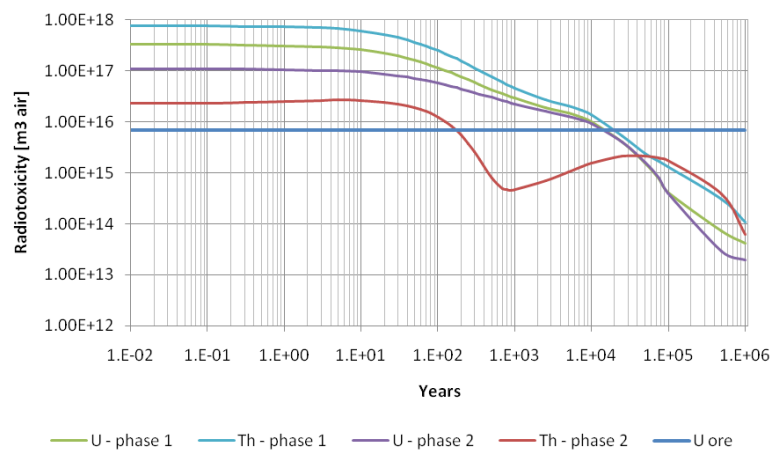


Figure 3.18: Radiotoxicity in m³ of air for the two fuel at the end of each phase.

3.4 Summary of Results and Future Works

A heterogeneous core design, named THETRU, with inner and peripheral radial blankets, has been developed to improve the breeding capabilities of the ARR design. The Th-nitride fuel, with nitrogen enriched at 95 atom percent in N-15, was chosen since it features the best combination between TRU incineration and U-233 breeding.

First, the THETRU performance has been compared with the ARR counterpart design, i.e. with N-15 enriched ThN fuel. For this purpose, 60 EFPYs of irradiation were simulated with legacy-TRU external feed. The in-bred uranium was assumed to be separated from the recycled fuel and set aside for later use. The main conclusions from this study follow:

- The generation of in-bred U is increased by ~ 150 kg/GWt-yr in the ARR to over 270 kg/GWt-yr in THETRU;
- The TRU consumption rate, yielded by the THETRU design versus the ARR, is only marginally decreased, from 315 kg/GWt-yr TRU burned in the ARR to 296 kg/GWt-yr in THETRU

Subsequently, a scenario involving the exhaustion of the TRU external supply has been simulated. Once the TRU supply is interrupted, there are still 3 MT of TRU to be burned within the THETRU core. The feed was, thus, changed to in-bred uranium. Additional external supply of U was necessary because the breeding gain was inferior to 1, i.e. 0.95. Therefore, the transition phase from a Th/TRU core to a pure Th/U-233 fuel cycle was explored. Such transition, i.e. from having a TRU external supply to a self-sufficient cycle, has been explored also for the ARR with U-238/Pu fuel cycle. For this case, the feed was changed to in-bred Pu. The performance of the two cycles, Th-based and U-238 based, were compared. The main conclusions that can be drawn are:

- The Th-based design can deeply burn the residual amount of TRU within the core. After 60 EFPYs from the stop of TRU supply, the

TRU content is reduced by $\sim 93\%$, and after 120 EFPYs by $\sim 99\%$. However, a complete destruction of all the TRU cannot be achieved. As a result of many recycles, the U-236 isotope builds-up, which, via neutron capture reaction and following decay, generates Np-237. From the latter, also Pu-238 is bred. Nevertheless, at equilibrium, the content of Np and Pu is ~ 22 and ~ 19 kg respectively. Content of Am and Cm is lower than 1 kg. The impact on the 300-year radiotoxicity deriving by this build-up is acceptable.

- In the U case, the TRU cannot be deeply burned, since new Pu is directly bred from the U-238 isotope. At equilibrium, the TRU content is decreased by $\sim 20\%$. This reduction is due to the decreased content of Pu, Am, and Cm. This is due the better Pu vector, i.e. with higher concentration of Pu-239 and lower concentration of higher Pu isotopes, fostered by the in-bred Pu feed.
- The smaller TRU core inventory of the Th design fosters a much lower long-term radiotoxicity, $\sim 1/10$, when compared to the U design.
- At equilibrium, the Th design features a core inventory, and so the radiotoxicity, typical of a pure Th/U-233 fuel cycle, which is dominated by the U isotopes, in particular U-233 and U-232.
- At equilibrium, the radiotoxicity of the U design is dominated by Pu and some Am.

Many studies could/should be conducted. Future works include the dynamics simulations in order to address the controllability of the THETRU with proposed fuel, studying the feedback coefficients; optimization of the fuel and blanket assembly; investigation of the impact of the radial blankets positions, e.g. two consecutive rows of blankets instead of one, a different pattern where the blanket assemblies (i.e. checkerboard instead of rings), and so forth; study the impact of a different coolant such as lead. Throughout the simulations, the blankets were reprocessed with the

same timing of the fuel, which may not be the best management scheme, so different timing may be considered. Last but not least, economic analyses should be carried out.

Chapter 4

Conclusions

In this thesis, the performance of Th-based and ^{238}U -based fuel cycles has been studied, with particular focus on the destruction of legacy TRU in a fast neutron spectrum environment. The evaluation has been carried out with comprehensive simulations covering all the relevant portions of the fuel cycle, with detailed cycle-by-cycle in-core irradiation performed through an automated procedure developed within the framework of the ERANOS code.

As the first step, the performance of Th-TRU fuel has been assessed for the Advanced Recycling Reactor (ARR), a Toshiba-Westinghouse fast sodium-cooled TRU burner reactor design. Firstly, the reference U-metal core design of the ARR has been modified and adapted to Th fuel. A comparison of the performance between the reference U-metal design and its Th-metal counterpart has then been undertaken, revealing up to 3 times higher legacy-TRU consumption rate in the Th design. The behavior of different Th fuel forms has also been investigated, namely, metallic, nitride (both with natural N and N enriched¹ in N-15), and oxide fuel. The results provided important insights on the TRU transmutation performance and U-233 breeding potential of the various options, and constituted the basis for the selection

¹Nitrogen was enriched to a 95% atom percent level in N-15 has been employed for reducing the (n,p) cross-section reaction for formation of C-14 from N-14, thereby improving neutron economy and mitigating the health hazards associated with C-14.

of an optimum fuel to carry forward into the ensuing design stage.

As the next step, a heterogeneous fast-reactor core design, named THETRU, has been developed. The design aimed at improving the U-233 breeding performance of the ARR while maintaining its favorably high TRU transmutation rate. This has been accomplished through the use of radial and axial blankets. ThN, with N enriched at 95 atom percent in N-15, has been chosen as fuel since it yields the best compromise between U-233 breeding and TRU burning. The results obtained confirm the effectiveness of THETRU in achieving its design objectives. The U breeding is nearly doubled, from the ~ 150 kg/GWt-yr generated in the ARR design to over 270 kg/GWt-yr in THETRU. This is accomplished with only a minor decrease of the TRU burning performance, from 315 kg/GWt-yr TRU burned in the ARR to 296 kg/GWt-yr in THETRU. The heterogeneous design has additional benefits, such as the potential for reduced reactivity variation over the cycle and improved safety coefficients.

In the last part of this work, the optimized core design developed has been employed as basis to perform a scenario calculation which encompasses the phases envisaged for thorium implementation, from a Th/TRU fuel cycle to a Th/U-233 fuel cycle. A first phase where legacy-TRU is supplied as an external feed and burned within the fast reactor core is followed by a second phase, where the external TRU stock is assumed to be exhausted, and the in-bred U is used to continue the destruction of the TRU accumulated in the core during the first phase. As the TRUs are being burned also from the fuel core inventory, the cycle transitions to a Th/U-233 fuel, virtually free of TRU. The HWL radiotoxicity from this cycle after 300 years of decay has then been evaluated and showed to be comfortably below that of the natural U ore.

Therefore this work has showed that it is possible, using thorium, to accomplish two main objectives of the Westinghouse backend strategy: deep burn of the legacy TRUs, achievement of a virtually TRU-free fuel with 300-year radiotoxicity comparable to that of the U ore.

Several aspects remain to be explored to ascertain the viability of the options proposed. This includes not only design aspects but also experimental work, such as Th-based fuel manufacturing and handling in presence of high TRU and/or U-232 content, irradiation and separation. The potential proliferation concerns represented by fuel with high content of TRU as well as U in-bred from Th should also be examined.

For what concerns the design aspects, optimization of the fuel and blanket assembly of the THETRU, and of their positioning throughout the core, is certainly possible.

Last but not least, economics analyses to compare the fuel cycles on a more comprehensive basis should be conducted.

Appendix A

Summary of studies conducted on thorium fuel cycle

The work presented in this thesis is focused on Liquid Metal Fast Reactors, in particular with sodium as coolant. For completeness, a brief summary of studies on Th-based fuel cycles, but in the context of different reactor types, is presented below.

A.1 Performance in LWRs

Thorium-based fuels can be used to reduce concerns related to the proliferation potential and waste disposal of the current light water reactor uranium fuel cycle. The main sources of proliferation potential and radiotoxicity are the plutonium and higher actinides generated during the burnup of standard LWR fuel. A significant reduction in the quantity and quality of the generated Pu can be achieved by replacing the ^{238}U fertile component of conventional low-enriched uranium fuel by ^{232}Th . Thorium can also be used as a way to manage the growth of plutonium stockpiles by burning plutonium, or achieving a net-zero transuranic production, sustainable recycle scenario [21].

Two main implementation scenarios have been the focus of recent studies

in a NERI-project for Pressurized Water Reactors (PWRs): homogeneous and heterogeneous fuels. The homogeneous designs are twofold: one kind employs a mixture of $\text{ThO}_2\text{-UO}_2$ within each fuel rod, in the other, called micro-heterogeneous, uranium and thorium fuel parts are spatially separated within a given fuel rod. The heterogeneous designs consider a seed-blanket approach, where U and Th fuel parts are spatially separated within a given assembly or between assemblies.

Heterogeneous fuels

The two approaches are described as follows and shown in Figure A.1:

- The Seed-Blanket Unit (SBU, also known as the Radkowsky Thorium Fuel, RTF) concept, which employs a PWR assembly where the center rods are the seed and the outer rods make the blanket. In other words, each assembly is a complete seed-blanket unit;
- The Whole Assembly Seed and Blanket (WASB), where each assembly is or all-seed-unit or all-blanket-unit and they are arranged as a checkerboard array.

For both the SBU and WASB concepts, there is a significant reduction in the quantity and “weapons quality” of the plutonium that is produced: the production of Pu is reduced by a factor of $\sim 3\text{--}5$ relative to a standard PWR/WWER, and the plutonium that is produced has a high content of ^{238}Pu , ^{240}Pu , and ^{242}Pu which makes it impractical for use in a weapon. A once-through fuel cycle was assumed for both approaches.

Homogeneous and microheterogeneous fuels

A homogeneous mixture of thorium and uranium will not be able to achieve the same burnup potential as the pure UO_2 fuel. Spatial separation by at least a few millimeters of the uranium and thorium parts of the fuel can improve the achievable burnup of the thorium-uranium fuel. The neutron

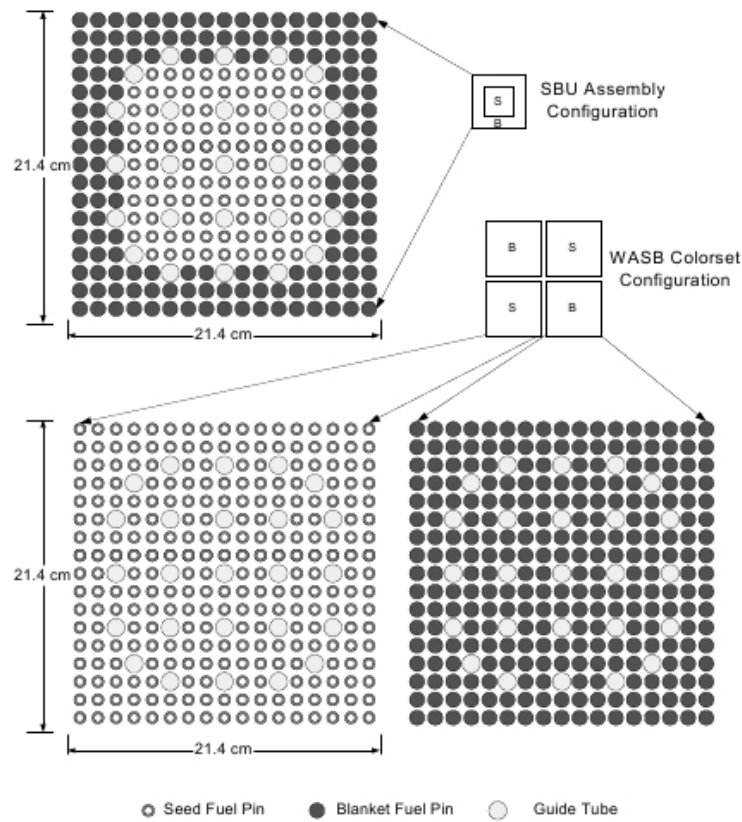


Figure A.1: SBU and WASB fuel assembly design.

spectral shift was identified as the primary reason for the enhancement of burnup capabilities. Mutual resonance shielding of uranium and thorium was found to be a smaller factor.

Three microheterogeneous designs were addressed:

- Duplex pellet both where the uranium is inside the thorium and vice-versa;
- Axially microheterogeneous;
- Checkerboard of uranium and thorium rods in one assembly.

It was found that the microheterogeneous fuel can achieve up to 15% higher burnup than the all-uranium fuel using the same initial ^{235}U . However, denaturing of the ^{233}U in the thorium portion of the fuel with a small amounts of

uranium significantly impairs this enhancement. The denaturing is necessary in some cases in order to reduce the power peaking in the seed-type fuel by improving the power share of the thorium region at the beginning of fuel irradiation. A combined axially heterogeneous fuel (with annular uranium fuel pellet region of 4 cm length separated by about 8 cm long region of duplex pellets where the uranium is inside the thorium) was found to meet thermal hydraulic design requirements while still providing higher achievable burnup than the all-uranium case. However, the large power imbalance between the uranium and thorium regions creates several design challenges, such as higher fission gas release and significant axial cladding temperature gradients.

Burning plutonium and other actinides

For same burnups, variable enrichment cases, the plutonium destruction rate (per megawatt-day per cubic centimeter) is ~ 2.5 times higher in the thorium-based fuels [22]. Destruction of up to 1000 kg of reactor grade Pu can potentially be burned in thorium based fuel assemblies per GWYear. Addition of minor actinides degrades the burning efficiency. Introduction of TRU containing fuels to a PWR core inevitably leads to lower control materials worths and smaller delayed neutron yields in comparison with conventional UO_2 cores.

A plutonium-thorium blended fuel was also studied and was found that is feasible to license and safely operate a reactor fueled with such fuel [23].

Waste and radiotoxicity

Thorium based fuel cycle produces much less minor actinides (Am, Np, Cm) but are associated with isotopes like ^{232}U and ^{228}Th , with relatively short half life and other radionuclides like ^{231}Pa , ^{229}Th and ^{230}U , which would have long term radiological impact. In addition, there would be fission products like ^{129}I and ^{135}Cs , which give the highest contribution to the total dose on short term basis and activation products like ^{59}Ni and ^{94}Nb . The residual

heat of spent TOX fuel is more than of MOX fuel mainly because of the ^{232}U and daughter products.

Studies conducted with both unirradiated and irradiated thoria-urania LWR fuel have demonstrated that $(\text{U,Th})\text{O}_2$ exhibited a measurable improvement over UO_2 with regard to matrix dissolution, suggesting that urania-thoria spent fuel may be a more stable long-term waste form than conventional UO_2 fuel [24].

Shippingport reactor

It is worth mentioning the reactor developed by the U.S. Department of Energy: a liquid water breeder reactor at Shippingport, Pennsylvania. The reactor started in the end of fifties and was in operation until 1982. The system, fueled by thorium and uranium, operated well, producing a breeding ratio between 1.01 and 1.02 as designed.

The core consists of hexagonal modules arranged in a symmetrical array surrounded by a reflector-blanket region (Figure A.2). Each module contains an axially movable seed-region and a stationary annular hexagonal blanket. Each of these regions consists of arrays of tightly packed, but not touching, fuel rods containing pellets of thoria and $^{233}\text{UO}_2$, the latter in varying amounts from 0 to 6 w/o in the seed and from 0 to 13 w/o in the blanket region (Figure A.3).

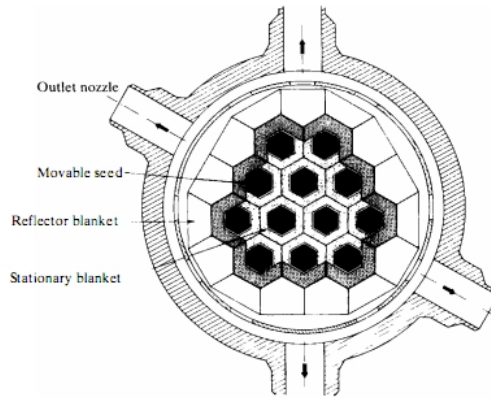


Figure A.2: LWBR core cross-section [6].

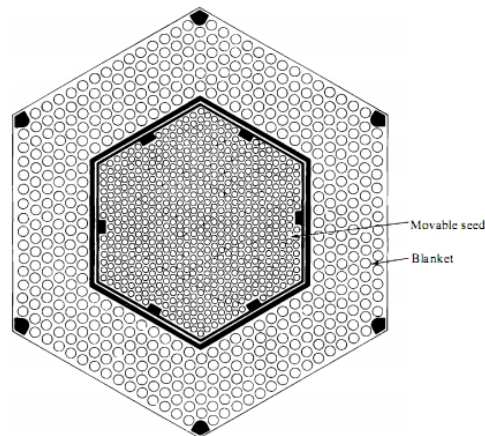


Figure A.3: LWBR fuel module cross-section [6].

A.2 Performance in HWRs

Heavy water has the moderation ratio (the ratio of moderating ability to neutron absorption) about eighty times that of light water, making good neutron economy for a breeding cycle. The majority of heavy water reactors in operation today are of a pressure tube design, employing small, simple fuel bundles and allowing on-power fueling. All of these features could be of great benefit in the implementation of thorium fuel cycles [25].

Because thorium does not contain a fissile isotope, neutrons must be initially provided by adding a fissile material, either within or outside the ThO_2 itself. How the neutrons are initially provided defines a variety of thorium fuel cycle options in HWRs that will be examined in this section. These include the following:

- The once-through thorium (OTT) cycles, where the rationale for the use of thorium does not rely on reprocessing the ^{233}U and recycling (but where reprocessing remains a future option);
- Direct self-recycle of irradiated thoria elements following the OTT cycle (no reprocessing);
- The self-sufficient equilibrium thorium cycle, a subset of the recycling options, in which there is as much ^{233}U in the spent fuel as is required in the fresh fuel;
- High burnup open cycle;
- Other recycling options, ranging from reprocessing to the selective removal of neutron absorbing fission products.

The once through thorium cycles

The OTT cycle relies on *in situ* generation and incineration of ^{233}U . However, the OTT cycle leaves behind substantial amounts of ^{233}U in the

spent fuel. Two options were addressed: the mixed *channel* approach and the mixed fuel *bundle* design.

In the mixed channel approach, the channels would be fueled either with ThO₂ bundles or with “driver” fuel, typically SEU. In such a system, the thorium would remain in the core much longer than the driver fuel would. As the residence time of the thorium in the core increases, the energy obtained from a unit of mined uranium will first decrease, then, after passing through a minimum, will start to increase, finally becoming higher than it would have been had no thorium been present at all. Studies has been conducted in order to optimize the OTT cycle from both the resource utilization and the monetary cost compared with either natural uranium or SE, without taking any credit for the ²³³U produced. It has shown that, even if such OTT cycles “exist ” , their implementation would pose technical challenges to fuel management because of the disparity in reactivity and power output between driver channels and thorium channels [26].

An alternative approach has been developed in which the whole core would be fueled with mixed fuel bundles, which contain both thorium and SEU fuel elements in the same bundle. Figure A.4 shows a CANFLEX mixed bundle containing ThO₂ in the central eight elements and SEU in the two outer rings of elements. This mixed bundle approach is a practical means of utilizing thorium in existing HWRs, while keeping the fuel and the reactor operating within the current safety and operating envelopes established for the natural uranium fuel cycle. It does not involve making any significant hardware changes. Compared with natural uranium fuel, this option has better uranium utilization, comparable fuel cycle costs are not as low as for SEU, or for an “optimized” OTT cycle using the mixed channel approach.

CANFLEX flexibility also allow burning of plutonium in a suited design of the bundle [25].

AECL has examined two mixed bundle strategies for burning thorium in existing CANDU reactors [27]: on one hand, only one fuel type used throughout the entire core, on the other hand, the reactor core is divided into three

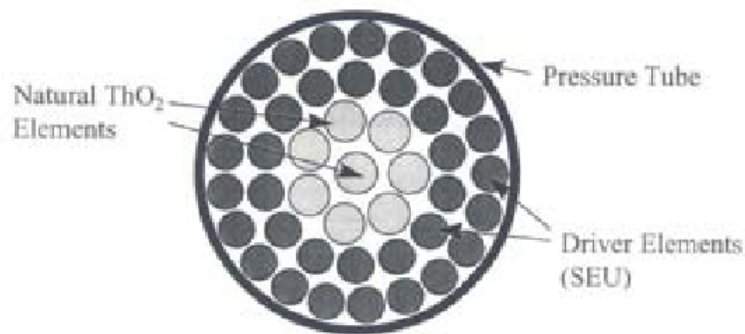


Figure A.4: CANFLEX mixed bundle.

regions, each containing a different type of thorium fuel bundle. The latter significantly increases the amount of thorium fuel in the core and improves the overall fuel efficiency of the thorium-burning reactor.

Direct self-recycle

Additional energy can be derived from the thorium by recycling the irradiated thorium fuel elements (which contain ^{233}U) directly, without any processing, into the center of a new mixed bundle [28]. Recycle of the central eight thorium elements results in an additional burnup of ~ 20 MWd/kg HE from the thorium elements, for each recycle. The reactivity of these thorium elements remains remarkably constant during irradiation for each recycle. This direct, self-recycling results in a significant improvement in uranium utilization compared with OTT: after the first recycle, the uranium requirements are $\sim 35\%$ lower than those of the natural uranium cycle, and more than 10% lower than those of the optimal SEU cycle, and remain fairly constant with further recycling. The cumulative uranium requirement averaged over a number of cycles is 30-40% lower than that of natural uranium fueled CANDU reactors.

Self-sufficient equilibrium thorium cycle

The ultimate uranium conserving fuel cycle would be the self-sufficient equilibrium thorium cycle, in which no fissile topping (and hence, no natural uranium) would be required in equilibrium, i.e. the ^{233}U concentration in the recycled fresh fuel matches the ^{233}U concentration in the spent fuel [29].

The major shortcoming of the self-sufficient equilibrium thorium cycle is its low burnup, between 10 and 15 MWd/kg HE, which will not be economic in a cycle that requires reprocessing and remote fabrication of the ^{233}U -bearing fuel. To address this issue, a small amount of ^{235}U could be added to each cycle allowing higher burnup [25].

High burnup open cycle

The high burnup thorium open cycle avoids the issues relating to closing the fuel cycle with reprocessing. In this cycle, the burnup is increased by trading off the conversion ratio. The thorium is enriched with ^{235}U to give whatever burnup fuel can achieve. The spent fuel is not recycled (although this option would not be precluded). High burnup is equally possible with SEU, but the advantage of thorium over SEU lies in the fact that for very high discharge burnups, the initial fissile content required is lower with thorium fuel. In the case of low enrichments, SEU gives a higher discharge burnup for a given ^{235}U enrichment, but with very high discharge burnups, the enrichment required for the thorium fuel is lower than that required for SEU. In theoretical assessments, pure ^{235}U has been added to the thorium.

The main advantage of this thorium cycle compared with an equivalent enriched uranium cycle stems from the fact that as ^{235}U is burnt, so ^{233}U is built up, and as ^{233}U is a superior fissile material than ^{235}U , the reactivity versus burnup curve falls off more gradually with thorium than it does with enriched uranium. This means that to attain the same discharge burnup, the initial ^{235}U content can be lower in the thorium cycle. Added to this is the fact that thermal neutron absorption in thorium is about three times than in ^{238}U , and that consequently the initial reactivity in the thorium core will be

well below that of the SEU core for the same discharge burnup. This leads to lower reactivity swings, which is a definite operational advantage. This cycle is also an attractive method of plutonium annihilation, as it would have a very high plutonium destruction efficiency [25].

Heavy water cooled PWR

Recently was addressed a fast PWR cooled by heavy water and fueled with ^{232}Th - ^{233}U mixed oxide [30]. It was studied the impact of moderator-to-fuel ratio (MFR) in order to accomplish breeding, negative void coefficient and acceptable burnup. It was shown that with a $\text{MFR} = 1$ and an enrichment of about 8% the following results can be reached:

breeding ratio $\text{BR}=1.1$;

void coefficient: negative;

burnup equal to or higher than standard PWRs.

This kind of reactor can be designed as a safe breeder exploiting current technologies.

A.3 Performance in MSRs

The MSR concept was first studied in the fifties at the Oak Ridge National Laboratory (ORNL), with the Aircraft Reactor Experiment of a reactor for plane based on a liquid uranium fluoride fuel circulating in a BeO moderator. Studies were then oriented on a civilian application of this concept to electricity production. The Molten Salt Reactor Experiment (MSRE) managed from 1964 to 1969 the operation of a 8 MWth graphite-moderated MSR, with a liquid fuel made of lithium and beryllium fluorides. A third component of the salt was first enriched uranium, then ^{233}U and finally plutonium fluoride.

Liquid fuel (generally $\text{BeF}_2\text{-LiF-(Heavy Nuclide)F}_4$), reprocessing and refueling on line are the peculiarities of such type of reactors.

MSRs seem to be best systems for thorium exploitation, though they are a long term program. Their advantages over other systems can be summarized as follows:

- No fuel meltdown concerns;
- Neutronics advantages: continuous fission gas removal and possibility of online reprocessing (in order to remove the poisonous Protactinium);
- Possibility of a two-fluid configuration, in which the thorium is dissolved only in a blanket. The uranium is produced in the form of liquid UF_4 , which can easily be converted to UF_6 (through fluorination), extracted, and dissolved in the fuel;
- Possibility of fast denaturing of the pure ^{233}U in the fuel by means of dedicated tanks containing depleted uranium fluorides. This could partly solve the proliferation issues which comes from having a pure fissile (^{233}U) in the fuel.
- Suitability for thorium-supported actinide burning. There is no need to handle the actinides for producing solid fuel elements. In some configurations, the LWR spent-fuel can be burnt “as it is”.

Previously, MSRs were mainly considered as thermal-spectrum graphite-moderated concepts. Since 2005 R&D has focused on the development of fast-spectrum MSR concepts (MSFR). In the following some MSR designs are briefly presented.

MSBR

The Molten Salt Breeder Reactor (MSBR) was the first thermal-spectrum breeder concept and it was developed during the 1960s by ORNL. It was a 2250 MWth reactor with a cylindrical core of 396 cm in height and 554 cm in diameter. This reactor relies on ^{232}Th – ^{233}U cycle and could bring a breeding ratio of 1.06 with a doubling time of about 20 years [31].

Fuji

Fuji is a thorium MSR nearly-breeder design developed in Japan in the research group of Professor Furukawa. The concept descends directly from the Molten Salt Reactor Experiment of ORNL. It is graphite moderated but does not require core-graphite replacement nor continuous chemical processing. FUJI is size-flexible with typical values that lies between 150-300 MWe. The cost of a 10 MWe FUJI prototype was estimated to be on the order of 300 millions USD [32]. The “International Thorium Energy and Molten Salt Technology Inc.” has been recently created, aiming at the Fuji construction.

MSFR

Molten Salt Fast Reactor¹ concept combines the generic assets of fast neutron reactors (extended resource utilization, waste minimization) with those relating to molten salt fluorides as fluid fuel and coolant (favorable thermal-hydraulic properties, high boiling temperature, optical transparency). In addition, MSFRs exhibit large negative temperature and void reactivity coefficients. MSFR systems have been recognized by GEN IV International Forum as a long term alternative to solid-fuelled fast-neutron systems with unique favorable features (negative feedback coefficients, smaller fissile inventory, easy in-service inspection, simplified fuel cycle, etc.) [33].

The primary feature of the MSFR concept is the removal of the graphite moderator from the core. Figure A.5 displays a schematic drawing of a vertical section of the reactor. In terms of fuel cycle, two basic options have been investigated, ²³³U-started MSFR and TRU-started MSFR. In both starting modes, safety requirements are met since all the feedback coefficients are negative. The total feedback coefficient is equal to $-6 \text{ pcm}/^\circ\text{C}$ when the equilibrium state of the reactor has been reached and the density coefficient (for MSRs can also be viewed as a void coefficient) is about $-3 \text{ pcm}/^\circ\text{C}$.

For a ²³³U-MSFR, the annual ²³³U production is 120 kg meaning a 50 years

¹The original name was Thorium Molten Salt Reactor (TMSR), recently it has been renamed as Molten Salt Fast Reactor.

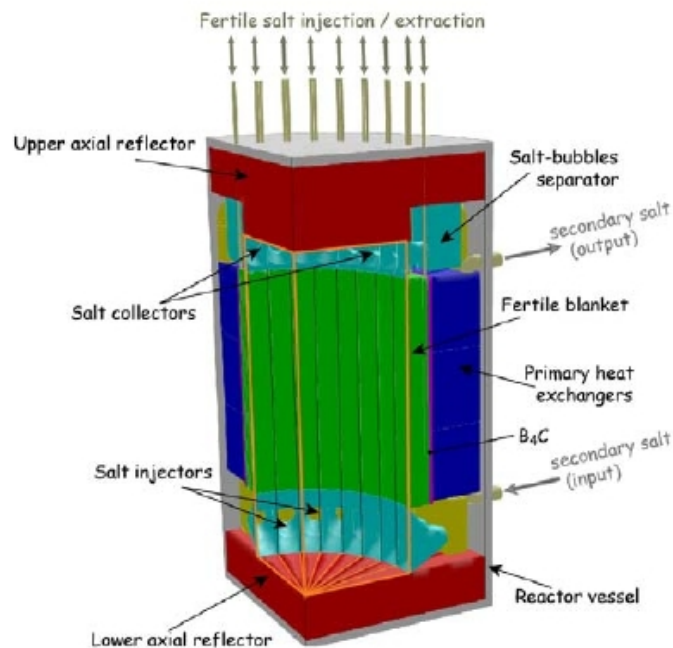


Figure A.5: Schematic view of a quarter of the MSFR.

doubling time per reactor. Starting a MSFR from actual reactors' spent fuel yields 35 years doubling time.

The assessment of structural materials remains challenging because of operation temperatures as high as 700-800 °C and irradiation damages [34].

The salt management combines a salt control unit, an on line gaseous extraction system and an offline lanthanide extraction by pyrochemistry. The gaseous extraction system, where helium bubbles are injected in the core, removes all non-soluble fission products. The reactivity can be set equal to one through the on line control and adjustment of the salt composition. In order to extract the lanthanides a fraction of salt is periodically withdrawn and reprocessed offline. Breeding performance is conditioned by the rate at which this offline salt reprocessing is done. The actinides are sent back into core to be burnt.

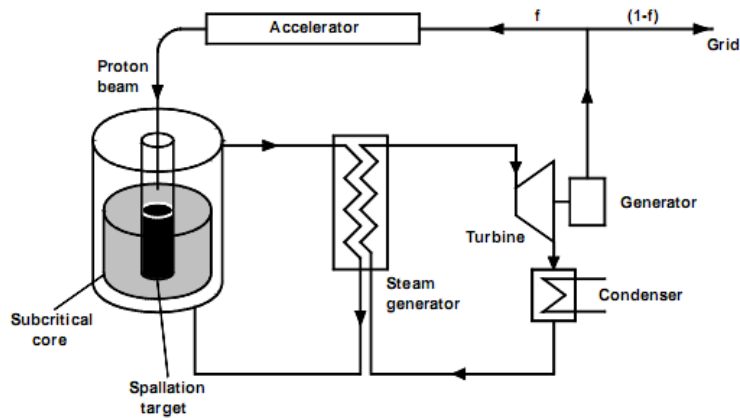


Figure A.6: Concept of an Accelerator Drive System [36].

A.4 Thorium in ADS

An Accelerator Driven System (ADS) is a subcritical reactor ($k_{\text{eff}} = 0.95-0.98$) in which necessary neutrons for the chain reactions sustainment come from an external source. A high energy proton beam (~ 1 GeV) hits a target and spallation reactions are generated and a large number of neutrons are emitted. The mean number of neutrons depends on the proton energy. For a 1 GeV proton beam, about 30 neutrons for each spallation reaction are emitted. The more subcritical the core is, the higher the power of the beam must be. For instance, for a core with $k_{\text{eff}} = 0.95$ the power beam must be around 25 MW. A beam power of 10 MW is more than the largest accelerators are capable today [35]. In Figure A.6 is showed the layout of a such system.

The reactor core is fueled mainly with thorium and at the starting of the ADS there will also be some ^{235}U or Pu or even transuranic waste in the fuel. Coolant usually is lead or lead-bismuth eutectic working in natural convection.

Incineration of minor actinides appears to be efficiently with ADS. Spallation neutrons can be used for increased breeding of ^{233}U or to transmute long-lived fission products and transuranics as well. Actually, the advantage

of ADS respect to critical cores is clearly showed for concentrated management of waste. Hybrid systems perform as excellent dedicated minor actinide incinerators and offer the required flexibility for transition scenarios [36]. To this end, the main advantage comes from the subcriticality of the system. Higher concentrations of minor actinides to be burnt is allowed respect to critical cores. Safety control of critical reactors relies on margin to prompt criticality given by delayed neutrons. Transuranics have a lower fraction of delayed neutrons than ^{235}U . For an ADS there is no control problem as it can be managed at a lower reactivity in order to regain the margin to prompt criticality lost. The reactor power can be kept constant increasing the beam power.

Mentioning worth is the Energy Amplifier (EA) proposed by Carlo Rubbia, in 1993, that could produce energy at the same time as destroys both its own waste and waste from other reactors [37]. An EA module consists of a 1500 MWth unit with its dedicated 1.0 GeV proton accelerator of 12.5 mA. The EA operates in a closed thorium fuel cycle and recycling of all the actinides. According to the authors, EA could achieve a burn-up well in excess of 100 MWd/kg and after about 700 years the radiotoxicity left is about 20 000 times smaller than the one of an ordinary PWR for the same energy.

The most active work on ADS in Europe is the MYRRHA project in Belgium, which started in 1997 and is planned to be in operation around the year 2016. MYRRHA is planned to have a subcritical core ($k_{\text{eff}} \simeq 0.95$) with MOX fuel (35 wt% plutonium) and will be cooled by lead-bismuth eutectic. The accelerator will be a 1.5 MW LINAC that delivers protons with an energy of 600 MeV. The power of the reactor is estimated at 60 MWth [35].

The major drawbacks of ADS systems are the following:

- The system is a combination of two complex machines, the reactor and the accelerator, each of which must be working for the system to produce power. The reliability of the accelerator is a particular concern for R&D. On the other hand, due to long burn-up and small reactivity swings, the core must be “touched” less frequent than critical reactors.

- A proton beam with energy as high as required for such systems induces a large production of volatile radioactive isotopes in the spallation target. The activity in the Cover Gas System (CGS) may be up to 100 000 times higher than in the CGS of “normal” reactors operating with lead-bismuth [36].
- Accelerator will be placed outside the containment building. The target (inside the core) is separated from the beam tube by a window which is exposed to an intense flux of high energy protons and neutrons as well. In the Rubbia EA project, this will be replaced one a year [37]. The primary containment is so weakened. Actually there are similar problems to the steam line in a BWR, but in the case of a BWR there are fast acting valves to close the steam lines in case of leakage. This can be achieved also in the beam tube of an ADS, but a misaligned proton beam of several MW may also melt the isolation valve [36].

Bibliography

- [1] “World Energy Outlook 2009.”
- [2] “Retrieved online from NRC website: <http://www.nrc.gov/waste/hlw-disposal/yucca-lic-app.html>.”
- [3] Carelli, M., Franceschini, F., Lahoda, E., and Petrovic, B., “Back to front: a comprehensive approach to deal with the everlasting nuclear waste “problem”,” *Radwaste Solutions*, vol. 18, N. 2, May-June 2011.
- [4] Salvatores, M., and Palmiotti, G., “Radioactive waste partitioning and transmutation within advanced fuel cycles: Achievements and challenges,” *Progress in Particle and Nuclear Physics*, vol. 66, pp. 144–166, 2011.
- [5] Hill, R.N., and Taiwo, T.A., “Transmutation impacts of generation-IV nuclear energy system,” in *PHYSOR*, 2006.
- [6] Lamarsh, J.R., and Baratta, A.J., *Introduction to Nuclear Engineering*. Prentice-Hall, Inc., third ed., 2001.
- [7] “JANIS nuclear data, available at: <http://www.oecd-nea.org/janis/>.”
- [8] Dobson, A., “GNEP deployment studies preliminary conceptual design studies,” in *Report for the Nuclear Fuel Recycling Center and the Advanced Recycling Reactor. Volume I*, Summary 2008.

- [9] Strawbridge, L.E., “Safety Related Criteria and Design Features in the Clinch River Breeder Reactor Plant,” in *ANS Fast Reactor Safety Meeting*, 1974.
- [10] Bubberley, A.E., Yoshida, Boardman, C.E., and Wu, T., “Super-PRISM oxide and metal fuel core designs,” in *ICONE 8*, Baltimore, MD USA, April 2-6, 2000.
- [11] Krepel, J., Pelloni, S., Mikityuk, K., and Coddington, P., “EQL3D: ERANOS based equilibrium fuel cycle procedure for fast reactors,” *Annals of Nuclear Energy*, vol. 36, pp. 550–561, 2009.
- [12] Rimpault, G., Plisson, D., Tommasi, J., Jacqmin, R., Rieunier, J.-M., Verrier, D., and Biron, D., “The ERANOS Code and Data System for Fast Reactor Neutronic Analyses,” in *PHYSOR 2002*, 2002.
- [13] “ERANOS 2.2 - Code documentation.”
- [14] Krepel, J., Pelloni, S., Mikityuk, K., and Coddington, P., “GFR equilibrium cycle analysis with the EQL3D procedure,” *Nuclear Engineering and Design*, vol. 240, pp. 905–917, 2010.
- [15] IAEA-TECDOC 1374, *Development status of metallic, dispersion and non-oxide advanced and alternative fuels for power and research reactors*, International Atomic Energy Agency, (Vienna, Austria), 2003.
- [16] Till, C.E., Chang, Y.I., Kittel, J.H., Fauske, H.K., Lineberry, M.J., Stevenson, M.G., Amundson, P.I, and Dance, K.D., “Fast Breeder Reactors Studies,” Argonne National Laboratory, Argonne, Illinois, July 1980.
- [17] Collins, P.J., Beck, C.L., McFarlane, H.F., Lineberry, M.J., and Carpenter S.G., “A comparison between physics parameters in conventional and heterogeneous LMFBRs using results from ZPPR,” Retrieved online from OSTI website: <http://www.osti.gov/bridge/purl.cover.jsp?purl=/6213599-gEVBmG/>.

- [18] van Rooije, W.F.G., Kloosterman, J.L., van der Hagen, T.H.J.J., and van Dam, H., "Definition of Breeding Gain for the Closed Fuel Cycle and Application to a Gas-Cooled Fast Reactor," *Nuclear Science and Engineering*, vol. 157, pp. 185–199, 2007.
- [19] Kang, J., and von Hippel, F.N., "U-232 and the Proliferation-Resistance of U-233 in Spent Fuel," *Science & Global Security*, vol. 9, pp. 1–32, 2001.
- [20] Kim, T.K., Yang, W.S., Grandy, C., and Hill, R.N., "Core design studies for a 1000 MW_{th} Advanced Burner Reactor," *Annals of Nuclear Energy*, vol. 36, pp. 331–336, 2009.
- [21] Todosow, M., Galperin, A., Herring, S., Kazimi, M., Downar, T., and Morozov, A., "Use of thorium in light water reactors," *Nucl. Tech.*, vol. 151, pp. 168–176, 2005.
- [22] Weaver, K.D., and Herring, J.S., "Performance of thorium-based mixed-oxide fuels for the consumption of plutonium in current and advanced reactors," *Nucl. Tech.*, vol. 143, pp. 22–36, 2003.
- [23] Dziadosz, D., Ake, T.N., Saglam, M., and Sapyta, J.J., "Weapons-grade plutonium-thorium PWR assembly design and core safety analysis," *Nucl. Tech.*, vol. 147, pp. 69–83, 2004.
- [24] Demkowicz, P.A., Jerden, J.L., Cunnane, J.C., Shibuya, N., Baney, R., and Tulenko, J., "Aqueous dissolution of urania-thoria nuclear fuel," *Nucl. Tech.*, vol. 147, pp. 157–170, 2004.
- [25] IAEA-TECDOC 1450, *Thorium fuel cycle - Potential benefits and challenges*, International Atomic Energy Agency, (Vienna, Austria), 2005.
- [26] Milgram, M.S., *Once through thorium cycles in CANDU reactors*, Report AECL-7516, Atomic Energy of Canada Ltd, 1982.

- [27] Boczar, P.G., Chan, P.S.W., Dyck, G.R., Ellis, R.J., Jones, R.T., Sullivan, J.D., and Taylor, P., “Thorium fuel-cycle studies for CANDU reactors,” in *IAEA-TECDOC-1319*, IAEA, pp. 25–41, 2002.
- [28] Boczar, P.G., Dyck, G.R., Chan, P.S.W., and Buss, D.B., “Recent advances in thorium fuel cycles for CANDU reactors,” in *IAEA-TECDOC-1319*, IAEA, pp. 104–122, 2002.
- [29] Critoph, E., et. al., *Prospects for self-sufficient thorium cycles in CANDU reactors*, Report AECL-8326, Atomic Energy of Canada Limited.
- [30] Permana, S., Takaki, N., and Sekimoto, H., “Breeding capability and void reactivity analysis of heavy-water-cooled thorium reactor,” *J. Nucl. Sci. Technol.*, vol. 45, no. 7, pp. 589–600, 2008.
- [31] Forsberg, C.W., “Molten salt reactors (MSRs),” in *The Americas Nuclear Energy Symposium*, 2002.
- [32] Furukawa, K., Arakawa, K., Erabay, L.B., Ito, Y., Kato, Y., Kiyavitskaya, H., Lecocq, A., Mitachi, K., Moir, R., Numata, H., Pleasant, J.P., Sato, Y., Shimazu, Y., Simonenco, V.A., Sood, D.D., Urban, C., and Yoshioka, R., “A road map for the realization of global-scale thorium breeding fuel cycle by single molten-fluoride flow,” *Energy Convers Manage*, vol. 49, pp. 1832–1848, 2008.
- [33] GEN IV Interantional Forum, *GIF symposium*, 2009.
- [34] Renault, C., Hron, M., Konings, R., and Holcomb, D.E., “The molten salt reactors (MSR) in generation IV: overview and perspectives,” in *GIF symposium*, pp. 191–200, 2009.
- [35] *Thorium as an energy source - opportunities for Norway*, 2008. Technical report.

-
- [36] *Accelerator-driven Systems (ADS) and Fast Reactor (FR) in advanced nuclear fuel cycles*, OECD NEA, 2002.
- [37] Rubbia, C., Rubio, J.A., Buono, S., Carminati, F., Fiétier, N, Galvez, J., Gelès, C., Kadi, Y., Klapisch, R., Mandrillon, P., Revol, J.P., and Roche, Ch., “Conceptual design of a fast neutron operated high power energy amplifier,” *CERN/AT/95-44 (ET)*, 1995.